Autophagy and apoptosis contribute to neuronal survival in a model system of oxytosis in vitro

Dissertation

zur

Erlangung des Doktorgrades

der Naturwissenschaften

(Dr. rer. nat.)

dem

Fachbereich

Pharmazie

der Philipps-Universität Marburg

vorgelegt von

Stefanie Neunteibl

aus Herborn

Marburg/Lahn 2014

Vom Fachbereich Pharmazie der Philipps-Universität Marburg als Dissertation am 15.07.14 angenommen.

Erstgutachter: Prof. Dr. Carsten Culmsee

Zweitgutachter: Prof. Dr. Moritz Bünemann

Tag der mündlichen Prüfung am 16.07.14

Meiner Familie

ERKLÄRUNG

Ich versichere, dass ich meine Dissertation

„Autophagy and apoptosis contribute to neuronal survival in a model system of oxytosis in vitro “

selbständig ohne unerlaubte Hilfe angefertigt und mich dabei keiner anderen als der von mir ausdrücklich bezeichneten Quellen bedient habe.

Die Dissertation wurde in der jetzigen oder einer ähnlichen Form noch bei keiner anderen Hochschule eingereicht und hat noch keinen sonstigen Prüfungszwecken gedient.

Marburg, den 11.06.14

.....

(Stefanie Neunteibl)

TABLE OF CONTENTS

1 Introduction

1.1 The role of autophagy and apoptosis for neuronal survival and death

Autophagy and apoptosis play major roles in determining the cellular fate. Accordingly, they participate in development, cellular homeostasis, and both in physiological as well as in pathological processes [1]. Apoptosis is executed by activated caspases, which are specific enzymes that participate in signaling cascades that culminate in the rapid removal of organelles and other cellular structures [2]. Autophagy is a highly conserved cytoprotective process whereby cytoplasmic contents are sequestered, transported via double-membrane autophagosomes to lysosomes, and degraded [3].

Along with regulated necrosis and other forms of programmed cell death [4], pathological mechanisms of autophagy and apoptosis have been detected in neurodegenerative diseases, such as Parkinson's disease (PD) or Alzheimer's disease (AD) and acute brain injuries [5].

1.1.1 Autophagy

The term autophagy, coined from the greek words of αυτς ('autos', self) and φαγειν ('phagein', eating), was first described by Christian de Duve in 1963 as a lysosome-mediated degradation process for non-essential or damaged cellular constituents [6]. Autophagy is a generic term for all pathways by which cytoplasmic materials are delivered to the lysosome or the vacuole in animal cells or plants [3]. In contrast to the ubiquitin-proteasome system (UPS), which serves as the primary route for degradation for thousands of short-lived proteins [7], autophagy is primarily responsible for degrading long-lived proteins and organelles. Recent studies indicated that there is a coordinated and complementary relationship between these two systems. Inhibition of proteasomal activities has been previously shown to induce autophagy [8]. In contrast, it was also described that proteasomes were activated in response to pharmacological inhibition of autophagy [9].

When autophagy was discovered over 50 years ago it was assumed to represent a general non-selective degradation pathway activated by nutrient limitation. Since then autophagy has been linked to human pathophysiology, including cancer, neurodegeneration, immune response and ageing [10].

In 1992, Yoshinori Ohsumi and his colleagues at the University of Tokyo discovered that autophagy also occurs in yeast. Being able to use yeasts as an experimental model opened the door for studying the molecular biology of the autophagic machinery [11]. Today, research on autophagy is a continuously growing field with increasing prominence because understanding the basic mechanisms of autophagy could lead to the development of new strategies for the treatment of various diseases, including neurological diseases.

1.1.1.1 Forms of autophagy

There are at least three types of autophagy, including macroautophagy, microautophagy and chaperone-mediated autophagy (CMA). They differ in terms of their mechanism for directing the cytoplasmic content to the lysosomes, where the engulfed content is degraded by lysosomal proteases into macromolecules and are released back into the cytoplasm [12, 13].

Macroautophagy is thought to be the major form of autophagy and it has been studied most extensively compared to the other classes. In this thesis I investigated macroautophagy, which I will hereafter refer to as autophagy. The initial step of autophagy is the elongation of isolated membranes surrounding cytoplasmic material, which forms a double-membrane structure, the autophagosome. Afterwards the autophagosome fuses with the lysosome, thereby generating the autophagolysosome, where their contents are degraded by lysosomal hydrolases [3, 14]. Recent studies revealed that post-translational modifications, in particular ubiquitination of macroautophagy regulators, lead to a selective degradation of certain cytoplasmic components such as protein aggregates, organelles, and intracellular pathogens [15–17]. Another post-translational modification demonstrated to facilitate selective targeting of cargo for macroautophagy is acetylation [18].

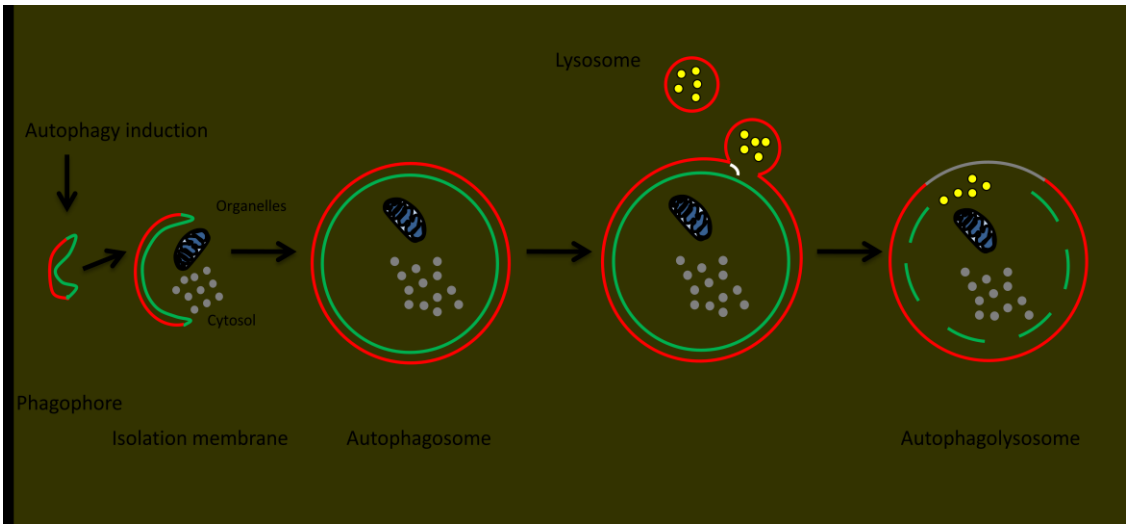

Figure 1. **Main steps of macroautophagy.** The main steps of the macroautophagy process are induction, autophagosome formation, sequestration and degradation. Autophagy induction involves the sequestration of portions of the cytoplasm, including organelles, within a double-membrane autophagic vacuole, named autophagosome. The autophagosome undergoes fusion with a lysosome to form an autophagolysosome, in which hydrolases degrade the cytoplasmic material [19].

During **microautophagy**, tiny portions of cytoplasm are directly sequestered and subsequently engulfed by lysosomes. In the past two decades, the growth in the understanding of microautophagic processes has come about almost entirely from studies performed in yeast. By contrast, few investigators have studied microautophagy in mammalian cells as a primary focus, and consequently the understanding has remained limited [20]. **Chaperone-mediated autophagy**, a selective form of autophagy, has only been identified in mammalian cells so far. Proteins degraded by CMA are identified individually by a cytosolic chaperone that delivers them to the surface of the lysosomes. There, the substrate proteins unfold and cross the lysosomal membrane. All the proteins internalized into lysosomes through CMA contain a pentapeptide motif (KFERQ) in their amino acid sequence that is essential for their targeting to lysosomes. These proteins are taken up by a complex, formed by the chaperone protein (hsc70) and co-chaperones (hip, hop, hsp40, hsp90, and bag1), directing them to a lysosome. At the lysosomal membrane the proteins are recognized by the LAMP-2A receptor that mediates their internalization into the lysosome [21].

1.1.1.2 Physiological and pathophysiological role of autophagy

Under physiological conditions, the process of autophagy occurs constantly. However, autophagic activity increases in conditions of cellular stress, such as starvation, hypoxia, drug treatment or exposure to radiation [22]. Autophagic activity is essential for various physiological processes, including cell survival, cell metabolism, development, aging and immunity [3]. Autophagy is generally considered to support cellular homeostasis and survival, but massive accumulation autophagosomes may represent either an alternative pathway of cell death (autophagic cell death) or an ultimate attempt of stress adaption [19]. More recent studies established a link between autophagy and disease. For example, macroautophagy deregulation at distinct steps including autophagosome nucleation, maturation and degradation has been demonstrated in many diseases such as neurodegenerative disorders, cancers and inflammatory disorders [12, 23, 24].

1.1.1.3 Autophagy in neurons

Autophagy in neurons was controversially debated for a long time based on the pre-conception that autophagy was only activated during nutrient deprivation and it was a general assumption that the brain was protected from such stress. Growing evidence however supports now that not only autophagy occurs naturally in neurons under physiological conditions, but that proper functioning of this catabolic pathway is required for function and maintenance of neuronal cells [25]. In the long run, autophagy is essential for neuronal health, while insufficient autophagy appears to be a contributing factor in chronic neurodegenerative diseases. For example, knockout mice lacking key mediator proteins regulating autophagy, such as Atg5 or Atg7 rapidly develop symptoms of neurodegenerative diseases with the presence of polyubiquitinated proteins in neurons as inclusion bodies [26, 27]. Moreover, basal autophagy is essential for maintaining axon homeostasis and morphology, and impaired autophagy results in axonal swelling, followed by progressive neurodegeneration [28, 29]. In neurodegenerative disorders, incomplete macroautophagic engulfment of cytosolic contents and mitochondria were observed in experimental models of Huntington's disease (HD) [30] and Parkinson's disease (PD) [31, 32], respectively, whereas in models of Alzheimer’s disease (AD) defects in autophagosome degradation were reported [33].

1.1.1.4 Molecular mechanisms of autophagy

Multiple autophagic proteins (Atg-proteins) that were discovered in the 1990s during genetic investigations in yeast regulate the autophagic process. In total, 35 Atg-proteins were discovered. Atg 1-10, 12-14, 16 and 18 are the so-called core Atg-proteins [34]. These core Atg-proteins are highly conserved in other eukaryotes and they act in a similar manner in yeast and mammalian cells [35, 36]. The biogenesis of autophagosomes is initiated with the formation of a pre-autophagosome (or phagophore), a membranous structure that contains all the proteins required for the creation of an autophagosome and that are assembled from membranes of preexisting organelles (endoplasmic reticulum, Golgi, mitochondria, plasma membrane) [37–40]. Induction of autophagy is initiated by the activation of the autophagy related gene-1 (Atg1) complex, comprising Atg1, Atg13 and Atg17, as well as accessory proteins [41]. After this, vesicle nucleation requires activation of the class-III phosphatidylinositol-3-kinase (Vps34) and Beclin-1/Atg6, as well as several other factors to recruit proteins and lipids for autophagosome formation. Vesicle elongation and completion are mediated by two-ubiquitin-like systems; Atg7 (E1-like) and Atg3 (E2-like) regulate the lipid modification (phosphatidylethanolamine, PE) of microtubule- associated protein light chain 3 (LC3, the mammalian orthologue of Atg8), which requires initial cleavage of LC3 by Atg4 protease; Atg7 and Atg10 (E2-like) regulate the conjugation of Atg12 to Atg5, followed by transfer to Atg16. The Atg12/Atg5/Atg16 complex mediates LC3-PE binding to the autophagosome membrane [42–44]. The fully assembled autophagosome is transported to the lysosome where the membranes fuse, resulting in breakdown of the autophagosome contents by the lysosomal enzymes [3, 41].

Furthermore, the Atg proteins LC3 (Atg8), Beclin-1 (Atg6) and Atg5 are well established markers for monitoring the autophagic process [45].

Microtubule-associated protein light chain 3 (LC3) is the most widely monitored autophagy-related protein and exists in two forms, LC3-I (16 kDa) and its lipidated form LC3-II (14 kDa), which are localized in the cytosol and in autophagosomal membranes respectively. The expression level of LC3-II can be used to estimate the abundance of autophagosomes before they are degraded by lysosomal hydrolases. The subcellular localization of LC3 redistributes from a cytosolic diffuse pattern to punctuate staining in vacuolar membranes when autophagy is induced [19, 46].

Beclin-1 is the mammalian orthologue of yeast Atg6 and belongs to the class III phosphatidylinositol-3-kinase (PI_3K) complex that participates in autophagosome formation. Beclin-1 has also been described as a B-cell lymphoma 2 (Bcl-2)-interacting protein. The ablation of autophagy by Bcl-2 is dependent on Beclin-1-Bcl-2 interaction. Dissociation of Bcl-2 from Beclin-1 leads to an induction of autophagy [47].

Atg5 is an E3 ubiquitin ligase which is necessary for autophagosome elongation [48]. Atg5 is activated by Atg7 and forms a complex with Atg 12 and Atg16L1. This complex is necessary for LC3-I conjugation to phosphatidylethanolamine (PE) to form LC3-II [49].

1.1.1.5 Major signaling pathways of autophagy upstream of the Atg machinery

The central player in autophagic signaling is the mammalian target of rapamycin (mTOR), which negatively regulates autophagy.

In mammals, mTOR can be included into two different complexes [50], mTORC1 and mTORC2. Both complexes display distinct cellular functions and phosphorylate different downstream targets [51]. The activity of mTORC1 is regulated via many signals including growth factors, insulin, nutrients, and cells stressors such as hypoxia, ROS and viral infections [52]. The two major pathways that regulate mTOR in mammalian cells are the PI_3K/Akt and AMP-activated protein kinase (AMPK) pathways.

The PI_3K/Akt pathway is triggered by the binding of insulin or growth factors to its receptor, thereby activating class I phosphatidylinosital-3 kinase (PI_3K). Activated PI_3K converts PIP_2 to PIP_3 to activate Akt [53]. Akt then phosphorylates and inactivates the tuberous sclerosis complex 1/2 (TSC1/2) resulting in activation of Rheb and mTORC1, thereby inhibiting autophagy.

The mammalian target of rapamycin can also sense changes in the cellular energy via AMPK. The activity of AMPK is required for autophagy to be induced in response to starvation in mammalian cells [54]. Activation of AMPK inhibits mTORC1 dependent signaling by interfering with the activity of Rheb, which leads to induction of autophagy.

Although the suppression of the mTOR is a major signaling pathway regulating autophagy, autophagy can also be activated independent of mTOR by various stimuli,

such as through altering macroautophagy genes transcription or by reducing the cellular level of inositol 1,4,5-trisphosphate (IP_3) [55, 56].

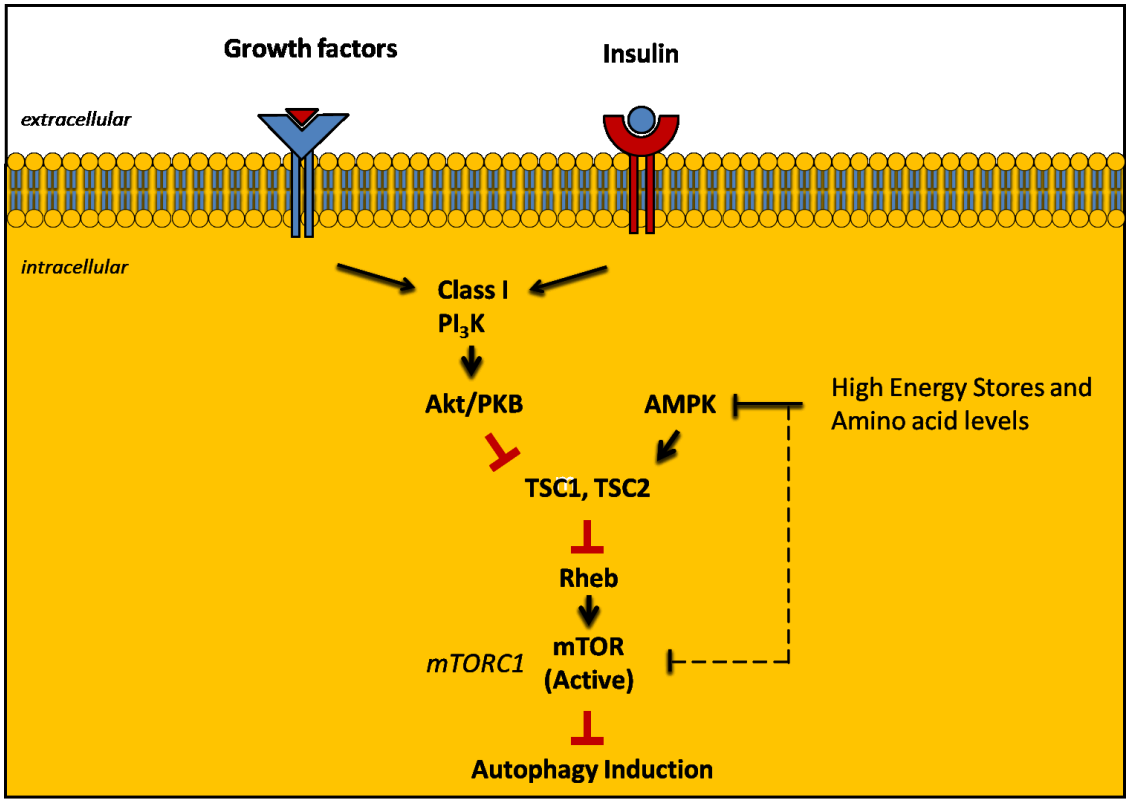

Figure 2. Major pathways that regulate mTORC1 in mammalian cells. The mTOR signaling pathway can receive input from growth factors and insulin via class I PI_3K, which activates Akt/PKB. In turn, Akt activates mTORC1 via the inhibition of TSC 1/2 and Rheb, leading to inhibition of autophagy. AMPK, which is activated when the AMP/ATP ratio increases, inactivates mTORC1 by activating TSC2, resulting in autophagy induction [57].

1.1.1.6 Activation of autophagic activity

The most frequently investigated physiological stimulus of autophagy is nutrient starvation [58]. But autophagy is also induced by physiological stimuli, such as growth factors and hormones, as well as by pathogen invasion. Moreover, reactive oxygen species (ROS) can be involved in this process [59]. Another approach to activate autophagy in experimental setups is through the modulation of nutrient-sensing signaling pathways. Further, rapamycin, an inhibitor of mTOR, and its analogs activate autophagy both *in vitro* and *in vivo* [60]. Starvation and mTOR inhibition affect a wide range of cellular responses, e.g. at the levels of protein synthesis and cellular metabolism, in addition to autophagy activation. Several mTOR independent autophagy inducers have also been reported. For example Lithium [61], BH3 mimetics [62], trehalose or small molecule enhancers of rapamycin (SMERs) [63, 64]. These substances also lack specificity for the autophagy process and may further induce various unrelated cell responses.

1.1.1.7 Inhibition of autophagic activity

Several pharmacological inhibitors are available and genetic manipulation techniques have also provided powerful tools to inhibit autophagic activity [65]. One of the most commonly applied pharmacological approaches to inhibit autophagy *in vitro* involves the use of PI_3-kinase inhibitors, such as wortmannin, LY294002 or 3-Methyladenine (3-MA) [66–68]. All of these substances inhibit both class I PI_3K activity (which inhibits autophagy) as well as class III PI_3K activity (which is required for autophagy) [69]. As PI_3-kinases regulate multiple diverse cell signaling and membrane trafficking processes, these PI_3-inhibitors are not specific for inhibition of autophagy. Additionally, 3-MA, which is used at very high concentrations, can target other kinases and affect other cellular processes, such as glycogen metabolism, lysosomal acidification [70], endocytosis [71] and the mitochondrial permeability transition [72]. 3-MA can suppress proteolysis even in Atg5-deficient cells, suggesting that its effects on protein degradation extend beyond its role in autophagy inhibition [48]. Other pharmacological inhibitors of autophagy block later stages of the process. Microtubule-disrupting agents (e.g. vinblastine) inhibit autophagosome-lysosome fusion [73, 74]. Final degradation of autophagic cargo inside autolysosomes can also be inhibited by ammonium chloride,

bafilomycin A1, chloroquine, and lysosomal protease inhibitors such as E64d and pepstatin [75]. A major limitation of these substances is that they affect other cellular processes besides autophagy such as mitosis and endocytosis.

Genetic approaches provide a more specific inhibition of autophagy. Autophagy deficiency or reduction has been confirmed in cells lacking Atg3 [76], Atg5 [48], Beclin-1 [77, 78], Atg 7 [79], Atg9a [80], Atg 16L [81, 82], FIP200 [83] and Ambra1 [84]. However, it is important to note, that even the Atg-proteins may not be entirely specific for autophagy. In fact they may exert autophagy-independent functions, including roles in cell death signaling, endocytosis, and immunity-related GTPase trafficking [85, 86].

1.1.1.8 Autophagic cell death

In many *in vitro* and *in vivo* systems cell death is often accompanied by features of autophagy. This led to the proposal of autophagic cell death [85, 87]. Autophagy is a pathway activated by cellular stress. Therefore it is not surprising that cells undergoing death after stress also show features of autophagy. This conundrum has led to some confusion in the literature where signs of autophagy in dying cells led to the interpretation that cells are in fact using autophagy as a death mechanism. In most known cases, autophagy constitutes a cytoprotective response activated by dying cells in the attempt to cope with stress, and its inhibition may thus accelerating, rather than preventing cell death [88]. However, there is accumulating evidence of a complex interplay between the apoptotic and autophagic machinery [1, 87]. First, autophagy has been shown to mediate physiological cell death *in vivo*, during the developmental program of Drosophila melanogaster [89]. Second, autophagy appears to be responsible for the death of some cancer cells *in vitro* [90, 91].

It is important then to discriminate between whether autophagy is determining cell death, or whether autophagy is altering the dynamics of death signaling. Shen and Codogno [92] have proposed that the following three criteria should be met to define cell death by autophagy: (i) cell death occurs independent of apoptosis; (ii) there is an increase in autophagic flux, not simply an increase in autophagy markers [93, 94]; and (iii) that suppression of autophagy using genetic deletion or chemical inhibitors is able to prevent cell death. Accordingly, all cases of cell death that exhibit markers of

autophagy such as the lipidiation of LC3 or an increased degradation of autophagic substrates like sequestosome 1 (SQSTM1), but cannot be blocked by autophagy inhibition should not be classified as autophagic cell death.

1.1.2 Apoptosis

The term apoptosis, derived from greek words (ἀπό *apo*, "away from" and πτῶσις *ptōsis*, "falling"), was first used by Kerr, Wyllie, and Currie in 1972 to describe a morphologically distinct form of cell death, although certain components of the apoptosis concept had been explicitly described many years previously [95, 96]. Apoptosis has been recognized and accepted as a distinctive and important mode of "programmed" cell death, which involves the genetically determined elimination of cells. The physiological function is the replacement of senescent or excessive cells [97]. Furthermore, apoptosis has an essential function during the development of the nervous system by controlling synapses and removing excessive and unneeded neural cells [98]. Apoptosis also occurs as a defense mechanism such as in immune reactions or when cells are damaged by disease or noxious agents [99]. Apoptotic cells show characteristic DNA fragmentation, nuclear condensation, membrane blebbing and the formation of apoptotic bodies. These apoptotic bodies are then phagocytosed by neighboring cells without causing any inflammatory response and damage to the surrounding tissues [95]. Pathological pathways of apoptosis have been associated with a lot of neurodegenerative diseases, such as AD and PD and also with acute brain damage as after cerebral ischemia or traumatic brain injury [100].

Apoptotic cell death can be divided into two biochemical cascades, described as the extrinsic and the intrinsic pathway.

1.1.2.1 Extrinsic apoptosis

The extrinsic pathway is induced by extracellular stress signals that are sensed and propagated by specific transmembrane receptors, the so-called death receptors [101, 102]. Binding of lethal ligands, such as FAS/CD95 ligand (FASL/CD95L), tumor necrosis factor α (TNFα) and TNF (ligand) superfamily member 10 (TNFSF10) to various death receptors (i.e., FAS/CD95, TNFα-receptor 1 (TNFR1) and TRAIL

receptor (TRAILR)1–2, respectively) can initiate extrinsic apoptosis [101]. The activation of these death receptors leads to the activation of several caspases, including caspase-8 and caspase-3. In some cell types including lymphocytes ('type I cells') active caspase-8 directly catalyzes the proteolytic maturation of caspase-3, thereby triggering the executioner phase of caspase-dependent apoptosis in a mitochondria-independent manner [103, 104]. In other cells such as hepatocytes and pancreatic B cells ('type II cells') [103, 104], caspase-8 mediates the proteolytic cleavage of BH3-interacting domain death agonist (BID), leading to the generation of a mitochondria-permeabilizing fragment (known as truncated BID, tBID) [105, 106]. While 'type I cells' undergo extrinsic apoptosis irrespective of any contribution by mitochondria, 'type II cells' succumb from the activation of death receptors while showing signs of MOMP, including the dissipation of mitochondrial transmembrane potential ($\Delta\Psi_m$) and the release of toxic proteins that are normally retained within the mitochondrial intermembrane space (IMS) [107]. Among these, cytochrome C drives – together with the cytoplasmic adaptor protein APAF1 and dATP – the assembly of the apoptosome, another caspase-activating multiprotein complex [108].

1.1.2.2 Intrinsic apoptosis

Intrinsic pathways of apoptosis are triggered by intracellular stress. The signaling cascades for intrinsic apoptosis are highly heterogeneous, but they are all linked to mitochondria-centered control mechanisms. Along with the propagation of pro-apoptotic signaling cascades, anti-apoptotic mechanisms are also activated in an attempt to allow cells to cope with stress. Both, pro- and antiapoptotic signals converge at mitochondrial membranes, which become permeabilized when proapoptotic signals are more potent than antiapoptotic signals [107]. The permeabilization can start at the outer mitochondrial membrane (mitochondrial outer membrane permeabilization, MOMP) or at the inner mitochondrial membrane due to the opening. Irreversible MOMP affecting most mitochondria within a single cell has multiple lethal consequences: (i) the dissipation of the $\Delta\Psi_m$, with cessation of mitochondrial ATP synthesis and $\Delta\Psi_m$-dependent transport activities; (ii) the release of toxic proteins from the intermembrane space (IMS) into the cytosol (apoptosis inducing factor (AIF), cytochrome C (CYTC), endonuclease G (ENDOG), SMAC/DIABLO (second mitochondria–derived activator

of caspase/direct IAP binding protein with low pI), OMI/HTRA2 (high temperature requirement protein A2)); and (iii) the inhibition of the respiratory chain (favored by the loss of CYTC), leading to ROS overproduction and hence activating a feed-forward circuit for the amplification of the apoptotic signal [107]. Upon MOMP, cytosolic CYTC forms a multi-protein complex with Apaf-1 (apoptosis protease- activating factor-1) and pro-caspase-9, the so-called apoptosome. The apoptosome catalyzes the activation of execution caspases including caspase-3, -6 and -7. These caspases induce the breakdown of the cellular framework through degradation of substrates like actin or by activation of caspase-activated deoxyribonuclease (CAD) [108, 109]. AIF and ENDOG relocate to the nucleus, where they mediate large-scale DNA fragmentation independently of caspases [110–112]. SMAC/DIABLO and OMI/HTRA2 inhibit the antiapoptotic function of several members of the inhibitor of apoptosis (IAP) family, thereby derepressing caspase activation [113, 114]. In addition, OMI/HTRA2 exerts caspase-independent pro-apoptotic effects [115, 116]. Caspase activation does not play a prominent role in stress-induced intrinsic apoptosis *in vitro*, as demonstrated by the fact that chemical and/or genetic inhibition of caspases rarely confers long-term cytoprotective effects [117, 118].

1.1.3 Regulated Necrosis

Necrotic cell death is described for several physiological and pathophysiological settings, but it has also be suggested to contribute to embryonic development [119, 120]. Characteristics of necrosis are mitochondrial swelling, depletion of ATP, massive calcium influx and cell membrane dysfunction accompanied by deregulation of the intracellular ion homeostasis. At later stages, hallmarks of necrosis are cell swelling, membrane lysis and inflammatory processes [121]. For a long time, necrosis has been considered as a merely accidental cell death mechanism and was defined by the absence of morphological traits of apoptosis or autophagy. But necrosis can also appear in a highly regulated manner through defined molecular signaling pathways that involve activation of receptor interacting protein (RIP) 1 and/or 3 [122]. The term ‘necroptosis’ has recently been used as a synonym of regulated necrosis, but it was originally introduced to define a specific cascade of regulated necrosis that is ignited by TNFR1 ligation and can be inhibited by the RIP 1-targeting compound necrostatin-1 [123].

1.2 Neural Stem Cells and Neurogenesis

Stem cells exhibit two defining characteristics, the seemingly unlimited capacity for self-renewal through cell division and the capacity for generating specialized cell types through differentiation [124]. In contrast, progenitor cells are proliferative cells with a limited capacity for self-renewal and are often unipotent. They are more determined for differentiation into a specific cell type than stem cells. Stem and progenitor cells are found in various tissues of adult organisms and they act physiologically as a repair system [125].

In the brain, stem and progenitor cells are the origin of adult neurogenesis. The process of adult neurogenesis occurs throughout life in two restricted brain regions in mammals, the subgranular zone (SGZ) in the dentate gyrus of the hippocampus, where new dentate granule cells are generated; and the subventricular zone (SVZ) of the lateral ventricles, where new neurons are generated and then migrate through the rostral migratory stream (RMS) to the olfactory bulb to become interneurons [124]. Adult neurogenesis is a dynamic, finely tuned process and subject to modulation by various physiological, pathological, and pharmacological stimuli. Neurogenesis in other adult central nervous system (CNS) regions is generally believed to be very limited under normal physiological conditions but could be induced after injury [126].

These findings demonstrated that neural stem and progenitor cells have the potential to compensate and recover neural functions after acute and chronic CNS diseases. Studies have also started to illustrate the functional impact of new neurons on the existing neural circuitry and their contributions to brain functions under both normal and disease states [127].

1.2.1 Transplantation of Stem cells or NPC for the treatment of acute or chronic neurodegenerative diseases

Acute neurodegenerative diseases such as cerebral ischemia or stroke, and chronic neurodegenerative disorders (e.g. AD, PD, HD, ALS) are characterized by progressive dysfunction and death of neurons leading to the severe neurological impairments [5]. Currently available therapeutic options to treat patients suffering from acute or chronic neurodegenerative diseases are limited. Most of the presently available treatments are

symptomatic and not curative. Thus, new therapeutic options to prevent neuronal cell death and to repair damaged neuronal tissue are highly warranted.
Therefore, stem cell-based therapeutic approaches, e.g. transplantation, hold much promise as potential novel treatments to restore brain function of patients that suffer from acute or chronic neurodegenerative diseases. Stem-cells and progenitor cells have the potential to perform neurorestorative processes like neurogenesis, angiogenesis and modulation of inflammation or trophic support, thus facilitating functional recovery and neuroprotection [128–131].

Neural cell types can be generated from various cell types by using different approaches. The spectrum of available stem cells and progenitor cells is reaching from neural stem cells (NSCs), pluripotent stem cells (PSCs), direct conversion of differentiated cells into induced neural stem cells (iNSCs), induced neuronal cells (iNCs) from different cell types to mesenchymal stromal stem cells (MSCs) from various tissues, like bone marrow, cartilage, umbilical cord blood, adipose tissue, adult muscle or amniotic fluid [132]. Also induced pluripotent stem cells (iPSCs) reprogrammed from fibroblasts [133] or hair follicle cells [134] can be used for stem cell-based therapy in acute or chronic neurodegenerative diseases.

Numerous studies have been performed studying effects of neural stem cells and progenitor cell transplantation in model systems of several neurodegenerative diseases. For example recent findings from studies in a model of 1-methyl-4-phenyl-1,2,3,6-tetrahydropyridine (MPTP) toxicity in monkeys demonstrated that transplantation of human NSCs led to behavioral improvement [135, 136]. Further, Blurton *et al*. have shown in 2009 [137] that NSCs along with brain derived neurotrophic factor (BDNF) can ameliorate complex behavioral abnormalities associated with AD pathology in transgenic mice that express pathogenic forms of amyloid precursor protein, presenilin, and tau. In a rat model of cerebral ischemia, transplanted fetal hNSCs have not only shown migration towards the ischemic lesion, but also generated mature neuronal cells within the infarcted/injured striatum [138, 139]. A recent study by Chen *et al.* showed that direct injection of iPSCs into injured areas of rat cortex significantly decreased infarct size, improved motor function, attenuated inflammatory cytokines, and mediated neuroprotection after middle cerebral artery occlusion (MCAo) [140]. Most

intriguingly, also intravenous application of stem cells may serve as a suitable route of application for efficient replacement of damaged neurons in the brain tissue. For example, in a model of MG-132-induced cell death of dopaminergic neurons, bone marrow mesenchymal stem cells (BM-MSCs) injected intravenously 3 weeks after the initial damage at a dose of at a dose of 1 million cells, displayed high increment of dopamine levels in striatum [141].

The innovative concept of stem cell therapy has also been translated to clinical applications. For example, several clinical trials have been performed in which adult stem cells (MSCs) were transplanted to stroke patients [142, 143] PD [144], or AD patients (www.clinicaltrials.gov). The studies showed that transplantation of MSCs is safe and leads to functional recovery. Moreover, NPCs derived from aborted fetal tissue were used in a clinical study investigating Cerebral Palsy (CP) in children confirming that NPC transplantation was safe and effective [145]. In addition to these studies, ReNeuron, a UK based company, is currently conducting a clinical trial with immortalized human NSCs in stroke patients (NCT01151124).

In summary, stem cell transplantation is safe and led to behavioral improvement, functional recovery, generation of mature neuronal cells, decreased infarct size and attenuated inflammatory cytokines in various model systems of neurodegenerative diseases.

Accordingly, stem cell based approaches may provide novel therapies especially for the treatment of PD, HD, AD or ALS, SCI and stroke [128, 129, 146]. It should be kept in mind, however that stem cell-based therapy still holds many risks. In particular, very little is known about long term side effects. Further, the exact mechanism of therapeutic effects observed after stem cell/progenitor cell transplantation into the brain still remains unclear.

To explain the benefit after stem cell/ progenitor cell transplantations, several hypotheses were discussed in the literature. A commonly applied hypothesis for the therapeutic effects observed after stem cell transplantation is the replacement of injured tissue by the transplanted stem cells through differentiation of the engrafted cells into new neuronal cells [128, 147]. However, only very few cells survive after transplantation which makes this explanation rather unlikely [148–150]. Further, studies demonstrated that functional improvement after stem cell transplantation occurs rapidly

and is often detectable within one week of transplantation, which is an insufficient time period for the transplanted cells to become neurons and integrate successfully into the brain circuitry [151]. A more reasonable hypothesis is that interaction of stem/ progenitor cells with the host brain may lead to neuroprotective effects through the release of trophic factors or the stimulation of endogenous growth factor synthesis, which may contribute to recovery of functional impairments [152]. It is also known, that NSCs exert antioxidant properties thereby rescuing the surrounding neurons [153]. Moreover, enhanced angiogenesis, inhibition of apoptosis and stimulation of recruitment, proliferation and differentiation of endogenous stem cells that reside in the brain tissue are further hypotheses to explain the beneficial effects of stem cell and progenitor cell transplantation [154–156].

1.2.1.1.1 Conditioned medium (CM) of stem cells or progenitor cells

Because of the finding that most stem cells die after transplantation *in vivo* and that trophic support is likely responsible for the beneficial effect after transplantation rather than cell or tissue replacements, conditioned medium (CM) of dead or alive stem cells or progenitor cells was used in previous studies investigating neurodegenerative diseases. This CM reflects the properties of the surroundings of the stem cell/progenitor cell transplants. Furthermore, investigation of CM may provide a deeper understanding for the protective components and the mechanisms involved in neuroprotective effects after stem cell transplantation. Studies on several types of conditioned medium (CM) were already performed. A previous study showed that application of adult bone marrow stromal cells (BMSC) CM attenuated staurosporine (STS) or amyloid-beta peptide-induced apoptosis and triggered endogenous survival signaling pathways that mediate protection against apoptotic insults in primary embryonic rat neurons [154]. NSC-conditioned medium (NSC-CM) was neuroprotective in an *in vitro* model of HD with modulating mutant huntingtin-induced cytotoxicity [157]. Recently, a study demonstrated that factors present in mesenchymal stem cells conditioned medium (MSC-CM) improved migration of resident stem cells from human cardiac tissue [158]. In a study using MSCs [159], the derived CM displayed significantly elevated levels of VEGF, monocyte chemoattractant protein-1 (MCP-1), macrophage inflammatory protein-1α (MIP-1α), MIP-1β and monokine induced by IFN-γ (MIG) compared to

control media. The MSC CM affected MSC migration, promoted angiogenesis and reduced apoptosis in H9c2 cells or canine jugular vein vascular endothelial cells (CVEC). Another study with human MSCs CM reported that MSCs secrete brain-derived neurotrophic factor (BDNF) which promoted neuronal survival in cultured rodent cortical neurons against trophic factor withdrawal or nitric oxide (NO) exposure [160].

1.3 In-vitro model systems to investigate neuronal cell death

1.3.1 Glutamate-induced oxidative stress in HT-22 cells

In order to investigate mechanisms of neuronal cell death, the well-established immortalized mouse hippocampal cell line (HT-22) that is particularly sensitive to glutamate was used for this thesis. HT-22 neurons have been generated from HT-4 cells, a cell line originating from primary mouse hippocampal neurons. Immortalization of these neuronal cells has been achieved using a temperature-sensitive SV-40 T-antigen [161]. Glutamate is an important excitatory neurotransmitter in the central nervous system that is largely involved in regulating learning and memory at the level of dendritic spines. At high concentrations, however it is highly neurotoxic, excessive glutamate release is, for example, thought to be involved in the development of acute brain damage and chronic neurodegenerative diseases including PD and AD [162, 163]. The HT-22 cells applied in this study do not express ionotropic glutamate receptors [164] and are thus not susceptible to glutamate-induced rapid calcium influx and excitotoxicity. In this model system of glutamate toxicity, cell death is mediated via the competitive inhibition of xCT, a glutamate/cystine antiporter, which is required for the delivery of cystine into neuronal cells [165]. Inhibition of cystine uptake by high concentrations of extracellular glutamate leads to an imbalance in cellular cysteine homeostasis. Cysteine is required for the synthesis of the cellular antioxidant glutathione (GSH). After treatment of cells with glutamate, a gradual drop in glutathione levels is detected, followed by impaired activity of the glutathionperoxidase-4 (GPx4), excessive accumulation of ROS and cellular death [166]. Such excessive ROS formation occurs through an activation of 12/15 lipoxygenases, which under physiological conditions are negatively regulated by GPx4. Downstream pathways of ROS accumulation include on the one hand the activation of

the proapoptotic BH-3 only protein Bid and on the other hand a direct effect on mitochondria, accompanied with the release of the AIF [167, 168]. In HT-22 cells, glutamate induces a form of programmed cell death with characteristics of both apoptosis and necrosis [169]. This kind of cell death has been termed oxytosis [170]. No significant caspase activation is observed during the development of glutamate-induced cell death [167].

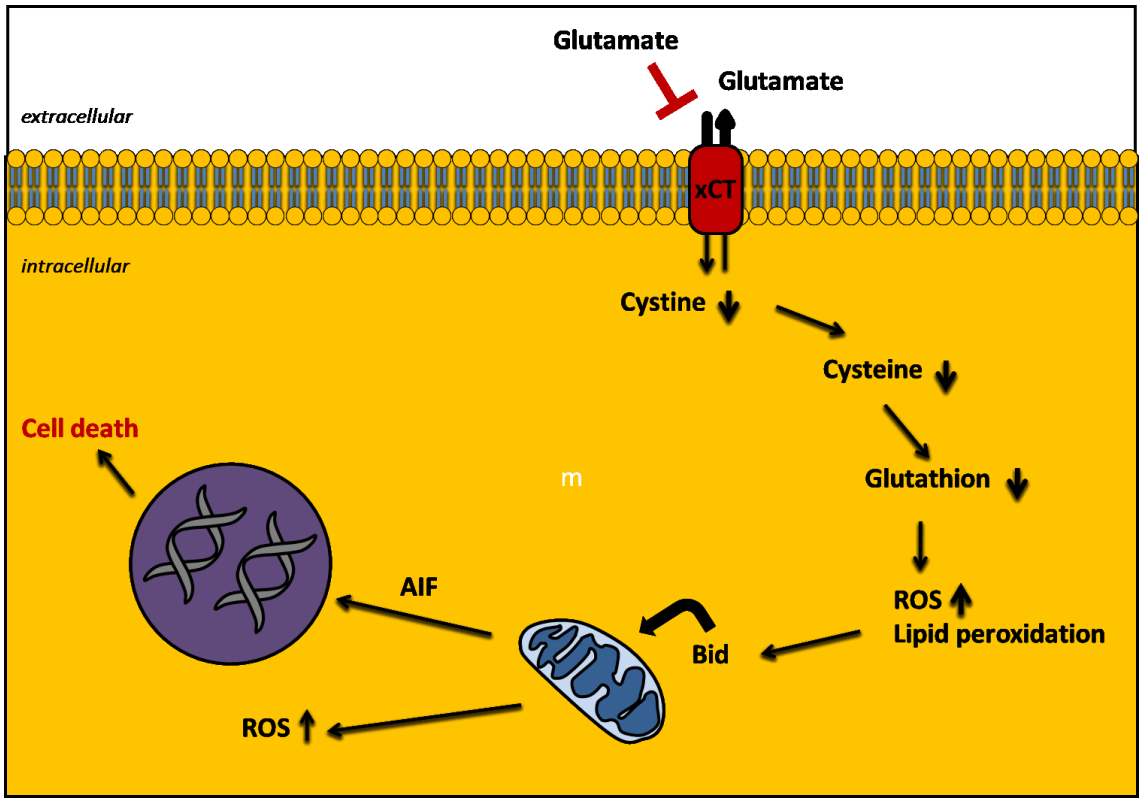

Figure 3. Model of glutamate-induced cell death in HT-22 cells. Exposure to millimolar concentrations of glutamate leads to an inhibition of the xCT transporter which results in a depletion of cystine and cysteine in the cell. This is followed by a decrease in glutathione levels and causes a fall in Gpx4 activity. In response to these events ROS formation is increased which leads to the translocation of Bid to the mitochondria where activated Bid induces mitochondrial fragmentation and mitochondrial membrane permeabilization. Consequently, the pro-apoptotic factor AIF translocates from mitochondria to the nucleus and cleaves DNA, thereby executing cell death [168].

1.3.2 Excitotoxicity in Primary Cortical Neurons

Primary cortical neurons were prepared from cortices of embryonic rats (E 16-18) (Sprague Dawley, Janvier) [171]. Besides the induction of oxidative stress in HT-22 cells, glutamate is able to induce receptor-initiated excitotoxicity in primary neurons [172]. Excitotoxicity is defined as cell death resulting from the toxic actions of excitatory amino acids. Because glutamate is the major excitatory neurotransmitter in the mammalian CNS, neuronal excitotoxicity usually refers to the injury and death of neurons arising from prolonged exposure to glutamate and the associated excessive influx of ions into the cell [173]. In physiological conditions, glutamate is the major neurotransmitter in primary perception and cognition in the brain, producing an excitatory response. However, many studies linked excitotoxicity to a variety of neuropathological conditions, suggesting that several neurodegenerative diseases may share excitotoxicity as a common pathogenic pathway that triggers neuronal demise [174, 175]. Thus, understanding the pathways involved in excitotoxicity is of critical importance for potential future treatment strategies in many neurodegenerative diseases.
The excitatory effects of glutamate are exerted via the activation of three major types of ionotropic receptors and several classes of metabotropic receptors linked to G- proteins. The major ionotropic receptors activated by glutamate are commonly referred to as the *N*-methyl-*D*-aspartic acid (NMDA), α-amino-3-hydroxy-5- methylisoxazole-4-propionate (AMPA) and kainic acid (KA) receptors. These ionotropic receptors are ligand-gated ion channels permeable to various cations, predominantly Na^+ and Ca^{2+} [176]. Transient Ca^{2+}-influxes triggered by these receptors lead to toxic disruption of the intracellular calcium homeostasis, increases in reactive oxygen species (ROS) and cell death. These detrimental downstream mechanisms include mitochondrial membrane depolarization, caspase activation, production of highly reactive oxygen (ROS) and nitrogen species (RNS), and cellular toxicity [177, 178].

1.4 Aims of the thesis

The aim of this thesis was to investigate the role of autophagy and apoptosis for neuronal resilience versus neuronal cell death in model systems of glutamate toxicity *in vitro*. Both mechanisms may play major roles in determining cellular survival or death. Accordingly, they participate in neural development, cellular homeostasis, and both, physiological as well as pathological processes [1].

Research on autophagy is a constantly increasing field of research in neuroscience, since autophagy is activated in neurodegenerative diseases and after acute brain injury, but proper functioning of this catabolic pathway is also required for the intracellular homeostasis of neuronal cells and thereby brain functions [25]. In the long term, autophagy is essential for neuronal function and survival, whereas impaired autophagy appears to be a contributing factor in chronic neurodegenerative diseases [26, 27]. There are, however, still many fundamental questions about the mechanisms governing autophagy in neuropathies. Therefore, **one aim of this study was to investigate the role of autophagy in neurons under stress**, in the model system of glutamate-induced oxytosis in neural HT-22 cells. Recently, it was shown that autophagy is activated by increased intracellular ROS levels [59]. Therefore, the objectives were to determine the effect of oxidative glutamate toxicity on autophagic flux and to investigate if oxytosis involves autophagy pathways of cell death. Moreover the neuroprotective effect of 3-Methyladenine (3-MA), a widely used autophagy inhibitor, was explored in the model systems of glutamate-induced oxytosis and excitotoxicity in neural HT-22 cells and primary cortical neurons, respectively.

The **contribution of apoptosis to neuronal survival** through intercellular signaling between dying cells and neurons was investigated using conditioned medium of neural progenitor cells and HT-22 cells. Stem cells as well as progenitor cells have been widely used in model systems of neurodegenerative diseases and acute brain injuries where transplantation of these cells into the brain improved neuronal survival and brain functions in experimental settings. However, most transplanted cells die after transplantation *in vivo* [148–150], and the exact mechanism of action of stem cell or progenitor cell transplantation still remains unknown. To investigate mechanisms of

intercellular signaling underlying the protective effects of transplanted stem cells, the transplantation conditions were mimicked *in vitro* by preparation of conditioned medium (CM) obtained from dying neuronal progenitor cells or HT-22 cells. This CM should contain similar cellular components as released during cell death of the progenitor cell transplants, and this CM should therefore also provide neuroprotective effects. Thus, the CM of apoptotic cells was applied in model systems of cell death *in vitro* for its potential to mediate neuroprotection. Further, the composition of the conditioned medium obtained from the dying cells was analysed for identifying the most potent protective components that may be applied as neuroprotectants *in vitro* and *in vivo* instead of the CM or the cellular transplants.

2 Materials and Methods

2.1 Cell culture

2.1.1 Cell culture materials

Sterile cell culture dishes and other materials were obtained from Greiner (Frickenhausen, Germany), Sarstedt (Nümbrecht, Germany), Ibidi (Munich, Germany), Whatman (Dassel, Germany), B. Braun (Melsungen, Germany), Millipore (Schwalbach, Germany). The xCELLigence system and E-plates were provided by Roche, Applied Science (Penzberg, Germany).

Table 1. Plastic ware

Plasticware	Company
T75 flasks	Greiner, Frickenhausen, Germany
T175 flasks	Greiner, Frickenhausen, Germany
6-well plates	Greiner, Frickenhausen, Germany
24-well plates	Greiner, Frickenhausen, Germany
96-well plates	Greiner, Frickenhausen, Germany
Ibidi slides 8-well plates	Ibidi, Munich, Germany
15 ml tubes	Sarstedt, Nümbrecht, Germany
50 ml tubes	Sarstedt, Nümbrecht, Germany
0.5, 1.5, 2 ml tubes	Sarstedt, Nümbrecht, Germany
Cellscraper	Sarstedt, Nümbrecht, Germany
0.22 µm sterile filter	Whatman, Dassel, Germany
5, 10 ml Injekt®	B. Braun, Melsungen, Germany
3, 10, 50 kDa Amicon® Ultra Centrifugal Filter Units	Millipore, Schwalbach, Germany

2.1.2 Cell lines

2.1.2.1 HT-22 cells

HT-22 cells are immortalized hippocampal neurons from mice. This cell line was obtained from Gerald Thiel with kind permission of David Schubert (Salk Institute, San Diego, California, USA). HT-22 cells were maintained in Dulbecco's modified Eagle medium (DMEM, Sigma-Aldrich, Taufkirchen, Germany) and cultured in a standard humidified incubator (Thermo Scientific, Dreieich, Germany) at 37°C and 5 % CO_2. DMEM was completed with 10% fetal calf serum, 100 U/ml penicillin, 100 µg/ml streptomycin and 2 mM glutamine (all Sigma-Aldrich). HT-22 cells were plated at different densities (table 2) on 6-, 24, 96-well plates (Greiner), E-plates (Roche Applied Science), or ibidi slides 8-well plates (Ibidi). Treatment of HT-22 cells started 24 h after plating the cells.

Table 2. HT-22 cells – cell densities

Cell culture format	Cell density (cells/well)
6-well plate	~ 180,000
24-well plate	~ 60,000
96-well plate	~ 8,000
Ibidi slide 8-well plates	~ 16,000
E-Plate	~ 10,000

2.1.2.2 Induction of cell death in HT-22 cells with glutamate

HT-22 cells were treated when cells reached 70-80 % confluency. For induction of cell death in HT-22 cells, glutamate was used at a final concentration ranging from of 3 to 7 mM. For the glutamate stock solution, D,L-glutamic acid monohydrate (Sigma-Aldrich) was dissolved in DMEM (Sigma-Aldrich) to a stock concentration of 1 M. The pH was adjusted to 7.2 with concentrated sodium hydroxide solution (NaOH). The stock solution was stored at -20°C. For the induction of cell death, the stock solution was diluted with DMEM to final concentrations directly before the treatment and added to the cells.

2.1.2.3 Neural progenitor cells

Neural progenitor cells (NPC) were kindly provided by Prof. Dr. Fred H. Gage (Salk Institute, La Jolla, USA) [179] and cultured in a standard humidified incubator at 37°C and 5 % CO_2. NPC were maintained in Dulbecco's modified Eagle's medium/nutrient mixture F-12 (1:1) medium (DMEM/ Ham's F12) (PAA Laboratories GmbH, Cölbe, Germany or Sigma-Aldrich). DMEM/ Ham's F12 was supplemented with 1% N2 100x (Invitrogen, Karlsruhe, Germany), 1% penicillin 10,000 U/ml/ streptomycin 10mg/ml (Invitrogen), 0.2 % epidermal growth factor (EGF) 10 µg/ml (Invitrogen), 0.2 % basic fibroblast growth factor (bFGF) 10 µg/ml (Invitrogen), 1 % L-Alanyl-L-glutamine 200 mM (Sigma-Aldrich) and 0.1 % heparine 5 mg/ml (Sigma-Aldrich). NPC growth medium was freshly prepared and used within 1-2 weeks since stability of the growth factors is limited. NPC were plated at different densities (table 3) on 24-, 96-well plates (Greiner) or E-plates (Roche Applied Science). Treatment of NPC cells started after 48 h in culture.

Table 3. NPC densities

Cell culture format	Cell density (cells/well)
24-well plate	~220,000
96-well plate	~ 40,000
E-Plate	~ 27,000- 40,000

2.1.2.4 Preparation of conditioned medium (CM) via starvation

Neural progenitor cells and mouse embryonic fibroblasts (MEF) were used for the production of conditioned medium. CM was prepared after EGF- and bFGF-deprivation or EBSS-treatment. Cells were grown in 75 cm^2 culture flasks until they reached ~70 % confluency or on 96-well plates at a density of 20,000 cells/well. Culture media was removed and cells were washed once with PBS and incubated with Earle's balanced salt solution (EBSS) (1x, Sigma-Aldrich) or DMEM/ Ham's F12 (Sigma-Aldrich), supplemented with 1 % N2-supplement (Invitrogen). NPC CM and MEF CM were collected 24 h after growth factor deprivation and stored at -80°C. For applications in HT-22 cells, conditioned medium was produced with EBSS. PCN were treated with

conditioned medium produced with DMEM/ Ham's F12 supplemented with 1% N2-supplement (Invitrogen). Before use, CM was centrifuged (1,000 rpm, 10 min) and filtered through a 0.22 μm membrane filter (Whatman) to remove dead cells and cell debris. For heat activation, CM was heated up to 90°C for at least 10 min. CM was used with 6 h pretreatment followed by glutamate treatment if not described otherwise.

2.1.2.5 Production of spermidine-conditioned medium (Sp CM)

HT-22 cells were used for the production of Sp CM. Conditioned medium was prepared after treatment with spermidine (1 μM, 10 μM and 25 μM). Cells were grown in 75 cm^2 culture flasks until they reached ~70 % confluency. Culture media was removed and cells were incubated with DMEM. DMEM was supplemented with 10% fetal calf serum, 100 U/ml penicillin, 100 μg/ml streptomycin, 2 mM glutamine and spermidine at different concentrations. Sp CM was collected 24 h after treatment stored at -80°C. Before use, CM was centrifuged (1,000 rpm, 10 min) and filtered through a 0.22 μm membrane filter (Whatman) to remove dead cells and cell debris.

Table 4. Phosphate buffered saline (PBS), pH 7.4

PBS, pH 7.4	
NaCl	9 g
Na_2HPO_4	0.527 g
KH_2PO_4	0.144 g
HCl (0.1 M)	q.s. for pH adjustment
Aqua demin.	add to a final volume of 1,000 ml

Table 5. Earl's balanced salt solution (EBSS 1x) containing phenol red

EBSS 1x, pH 7.4	
EBSS 10x	100 ml
$NaHCO_3$	2.2 g
Aqua demin.	add to a final volume of 1,000 ml
HCl (0.1 M)	q.s. for pH adjustment

2.1.3 Primary cultures

2.1.3.1 Primary cortical neurons

Primary neurons were prepared from cortices of embryonic rats (E 16- 18) (Janvier, Le Genest St. Isle, France). Briefly, cortices were removed and neurons were separated by mechanical dissociation after mild trypsinisation of the isolated cortical tissue. Isolated cortices were incubated in Hank's balanced salt solution (HBSS, diluted from 10x HBSS, Invitrogen) containing 1 mg/ml trypsin (Sigma-Aldrich) for 15 min at 37°C. The cortices were then washed with HBSS and mixed with HBSS containing 1 mg/ml trypsin inhibitor (Sigma-Aldrich) and the cell suspension was incubated for further 2 min at room temperature. Afterwards, the cortices were washed two times with HBSS, and triturated in MEM+ obtained from Eagle's minimum essential medium (Invitrogen) by addition of 1 mM HEPES (Biomol, Hamburg, Germany), 26 mM $NaHCO_3$, 40 mM glucose, 20 mM KCl, 1.2 mM L-glutamine (each Sigma-Aldrich), 1 mM sodium pyruvate (Biochrom, Berlin, Germany), 10% (v/v) fetal calf serum (FCS) (Invitrogen) and 10 mg/l gentamicin sulfate (Sigma-Aldrich). Cortical cells were plated at a density of $7x10^5$ cells/ cm^2 on polyethylenimine (Sigma-Aldrich) pre-coated 96-well plates (Greiner) or 35 mm culture dishes (Greiner). Primary neurons were cultured in Neurobasal medium (Invitrogen), supplemented with HEPES 5 mM (Sigma-Aldrich), glutamine 1.2 mM (PAA), B27 supplement 2% (v/v) (Invitrogen), and gentamicin 0,1 mg/ml (Sigma-Aldrich). After 48 h, neurons were treated with cytosine arabinofuranosid for another 48 h. All experimental treatments were performed in 6-8 day-old cultures.

2.1.3.2 Mouse embryonic fibroblasts

Mouse embryonic fibroblasts (MEF) were prepared from C57BL/6mice on gestation day 18. Small pieces of embryonic skin were dissected and put into MEF culture media, consisting of Dulbecco's modified Eagle's medium (DMEM) high glucose (4.5 g/L) and 110 mg/l sodium pyruvate (PAA) with FCS 15 % (PAA), penicillin 10.000 U/ml / streptomycin 10mg/ml 1 % (Invitrogen), L-Alanyl-L-glutamine 200 mM 2 % (PAA). MEF attached and began to divide in 1-3 days. Cells were split in the same procedure as HT-22 cells when reaching ~80 % confluency on the flask bottom. Passages 1-3 were used for further experiments and plated at a density of 20.000 cells/cm^2. All cell types were incubated at 37°C in a humidified atmosphere containing 5% CO_2.

2.2 Chemicals and Reagents

All chemicals and reagents were obtained from Sigma-Aldrich and Carl Roth (Karlsruhe, Germany), if not described otherwise.

Buffers and solutions were prepared using demineralized, ultrapure water, prepared with the SG Ultra Clear UV plus Reinstwassersystem (VWR, Darmstadt, Germany). Steam autoclaving (steam autoclave, Systec V-40, Systec GmbH, Wettenberg, Germany) was used to further sterilize ultrapure, demineralized water for the use in cell culture preparations. All media and solutions that were used for cell culture experiments were sterilized by filtration using 0.22 µm filter sets (Sarstedt).

2.2.1 Pharmacological inhibitors or activators

For inhibition of caspases, the cell-permeable, irreversible, broad-spectrum caspase inhibitor Qvd-OPh (Calbiochem, Darmstadt, Germany) was used. The solution dissolved in DMSO (10 mM) was used at a final concentration of 20-40 µM.

Brain-derived neurotrophic factor (BDNF, R&D Systems GmbH, Wiesbaden, Germany) was dissolved in DMSO at a stock concentration of 10 µg/ml and stored at -20°C. For treatment in primary neurons, a final concentration of 10 ng/ml was used.

For inhibition of phosphoinositide-3-kinase (PI_3K) the cell-permeable, reversible inhibitor LY294002 (2-(4-morpholinyl)-8-phenyl-4H-1-benzopyran-4-one, Sigma-Aldrich) was used. LY294002 was dissolved in DMSO resulting in a 1 mM stock solution. For HT-22 cell treatment a final concentration of 10 µM was applied. Cells

were pretreated with the inhibitor for 1 h followed by a pretreatment containing CM and the inhibitor together. Afterwards, cells were damaged by glutamate.

3-MA (Sigma-Aldrich), a widely used inhibitor of autophagy, was used at a final concentration of 5 mM. The stock solution (100 mM) was stored at -20°C. Before use, the stock solution was heated (60°C) until the solution was clear.

The selective Bid inhibitor BI-6C9 (Sigma-Aldrich) was dissolved in DMSO at a concentration of 10 mM. For experiments in HT-22 cells a final concentration of 10 µM was used.

For inhibition of the activation of mitogen-activated protein kinase kinase (MAPKK) the specific inhibitor PD 98059 (Sigma-Aldrich) was used. PD 98059 was dissolved in DMSO resulting in a 10 mM stock solution. For HT-22 cell treatment a final concentration of 50 µM was applied. Cells were pretreated with the inhibitor for 1 h followed by a treatment containing 3-MA and the inhibitor together.

Blebbistatin (Sigma-Aldrich) is a cell permeable, specific inhibitor of non-muscle myosin II. The substance was dissolved in DMSO (50 mM). Blebbistatin was used at concentrations ranging from 5 µM-100 µM.

Y-27632 (Sigma-Aldrich) is a highly potent, cell-permeable, selective ROCK (Rho-associated coiled coil forming protein serine/threonine kinase) inhibitor. Y-27632 was dissolved in DMSO (10 mM) and used at final concentrations ranging from 1 µM-50 µM.

2.3 Cell viability assays

2.3.1 MTT-assay

The MTT (3-[4, 5-Dimethylthiazol-2-yl]-2, 5-diphenyltetrazolium bromide) (Sigma-Aldrich) -assay, was used to determine cell viability in NPC, MEF, HT-22 cells and primary neurons. The MTT assay is a colorimetric assay for measuring the activity of enzymes that reduce MTT to a formazan by either a lysosomal/endosomal compartment or mitochondria [180], resulting in a purple color. After indicated time points, when the typical rounded formation of cells indicated cell death, the MTT reagent was added to the media at final concentrations of 0.25-0.5 mg/ml followed by 1 h incubation at 37°C. The reaction was terminated by removing the media from the cells and freezing the plate at -80°C for at least 1 h. Absorbance was determined after solving the formazan

crystals in dimethyl sulfoxide (DMSO, Sigma-Aldrich) at 570 nm with the FLUOstar Optima reader (BMG Labtech, Offenbach, Germany). The background was detected at 630 nm and substracted accordingly. Cell viability was expressed as absorption level relative to controls, which were set to viability values of 100%.

2.3.2 The xCELLigence system

The xCELLigence system monitors cellular events in real time by measuring electrical impedance across interdigitated gold micro-electrodes integrated on the bottom of tissue culture E-plates. Usually, cells have a high electrical resistance and, thus, the more cells cover the electrodes, the larger are the increases in impedance. Following this, the system is able to detect changes in cell number (proliferating cells), altered attachment properties (cellular death), and especially the kinetics of these processes. The results are depicted as a curve indicating the cell index as a function of time [181]. For using this system 8,000 HT-22 cells or 30,000-40,000 NPC per well were seeded into 96-well E-plates. Prior to seeding the cells, background impedance was determined using 100-200 µl of cell culture medium or EBSS. Next, cell suspension was added to a total of 100 µl/well for HT-22 neurons and 200 µl/well for NPC. Treatment of cells was initiated when the cell index exceeded a value of about one. Cell index values were recorded using RTCA Software 1.2 (Roche Diagnostics). After concluding each experiment, E-plates were recycled by removing media, washing the plates twice with demineralized water and adding standard Trypsin/EDTA (TE) for 15-20 min. Afterwards 1x TE was removed, the plates were washed a further 3 times and irradiated with UV light for 30 min to reassure sterility.

2.3.3 FACS-Annexin V-FITC/ PI Apoptosis-Necrosis measurement

Annexin V-FITC/ propidiumiodide (PI) staining identifies cells in early apoptosis by detecting externalized phosphatidylserine, and PI identifies cells that have lost plasma membrane integrity (i.e., necrotic or late apoptotic cells). For annexin V-FITC/ propidium iodide-staining, HT-22 cells were cultured in 24-well plates and treated with glutamate. Cells were harvested 15 h after the onset of the glutamate, washed and resuspended in binding buffer (PromoKine, Heidelberg, Germany). Then 2.5 µl of each

propidium iodide and annexin-V-FITC solutions (PromoKine Annexin V-FITC Detection Kit, PromoKine) were added respectively, and incubated for 5 min at room temperature in the dark. Apoptotic and necrotic cells were detected using a FACScan (Guava Easy Cyte, Merck Milipore, Darmstadt, Germany). Annexin-V and propidiumiodide fluorescence were excited at a wavelength of 488 nm. Emissions were detected at 530±40 nm for annexin-V and at 680±30 nm for propidiumiodide. Data were collected from at least 10,000 cells. Measurements are representative of at least three independent experiments.

2.3.4 DAPI-Counting

For quantification of pyknotic nuclei in primary cortical neurons exposed to trophic factor withdrawal or glutamate, cells were fixed with PFA 4% after 16-24 h of treatment and incubated with the fluorescent DNA binding dye DAPI (4', 6-diamidino-2-phenylindole dihydrochloride (DAPI), 1 µg/ml, Sigma-Aldrich). The percentage of pyknotic nuclei was quantified from pictures obtained with a fluorescence microscope (DMI 6000 B, Leica, Wetzlar, Germany) connected to a CCD camera (DFC 360 FX, Leica, Wetzlar, Germany). Neurons with condensed and fragmented nuclei were considered apoptotic. About 1000 cells per treatment condition were counted, and counts were made in five separate cultures without knowledge of the treatment history.

2.4 Analysis of cellular morphology

To analyze cellular morphology of HT-22 cells or NPC, light microscopy was performed using the Axiovert 100 microscope (Zeiss, Jena, Germany). Pictures were taken using the Infinity 2 camera running Infinity Capture Software (Lumenera, Ottawa, Canada).

2.5 Visualization and characterization of mitochondria

For analysis of mitochondrial morphology, cells were stained with MitoTracker Deep Red (Invitrogen). HT-22 cells were seeded onto Ibidi slides at least 24 h before the treatment (16,000 cells/well). MitoTracker DeepRed was dissolved in DMSO at a final

stock concentration of 50 μM and kept protected from light. For cell treatment MitoTracker reagent was diluted 1:250 in culture medium (final working concentration 200 nM) together with DAPI (1 μg/ml) for counterstaining the nuclei. Staining solution was added to the cells for 20 min before the treatment. At indicated time points, cells were fixed with paraformaldehyde 4 % (PFA, Sigma-Aldrich). Nuclei were counterstained with DAPI (1 μg/ml). Evaluation and classification of mitochondrial morphology was performed as described before [182]. Mitochondria were counted manually and categorized in 3 groups, depending on the degree of fragmentation: Category I represented cells with intact tubular network with elongated mitochondria that are found in cells under control conditions. Category II and III indicated an increasing number of fragmented mitochondria. Mitochondrial fragmentation was accompanied by an apoptotic phenotype, showing nuclear condensation and the peri-nuclear arrangement of the mitochondrial fragments. At least 500 cells per condition were counted blind to treatment conditions in at least three independent experiments. Images for counting were acquired using a fluorescence microscope (DMI 6000B, Leica) equipped with LAS AF software (Leica). Pictures were taken using confocal laser scanning microscopy (Leica, TCS SP 5). Emission was measured at 665nm with a LP650 filter (Leica).

2.6 ATP-assay

HT-22 cells were seeded in white 96-well plates (Greiner). Twenty-four h after plating, cells were cotreated with glutamate (5 mM) and 3-MA (5 mM). ATP levels were detected 14 h after treatment by detection of luminescence using the ViaLight MDA Plus-Kit (Lonza, Verviers, Belgium). The kit is based upon the bioluminescent measurement of ATP that is present in all metabolically active cells. The bioluminescent method utilizes an enzyme, luciferase, which catalyses the formation of light from ATP and luciferin according to the following reaction:

Cells were treated first with a 'nucleotide releasing reagent', afterwards 'ATP monitoring reagent' was injected into each well. Luminescence was detected with the FLUOstar Optima reader (BMG Labtech). The emitted light intensity is linearly related to the ATP concentration. The values are given as relative values in % to control.

2.7 Detection of lipid peroxides

For detection of cellular lipid peroxidation, cells were loaded with 2 mM BODIPY 581/591 C11 (Invitrogen) in regular medium for 60 min. Fourteen h after glutamate treatment, attached cells and supernatants were collected, washed and resuspended in PBS. Until the measurement cells were kept on ice. Flow cytometry was performed using the Guava Easy Cyte (Merck Milipore) system, including Guava Clean 1.3 software (Merck Milipore) for data analysis. A 488 nm UV line argon laser was used for excitation measurements. BODIPY emission was recorded at 530 nm and 585 nm. Data were collected from at least 10,000 cells. Measurements are representative of at least three independent experiments.

2.8 Detection of mitochondrial membrane potential

For detection of changes of MMP ($\Delta\Psi m$), the MitoPTTM TMRE kit (Immunochemistry Technologies, Hamburg, Germany) was used. HT-22 cells were incubated for 20 min at 37° C with tetramethylrhodamin ethyl ester (TMRE) after glutamate treatment. As a positive control for a complete loss of ($\Delta\Psi m$), FCCP (50 µM) protonophore was applied on intact HT-22 cells. Cells were collected, washed with PBS and resuspended in assay buffer. Flow cytometry was performed using the Guava Easy Cyte system (Merck Milipore). Emission was measured at 680 nm. Data were collected from at least 10,000 cells from at least three independent experiments.

2.9 Measurement of cellular oxygen consumption rate (OCR)

OCR measurements were performed as previously described with minor modifications [183] with the help of Dr. Amalia Dolga. HT-22 cells were seeded in a XF 96-well microplate (Seahorse Bioscience, Copenhagen, Denmark) at a density of 10,000 cells/ well in 4.5 g/L glucose containing growth medium and incubated at 37°C and 5 % CO_2

for about 20 h. Before each measurement, growth medium was washed off and replaced with 180 ml of assay medium (with 4.5 g/L glucose, 2 mM glutamine, 1 mM pyruvate, pH 7.35) and then incubated for 60 min at 37°C. Three baseline measurements were recorded before the addition of compounds started. Oligomycin was injected in Port A (20 µl) at a final concentration of 3 µM. Oligomycin was used to inhibit ATP synthase and to determine the leak respiration. Subsequently, carbonylcyanide-4-(trifluoromethoxy) -phenylhydrazone (FCCP) was injected in port B (22.5 µl) at a concentration of 0.4 µM to uncouple respiration and to determine mitochondrial functional capacity. Respiration was finally inhibited with Rotenone/ Antimycin A (Port C, 1 µM). Three measurements were performed after the addition of each compound (4 min mixing followed by 3 min measuring).

2.10 Knockdown of protein expression by siRNA

For siRNA transfections, the cationic lipid formulation Lipofectamine RNAiMax (Invitrogen) was used. Transfections were performed in 24- or 96-well plates as reverse transfections. For each well, 1.2 µl (24-well plate) or 0.24 µl (96-well) Lipofectamine RNAiMax were mixed with siRNA and filled up to 100 µl (24-well pate) or 20 µl (96-well plate) with Optimem I (Invitrogen). The mixture was incubated for 20 min at room temperature. Afterwards 500 µl (24-well plate) or 100 µl (96-well plate) of an antibiotic free cell suspension (18,000 cells/cm^2) was added. Treatment of cells started 48 h after transfection. Gene silencing was verified by Western Blot analysis. Small interfering RNA specific for Beclin-1 was purchased from Sigma-Aldrich, siRNA specific for Atg5 and siRNA specific for class III PI_3K were purchased from Thermo Scientific bio (Schwerte, Germany) and siRNA targeting MAP LC3β was purchased from Santa Cruz (Heidelberg, Germany). Non targeting siRNA was purchased from Eurofins MWG Operon (Ebersberg, Germany). The following target sequences were used: siGenome mouse PI_3K class III siRNA 5'-AUAGAUAGCUCCCAAAUUA-3', non-targeting siRNA 5'-UAAUGU-AUUG-GAACGCAUA-3', Beclin-1 siRNA duplex of 5'-CUGAGAAU-GA-AU-GUCAGAA-3' and 5'-UU-CUGACAUUCAUUCUCAG-3', Atg5 siRNA 5'CCAAUU-GGU-UUA-CUAU-UUG-3' and MAP LC3β siRNA (Santa Cruz, sc-43391).

2.11 Protein analysis

2.11.1 Buffers for SDS PAGE and Western Blot analysis

The separation gel	**12.5 %**
1.5 M Tris HCl solution pH 8.8	2.5 ml
Acrylamide/bisacrylamide (37, 5:1) 30 %	4.0 ml
Sodiumdodecylsulfate solution 10 %	0.1 ml
Ammoniumpersulfate solution 10 %	0.05 ml
Tetramethylethylenediamine (TEMED)	0.01 ml
Aqua demin.	ad 10 ml

The stacking gel, 3.5 %	
0.5 M Tris HCl solution pH 6.8	2.5 ml
Acrylamid/bisacrylamide (37.5 : 1) 30 %	1.2 ml
Sodiumdodecylsulfate solution 10 %	0.1 ml
Ammoniumpersulfate solution 10 %	0.05 ml
TEMED	0.01 ml
Aqua demin.	ad 10 ml

1 x Electrophoresis buffer	
Tris base	3 g
Glycine	14.4 g
Sodiumdodecylsulfate (SDS)	1 g
Aqua demin.	ad 1000 ml

5x Sample buffer Western Blot

1M Tris-HCl pH 6.8	3.75 ml
Glycerol	7.5 ml
D,L-Dithiothreitol (DTT)	1.16 g
SDS	1.5 g
β-Mercaptoethanol	5 ml
Bromophenol blue sodium salt	0.0015 g
Aqua demin.	ad 15 ml

1x Transfer buffer, pH 8.3

Tris base	3 g
Glycine	14.4 g
Methanol	100ml
HCl 0.1 M	q.s
Aqua demin.	ad 1000 ml

1x TBS, pH 7.5

Tris base	2.4 g
NaCl	29.2 g
HCl 0.1 M	q.s.
Aqua demin.	ad 1000 ml

1x TBST, pH 7.5

Tween 20	500 µl
1x TBS	ad 1000 ml

Stripping buffer, pH 2.2

Glycine	15 g
SDS	1 g
Tween 20	10 ml
HCl conc.	q.s.
Aqua demin.	ad 1,000 ml

1x PBS pH 7.4

NaCl	8 g
KCl	0.2g
Disodiumhydrogenphosphate (Na_2HPO_4)	1.15g
Potassiumdihydrogenphosphate (KH_2PO_4)	0.2
Aqua demin.	ad 1000 ml

1x Blocking buffer

Skim milk powder	25 g
1x TBST	ad 500 ml

2.11.2 Protein preparation and determination

For obtaining total cell protein extracts, cells were seeded into 24-well or 6-well cell culture plates (Greiner). After indicated time points, cells were washed with PBS, detached with a cell scraper and exposed to lysis buffer containing mannitol 0.25 M, tris base 0.05 M, EDTA 1 M, EGTA 1 M, DTT 1 mM and triton-X 1 % (all Sigma-Aldrich). The lysis buffer was supplemented with cOmplete ULTRA Mini, EDTA-free, EASYpack, Protease Inhibitor Cocktail (Roche) (1 tablet per 10 ml) and PhosSTOP, Phosphatase Inhibitor Cocktail (1 tablet per 10 ml). To remove insoluble membrane fragments, extracts were centrifuged at 13,000 g for 15-30 min at 4°C. Extracts were

frozen at -80°C until further use. Protein concentration was determined in the supernatant using a BCA (bicinchoninic acid) protein kit (Thermo Fisher Scientific, Bonn, Germany). The BCA protein assay combines the reduction of Cu^{2+} to Cu^{1+} by protein in an alkaline medium with the detection of Cu^{1+} by bicinchoninic acid. The amount of Cu^{2+} reduced is proportional to the amount of protein present in the solution. The first step is the chelation of copper with protein in an alkaline environment to form a light blue complex (Biuret reaction). In the second step, bicinchoninic acid reacts with the reduced cuprous cation that was formed in step one, which leads to a formation of a purple-colored chelate complex. Responsible for this color reaction of the BCA are the macromolecular structures of the protein, the amount of peptides and the four amino acids cysteine, cystine, tryptophan and tyrosine. The BCA/copper complex exhibits a strong linear absorbance at 562 nm with increasing protein concentrations [184]. A standard curve containing 0-200 µg bovine serum albumin (BSA) (Perbio Science, Bonn, Germany) per 100 µl PBS 1x was prepared. Then, 200 µl of a 1:50 mixture of reagent B: reagent A (Perbio Science) was prepared and transferred to each tube. Immediately, 5 µl of standards or samples were added. Next, samples were incubated for 30 min at 60 °C, followed by pipetting 100 µl of each sample into a 96-well plate (Sarstedt). Absorption at 590 nm was determined using a microplate reader (Fluostar OPTIMA, BMG Labtech). Protein amounts of the test samples were calculated from the standard curve via linear equation.

2.11.3 Gel electrophoresis and Western Blotting

Sodiumdodecylsulfate polyacrylamide gel electrophoresis (SDS-PAGE) has been used to separate proteins according to their different molecular mass. Gels were prepared using Bio-Rad gel casting stand and casting frames (Bio-Rad, Munich, Germany). Gels were prepared using a polyacylamide separation gel with a concentration of 12.5 % and a stacking gel with 3.5 %. The specific buffers used for the generation of gels and subsequent electrophoresis are provided under 2.11.1. Prior to electrophoresis, samples were prepared using 25-40 µg of raw protein extract and adding 5 x SDS sample buffer. Samples were heated at 90°C for 10 min and loaded onto the gel after reaching room temperature. For comparative evaluation of molecular mass, 5 µl of PageRuler TM Plus Prestained Ladder (Fermentas, St. Leon-Rot, Germany) were loaded next to the

samples. Electrophoresis was performed initially at 60 V for about 30 min to allow for sample collection and increased later to 125 V. After electrophoretic separation, proteins were transferred on a polyvinylidene fluoride membrane (PVDF, Bio-Rad) according to the recommendations by Bio-Rad at 15 V for about 60-120 min. PVDF membranes were first activated in methanol and then incubated for 10 min in 1 x transfer buffer before blotting. Meanwhile, Whatman blotting paper and the acrylamide gel were incubated for 10 min in transfer buffer. Blotting was carried out by stacking one layer of Whatman paper on top of the anodic plate, followed by the PVDF membrane, the acrylamide gel as the third, and another final layer of Whatman paper on top. Blotting was carried out in a Trans-Blot SD semi-dry transfer cell (Bio-Rad) using extra thick Whatman filter paper (Bio-Rad) and 1x transfer buffer. After blotting, the PVDF membranes were transferred directly into blocking buffer to avoid unspecific binding and incubated for 1 h at room temperature.

Afterwards blots were incubated with the primary antibodies (diluted in blocking buffer) overnight at 4°C. The following primary antibodies were used for this thesis: anti LC3B, anti Beclin-1, anti p62, anti Atg5, anti class III PI_3K, anti cleaved caspase-3, anti PARP, anti Akt, anti phospho-Akt, anti Erk1/2, anti phospho-Erk 1/2, anti AMPKα, anti phospho AMPKα (all Cell signaling, Danvers, USA, 1:1000), anti actin (1:100,000, MP Biomedicals) anti α-tubulin (1:10,000, Sigma-Aldrich), peroxidase-conjugated anti-rabbit or anti mouse IgG (Vector Laboratories, Peterborough, UK, 1:2500). Actin or Tubulin was used as a loading control. The next day, membranes were washed three times with TBST for 5 min and incubated with the appropriate HRP-conjugated secondary antibody (diluted in blocking buffer, 1:2500, Vector Laboratories) for 1 h at room temperature. After washing 3 times with TBST for 15 min each, membranes were incubated with chemiluminescent substrate solution HRP-Juice (PJK GmbH, Kleinblittersdorf, Germany). Chemiluminescence signals were recorded using x-ray films (Thermo Scientific) or by densitometric analysis using the semi-automated Chemidoc-XRS Imaging System (Bio-Rad). Quantification of Western Blots was performed by using Quantity One analysis software (Bio-Rad). Western Blots of protein extracts of PCN were performed with the help of Dr. Amalia Dolga.

2.12 Immunocytochemistry

After indicated time points, NPC or HT-22 cells (plated in Ibidi 8-well plates) were washed once with warm PBS and then incubated with 4 % PFA solution for 30 min to fixate the cells, followed by a washing step with cold PBS. For permeabilisation cells were treated with 0.4 % Triton-X-100 /PBS for 5 min at room temperature. Again a washing step with PBS was performed. Cells were then incubated in blocking solution (3 % goat serum in PBS, PAA) for 30 min and then exposed to an anti-LC3B antibody (1:150 in blocking solution) overnight at 4° C. Negative control cells were not incubated with the anti-LC3B antibody. The next day and after two h remaining at room temperature, cells were washed three times with PBS and incubated with a Dylight antibody (goat Dylight anti rabbit 488, Vector Laboratories, 1:200) for 1.5 h at room temperature. After washing three times with PBS cells were ready for microscopic analysis. The specificity of LC3B immunoreactivity was controlled by omission of the primary antibody. Nuclei were counterstained with DAPI. Fluorescence images were obtained using a DMI6000 B inverted microscope (Leica, Germany) and analysed using LAS AF Software (Leica Application Suite, Advanced Fluorescence 2.2.0, Leica Microsystems).

2.13 Statistical analysis

The experiments were each performed at least three times. All data points are given as means ± standard deviation (S.D.). Statistical comparisons between groups were performed with ANOVA (analysis of variance), followed by Scheffé's or Duncan's test as indicated. A p value of <0.05 was considered to indicate significant differences of the compared mean values. Calculations were performed with Winstat standard statistical software package (R. Fitch Software, Bad Krozingen, Germany).

3 Results

3.1 3-Methyladenine mediates neuroprotection independent of autophagy inhibition

Oxidative stress has been proposed as a major underlying mechanism of progressive neurodegeneration in chronic neurodegenerative diseases, such as AD or PD. Oxidative stress has also been linked to activation of autophagy, a pathway by which cytoplasmic components are delivered to the lysosome for degradation. However, the impact of autophagy on neural cell viability in paradigms of oxidative stress has not been elucidated.

Therefore, the objectives were to determine the effect of the glutamate challenge on autophagic flux and to investigate if glutamate-induced toxicity involved autophagic cell death. Moreover the neuroprotective effect of 3-Methyladenine (3-MA), a widely used autophagy inhibitor, was explored in model systems of glutamate-induced oxytosis and excitotoxicity in neural HT-22 cells and primary cortical neurons, respectively.

3.1.1 Glutamate treatment induces autophagy in HT-22 cells and PCN

Accumulating evidence demonstrates that glutamate-mediated neuronal death involves increased formation of ROS and also pathological activation of autophagic pathways. Therefore, the question was addressed, whether there is a link between oxidative stress and autophagy in the model system of neuronal oxytosis. To this end, first the expression levels of LC3 proteins as a major hallmark of autophagic pathways were evaluated. The analysis of LC3 in HT-22 cells treated with glutamate (Glu, 5 mM) and chloroquine (CQ, 10 μM), a lysosomal inhibitor [185, 186], showed that glutamate increased LC3-I to LC3-II conversion (Fig. 4 A). Further, CQ treatment led to a strong accumulation of LC3-II in both, controls and glutamate treated cells. These results were further confirmed with immunocytochemistry studies. As shown in Fig. 4 B, the formation of punctuated LC3 staining indicated the conversion of LC3 (form I to II) and its recruitment into autophagosomes. The punctuated LC3 staining increased in HT-22 cells exposed to 16 h of glutamate in comparison to control cells. CQ treatment led to a stronger increase of punctuated LC3 staining in control and in glutamate treated cells. In order to evaluate effects of CQ on cell viability after the glutamate treatment, the MTT

assay was performed 16 h after the onset of the treatment. Fig. 5 demonstrated that CQ had no effect on cell viability in glutamate-treated cells. Together, these results indicated an increase of autophagic flux after glutamate exposure in HT-22 cells.

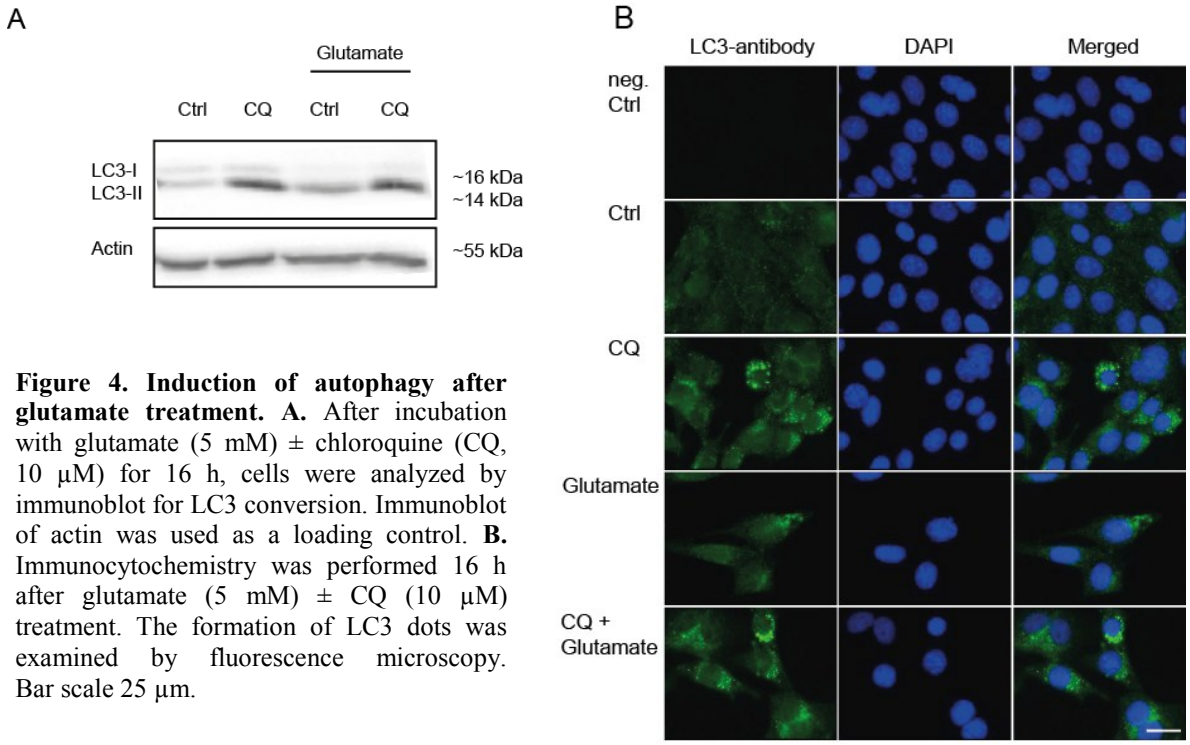

Figure 4. Induction of autophagy after glutamate treatment. A. After incubation with glutamate (5 mM) ± chloroquine (CQ, 10 µM) for 16 h, cells were analyzed by immunoblot for LC3 conversion. Immunoblot of actin was used as a loading control. **B.** Immunocytochemistry was performed 16 h after glutamate (5 mM) ± CQ (10 µM) treatment. The formation of LC3 dots was examined by fluorescence microscopy. Bar scale 25 µm.

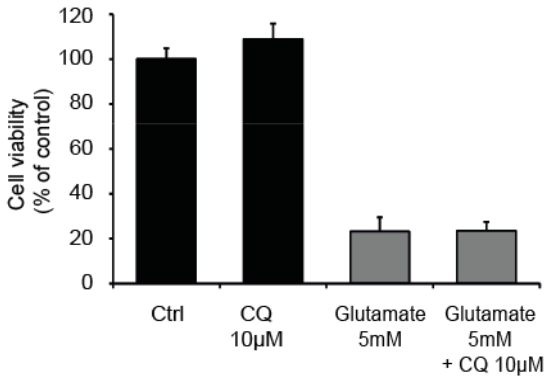

Figure 5. Chloroquine does not affect cell viability after glutamate treatment. HT-22 cells were treated with glutamate (5 mM) ± CQ (10 µM). Cell viability was determined using MTT assay 16 h after treatment.

In PCN, Western Blot analysis of total LC3 I and LC3-II revealed that glutamate treatment (10 µM, 20 µM) enhanced the protein levels of LC3-II in comparison to control cells (Fig. 6 A). The calculation of the LC3-II/LC3-I ratio showed a dose-dependent increase after glutamate treatment, which further indicated that glutamate-induced excitotoxicity was also able to induce autophagic activity (Fig. 6 B).

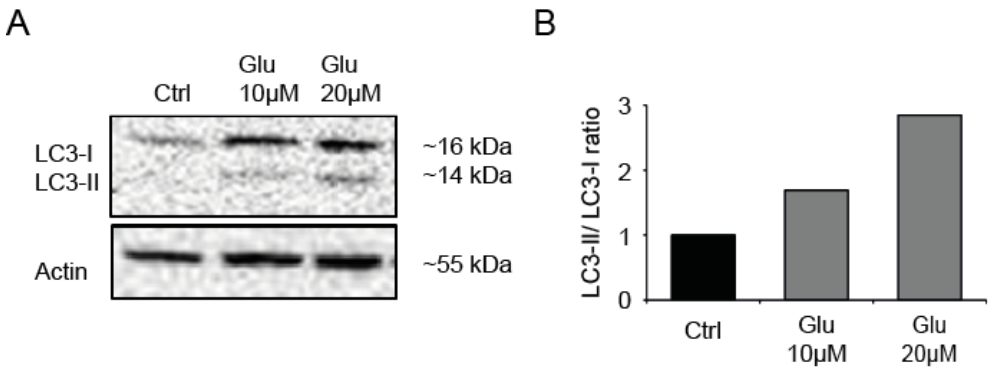

Figure 6. Excitotoxicity is accompanied by activation of autophagy in primary neurons. A. Western Blot analysis of LC3 protein levels 24 h after the onset of glutamate (Glu) exposure in primary cortical neurons (PCN). Actin immunoblot was used as a loading control. **B.** LC3-II/LC3-I ratio calculation revealed an increase of autophagic activity in PCN challenged with glutamate (Glu).

3.1.2 3-MA protects HT-22 cells against glutamate- induced neurotoxicity

To further investigate the role of autophagy in the model system of glutamate-induced cell death, 3-MA was applied as a widely used inhibitor of autophagy [187]. HT-22 cells were simultaneously treated with glutamate (5 mM) and 3-MA (5 mM) for 16 h. Interestingly, 3-MA did not decrease the conversion of LC3-I to LC3-II, neither in controls nor in glutamate-treated cells (Fig. 7). Additional treatment with CQ showed an increase of LC3-II after 3-MA and glutamate exposure in comparison to control cells, indicating that 3-MA even induced autophagic activity. Levels of total p62 were also degraded after 3-MA ± glutamate treatment, which was further confirming the ability of 3-MA to increase the autophagic flux.

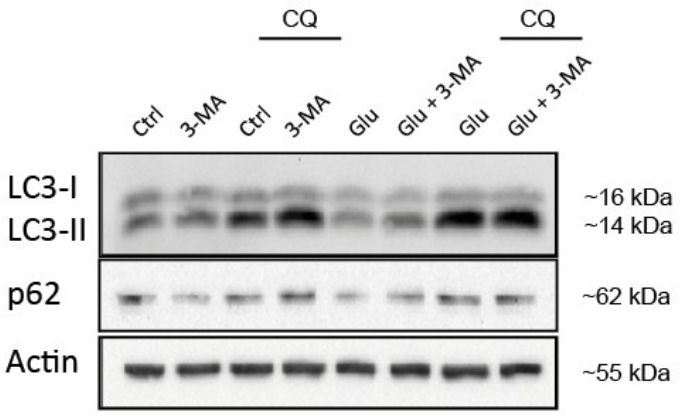

Figure 7. 3-MA increases molecular hallmarks of autophagy in HT-22 cells. Immunoblot analysis was performed 16 h after simultaneous treatment with 3-MA (5 mM) and glutamate (Glu, 5 mM). LC3-II protein levels conversion and p62 levels were analyzed to monitor autophagy. Actin immunoblot was used as a loading control.

Cell viability measurements performed using MTT assay showed that 3-MA significantly reduced glutamate toxicity (Fig. 8 A). Post treatment with 3-MA at 1, 3 and 6 h after glutamate exposure was also determined using the MTT assay. 3-MA was able to protect cells from glutamate-induced cell death when applied even 3 h after the induction of oxidative stress (Fig. 8 B).

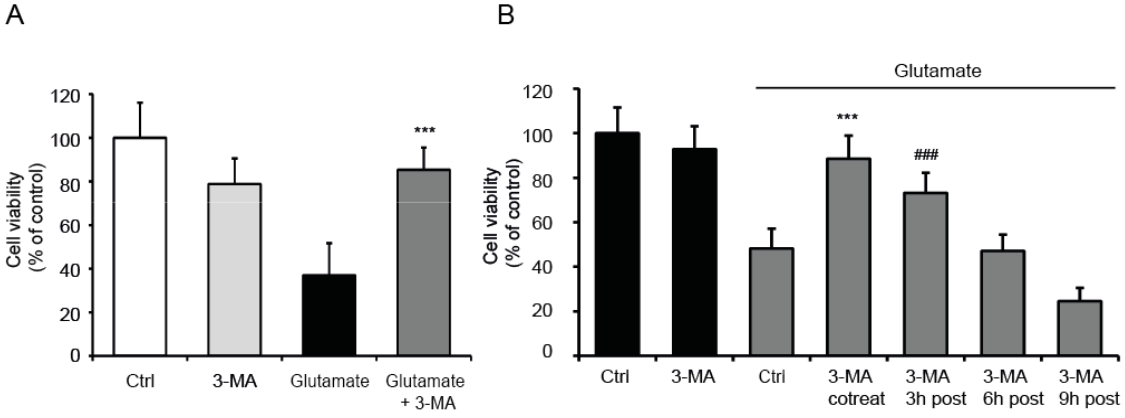

Figure 8. 3-MA significantly improves cell survival following glutamate exposure. A. 3-MA (5 mM) was added simultaneously with glutamate (5 mM) and the cell viability was measured after 16 h of glutamate exposure using the MTT assay (n=8; ***p<0.001, compared to glutamate treated control, ANOVA, Scheffé test). **B.** Post-treatment with 3-MA in the model system of glutamate toxicity. Bar graph shows 3-MA post-treatment of HT-22 cells at 1, 3 and 6 h after glutamate exposure. Protective effects of 3-MA post-treatment were assessed after 16 h of glutamate exposure using the MTT assay (n=8; ***p<0.001, compared to glutamate treated control, ###p<0.001 compared to glutamate treated control, ANOVA, Scheffé test).

Furthermore, morphological analysis showed that 3-MA prevented HT-22 cell death induced by glutamate (Fig. 9 A). 3-MA also significantly reduced the number of Annexin V/ PI- positive cells after the glutamate treatment (Fig. 9 B, C). These findings were supported by real time measurements with the xCELLigence system showing that 3-MA prevented the glutamate-induced decrease of the cell index (Fig. 9 D). Taken together, these results demonstrated that 3-MA mediated neuroprotection against glutamate-induced oxidative stress and 3-MA exerted this protective effect likely independently of autophagy inhibition.

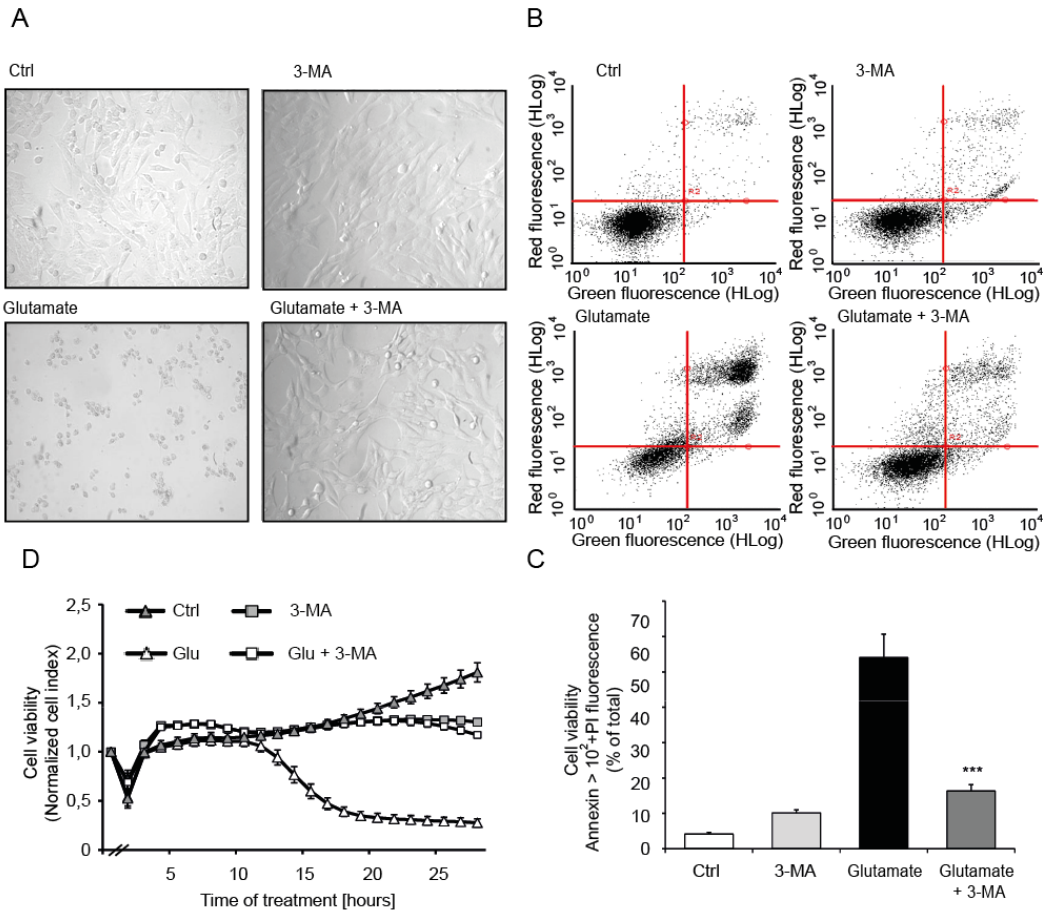

Figure 9. Neuroprotective effects of 3-MA against glutamate cytotoxicity. A. 3-MA preserved cellular morphology following glutamate (5 mM) treatment. **B/C.** Representative diagrams of Annexin V-FITC/ Propidiumiodide staining/ flow cytometry in 3-MA (5 mM) and glutamate (5 mM) treated cells. 3-MA was an effective inhibitor of cell death. The values of the upper right (late apoptosis and necrosis) and the lower right quadrant (early apoptosis) were combined and statistically analyzed (n=6; ***p<0.001, compared to glutamate treated control, ANOVA, Scheffé test). **D.** xCELLigence real-time measurement of HT-22 cells treated with glutamate (5 mM) and 3-MA (5 mM) showed a neuroprotective effect (n=6). Cell viability was monitored for 30h.

In PCN, 3-MA was also able to protect against glutamate-induced neurotoxicity, suggesting a similar pathway for neuronal survival like in HT-22 neuronal cells (Fig. 10).

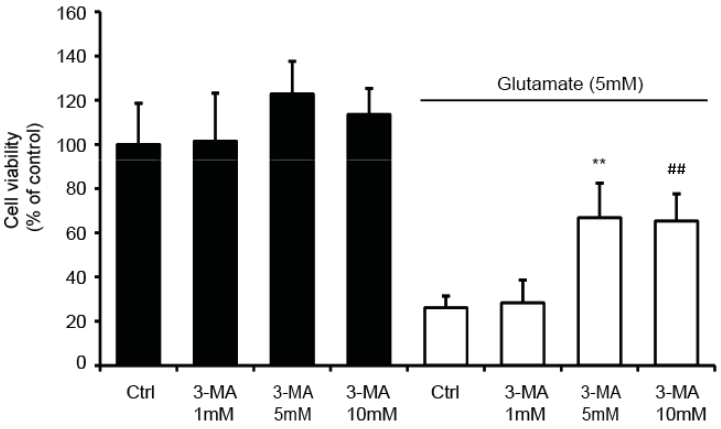

Figure 10. 3-MA mediates protection against glutamate treatment in PCN. MTT assay of PCN was performed 24 h after 3-MA and glutamate cotreatment (n=6; **p<0.01, compared to glutamate treated control, ##p<0.01, compared to glutamate treated control, ANOVA, Scheffé test).

3.1.3 Selective inhibition of essential autophagy proteins does not protect HT-22 cells

To investigate the involvement of autophagy in glutamate-mediated toxicity, siRNA-mediated gene silencing of Beclin-1 and Atg5 was applied for inhibition of these two key regulators of the autophagic process. Both siRNAs used specifically reduced Beclin-1 or Atg5 expression after 48 h as shown by immunoblot analysis (Fig. 11 A, B). In order to control that reduction of either Beclin-1 or Atg5 protein levels reduced autophagic activity, transfected cells were treated with CQ (10 µM) 48 h after transfection. Reduction of total Beclin-1 (Fig. 11 A) and Atg5 (Fig. 11 B) led to the reduction of both, LC3-I and LC3-II in comparison to vehicle and scrambled siRNA. Treatment with CQ led to a strong accumulation of LC3-II in cells incubated with vehicle or scrambled siRNA, whereas no accumulation was documented in cells exposed to Beclin-1 or Atg5 siRNA. These results confirmed a reduction in autophagic flux and the dependency of Beclin-1 and Atg5 for the autophagic process in HT-22 cells. Further, the selective knockdown Atg5 did not protect HT-22 cells against glutamate induced toxicity as shown by MTT analysis (Fig. 11 C) and impedance measurements using the xCELLigence system (Fig. 11 D). Interestingly, Beclin-1 siRNA treatment led to a transient protection against glutamate toxicity as shown by

real time impedance measurements (Fig. 11 D). MTT analysis only showed a tendency of a protective effect by Beclin-1 siRNA in the model system of glutamate toxicity. Further, MTT assay of Atg5 siRNA transfected cells that were simultaneously treated with 3-MA and glutamate (Fig. 11 C) demonstrated that the reduction of autophagic flux did not affect 3-MA mediated neuroprotection. Notably, Beclin-1 siRNA treatment increased the neuroprotective effect of 3-MA in the model system of glutamate toxicity. Also the combination of Atg5 and Beclin-1 siRNA (each 40 nM) (data not shown) and LC3 siRNA (40 nM) (Fig. 12) were tested in the model system of glutamate toxicity, but no significant protection was observed using the MTT assay. Efficient knockdown of total LC3 protein by applied siRNA was validated before (personal communication, Ganjam and Neitemeier).

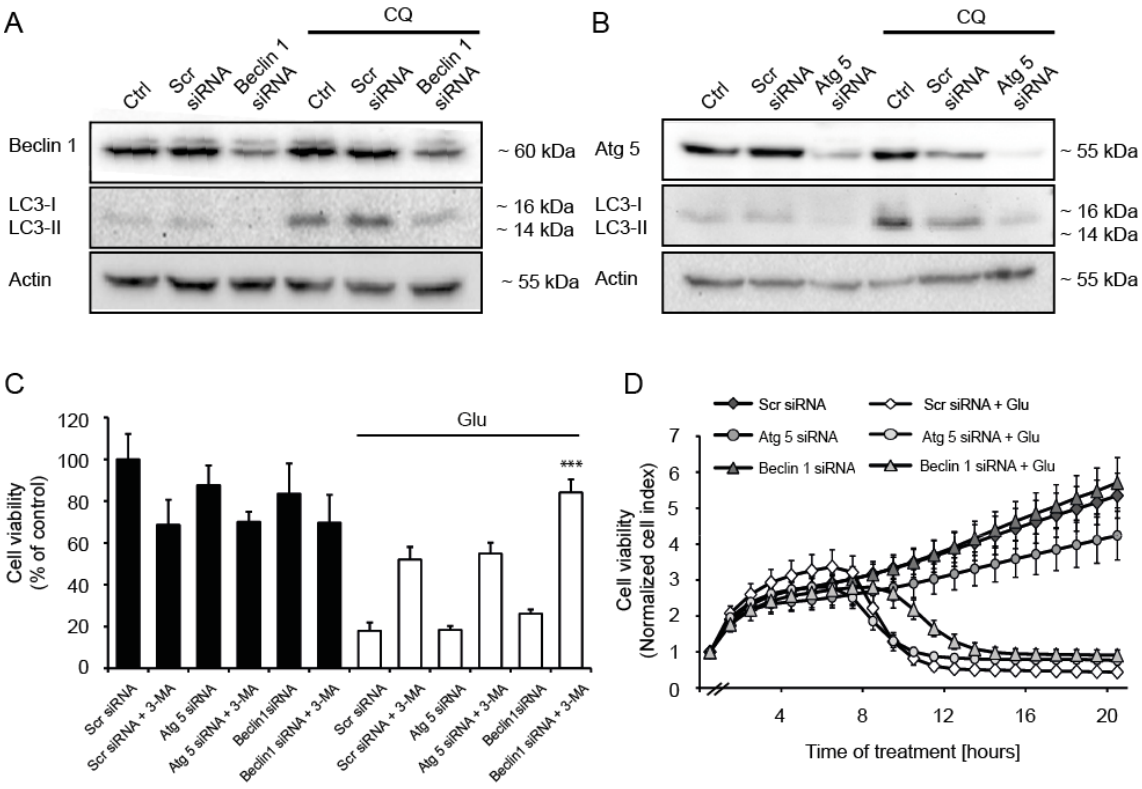

Figure 11. Knockdown of total Beclin-1 or Atg5 protein levels in HT-22 cells. A/B. Beclin-1 and Atg5 knockdown was verified by immunoblot analysis 48 h after transfection. Beclin-1 and Atg5 expression of Beclin-1 and Atg5 siRNA (40 nM) transfected cells were compared to non-transfected control cells and cells treated with scrambled siRNA. The amount of LC3 conversion was detected in transfected cells ± CQ (10 µM) treatment. Actin immunoblot was used as a loading control. **C.** Cells were challenged with glutamate (Glu, 7 mM) 48 h after siRNA transfection. Cell viability was determined using MTT assay 16 h after treatment (n=6; ***p<0.001, compared to glutamate, scr siRNA and 3-MA treated cells, ANOVA, Scheffé test). **D.** Cells were challenged with glutamate (Glu, 7 mM) 48 h after siRNA transfection. Cellular impedance was determined using the xCELLigence system.

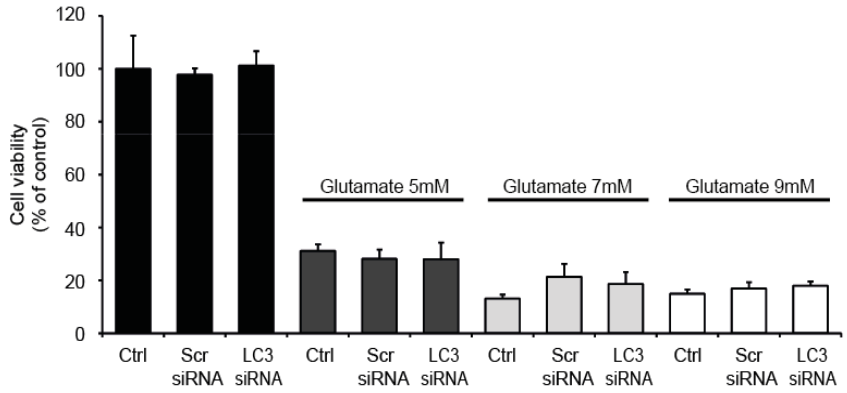

Figure 12. LC3 siRNA did not protect HT-22 cells against glutamate toxicity. HT-22 cells were transfected with LC3B siRNA (40 nM). 48 h after transfection, cells were treated with glutamate in different concentrations. MTT analysis was performed 16 h after the onset of glutamate.

In summary, these results indicated that selective inhibition of the autophagic process is not sufficient for persistent protection of HT-22 against oxidative stress. Further, 3-MA mediated its neuroprotective effects not through direct inhibition of the autophagic process. Most interestingly, Beclin-1 silencing further increased the protective effect of 3-MA in an additive manner.

In addition, the effects of Beclin-1 and Atg5 siRNA were investigated in the model system of serum deprivation. Starvation is the best characterized model system to induce autophagy in various cell types, including neurons. HT-22 cells were transfected with Beclin-1 or Atg5 siRNA (40 nM). MTT assay of transfected cells deprived of FCS for 24 h revealed that selective inhibition of autophagy did not prevent cell death (Fig. 13 A, B). The results that autophagy inhibition did not rescue the cells in the model systems of glutamate toxicity and also serum deprivation confirmed the assumption that autophagy itself is not causing cell death. This goes along with the perception of the majority of recent publications that autophagy is most likely a pro-survival mechanism, and even if dying cells show markers of autophagy this alone does not allow the conclusion that autophagy mediates cell death [188].

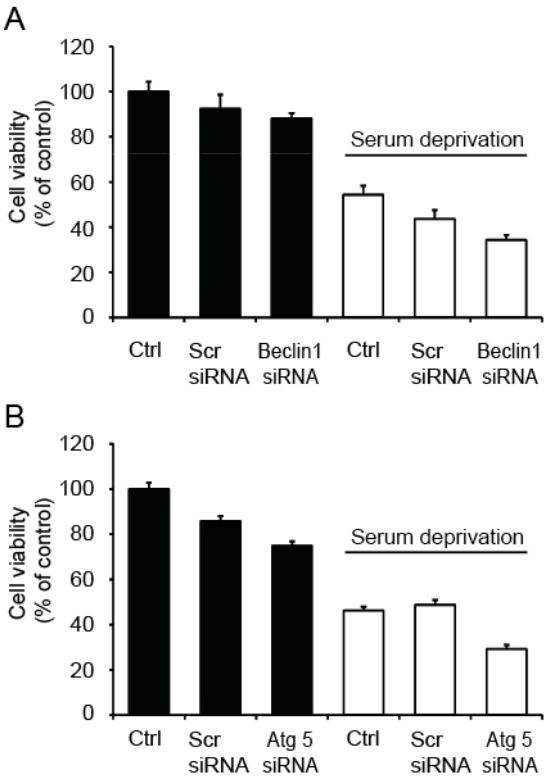

Figure 13. Knockdown of essential autophagy proteins does not protect against serum deprivation. Cells were deprived of serum 48 h after siRNA transfection. MTT assay was performed 24 h after serum deprivation to determine cell viability. **A.** Beclin-1 siRNA (40 nM) did not protect HT-22 cell against serum deprivation. **B.** Atg5 siRNA (40 nM) did not protect HT-22 cell against serum deprivation.

3.1.4 Selective knockdown of class III PI_3K does not protect HT-22 cells against glutamate-induced oxidative stress

3-MA is known to inhibit class III PI_3K in various cell types, thereby leading to inhibition of autophagy. Accordingly, siRNA against PI_3K class III was applied to investigate the effect of reduced protein levels of PI_3K class III in the model system of glutamate toxicity in HT-22 cells. The effects of class III PI_3K siRNA and 3-MA were compared in the presence or absence of glutamate challenge. Western Blot analysis of HT-22 cells transfected with siRNA targeting class III PI_3K (40 nM) showed a reduced expression of total class III PI_3K protein 48 h after transfection (Fig. 14 A). The analysis of the MTT cell viability assay revealed that knockdown of class III PI_3K did not protect HT-22 cells against glutamate toxicity (Fig. 14 B). Further, the protective effect of 3-MA against glutamate was not changed in cells that were transfected with class III PI_3K siRNA. These results indicated that the protective effect of 3-MA is not mediated through direct inhibition of class III PI_3K.

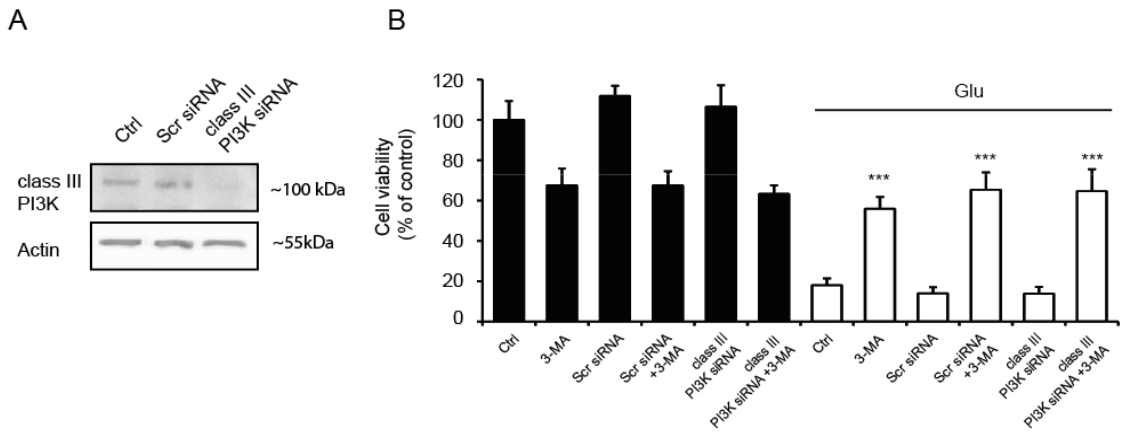

Figure 14. PI_3K class III knockdown did not attenuate glutamate toxicity. A. PI_3K class III knockdown was verified by immunoblot analysis 48 h after transfection. PI_3K class III expression of PI_3K class III siRNA (40 nM) transfected cells was compared to non-transfected control cells and cells treated with scrambled siRNA (40 nM). **B**. MTT analysis demonstrated that class III PI_3K siRNA (40 nM) did not protect HT-22 cells against glutamate toxicity (Glu, 5 mM). The protective effect of 3-MA was not changed in the presence of class III PI_3K siRNA (n=8; ***$p<0.001$, compared to glutamate treated control, ANOVA, Scheffé test).

3.1.5 Akt-inhibitor LY924002 reduces the protective effect of 3-MA against glutamate induced oxidative stress

The PI_3K/Akt and the MAPK/Erk-1/2-pathways are important signaling cascades that can mediate growth, differentiation and survival in neurons [189]. In order to evaluate the functional role of such potential, first, PI_3K/Akt activation in the neuroprotective effect of 3-MA was blocked by a specific inhibitor. For inhibition of phosphoinositide-3-kinase (PI_3K) class I and thereby indirect inhibition of Akt, the cell-permeable, reversible PI_3K-inhibitor LY294002 was applied at a final concentration of 10 µM. Cells were pretreated with the inhibitor for 1 h followed by a treatment with glutamate (5 mM) and 3-MA (5 mM). Cell viability determined by an MTT assay (Fig. 15 A) and impedance measurements with the xCELLigence system (Fig. 15 B) showed that LY294002 significantly reduced the protective effect of 3-MA in glutamate-treated HT-22 cells. This result suggested the functional involvement of the PI_3K/Akt survival signaling pathway in the observed protective effect of 3-MA against glutamate-induced neurotoxicity. To demonstrate that LY294002 did not generally inhibit protective

mechanisms, HT-22 cells were simultaneously treated with BI-6C9 (10 µM), a widely used inhibitor of Bid. The MTT assay revealed no reduction of the protective effect that was obtained with BI-6C9 alone (Fig. 15 A).

Further, immunoblot analysis of protein extracts from HT-22 cells showed a decrease of Akt-phosphorylation in 3-MA treated cells with or without glutamate. The decrease was prominent already after 30 min of 3-MA treatment (Fig. 15 C) and stable for at least 16 h (Fig. 15 D). The levels of total Akt remained unchanged. These findings demonstrated that 3-MA negatively modulated the PI_3K/Akt signaling pathway.

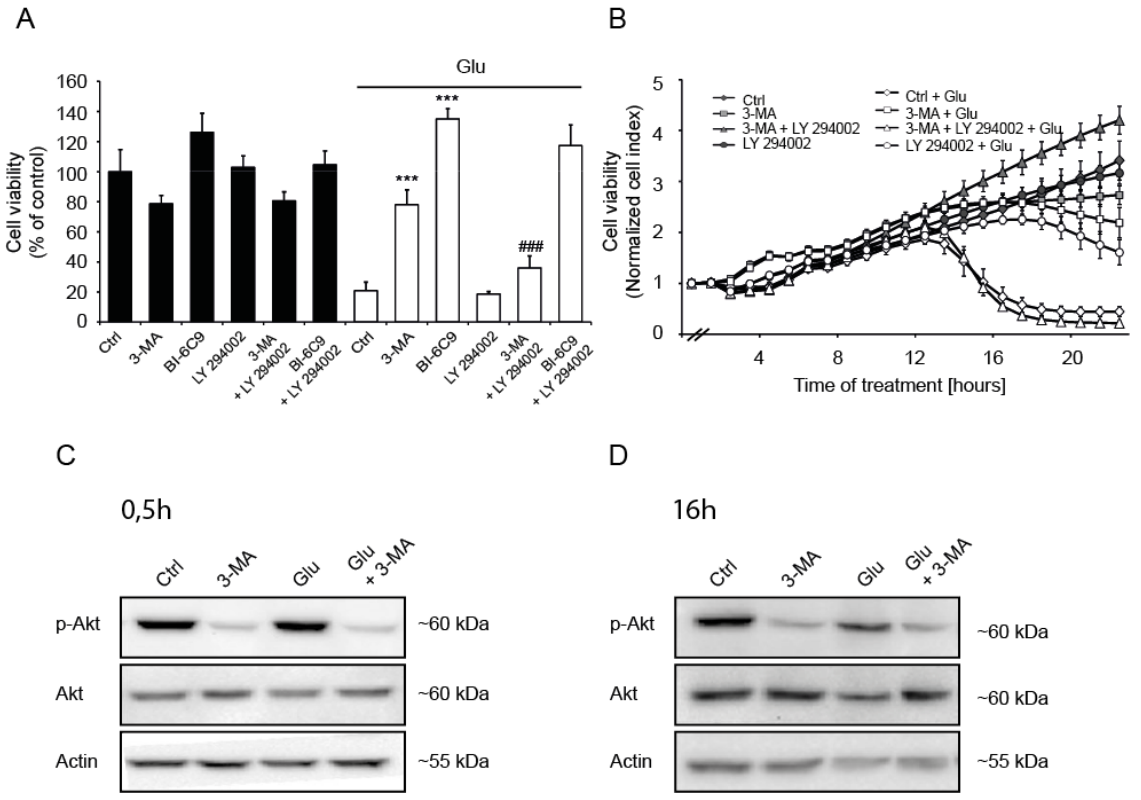

Figure 15. Involvement of the PI_3K/Akt pathway in 3-MA-mediated neuroprotection. HT-22 cells were pre-treated with LY294002 (10 µM), followed by the incubation with either 3-MA (5 mM) or BI-6C9 (10 µM) and glutamate (Glu, 5 mM). **A.** Cell viability was determined using MTT assay 16 h after the onset of glutamate (n=8,***p< 0.001 compared to glutamate treated control, ###p< 0.001 compared to glutamate and 3-MA treated cells, ANOVA, Scheffé's test). **B.** The xCELLigence system was used additionally to monitor the effect of LY294002 (10 µM) on 3-MA mediated neuroprotection. **C/D.** Immunoblot analysis of HT-22 cells treated with 3-MA (5 mM) and/or glutamate (Glu, 5 mM). Phospho-Akt (p-Akt) and Akt levels were determined after 0.5 h (C) and 16 h of treatment (D).

The PI_3K/Akt signaling pathway is one of the main regulators of mTOR and thereby linked to regulation of autophagic activity. In addition to Akt, the AMP-activated protein kinase (AMPK) signaling pathway is another main regulator of mTOR [190].
Immunoblot analysis of HT-22 cells treated with 3-MA (5mM) ± glutamate (5mM) demonstrated a transient decrease of AMPK phosphorylation after a treatment of 1.5 h (Fig. 17). Together, these findings suggested that 3-MA affects at least two different signaling pathways, namely the PI_3K/Akt and AMPK signaling pathways, which modulate cell growth, differentiation, energy homeostasis and survival in neurons.

3.1.6 Role of the MAPK/Erk-1/2 signaling pathway in 3-MA mediated neuroprotection

In order to investigate the involvement of the MAPK/Erk-1/2 pathway in 3-MA mediated neuroprotection, immunoblot analysis of Erk phosphorylation and pharmacological studies with the MEK 1 inhibitor PD98059 were performed, respectively. Immunoblot analysis of protein extracts from HT-22 cells revealed enhanced phosphorylation of MAPK/Erk-1/2 within 30 min after exposure of the cells to 3-MA ± glutamate. This enhanced phosphorylation of MAPK/Erk-1/2 appeared to be transient. Afterwards the signals representing phospho-MAPK/Erk-1/2 declined to control levels. The levels of total MAPK/Erk-1/2 remained unchanged, as was observed after incubation of the immunoblots with anti-Erk 1/2 antibodies (Fig. 17).
In addition, the MAPK/Erk-1/2 signaling pathway was blocked using the specific MEK 1 inhibitor PD98059 (50 μM). PD98059 binds to the inactive forms of MEK1 and prevents activation by upstream activators such as c-Raf [191]. MTT analysis demonstrated that pre-incubation for 1h with PD98059 protected HT-22 cells against glutamate-induced toxicity (Fig. 16). This result indicated that the MAPK/Erk-1/2 pathway is not involved in 3-MA-mediated neuroprotection, however a transient increase in Erk 1/2 phosphorylation was detected within 30 min after exposure of 3-MA ± glutamate.

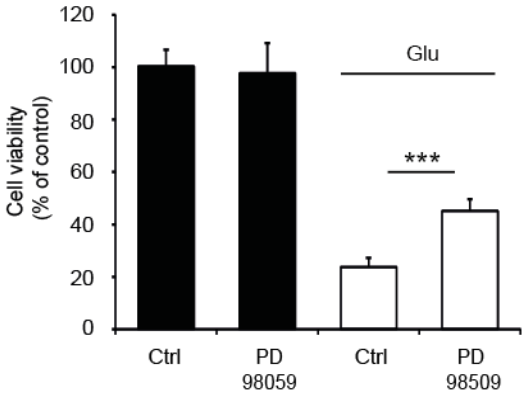

Figure 16. PD98059 protects HT-22 cells against glutamate toxicity. MTT analysis was used to determine the effect of PD98059 (50 µM) in the model system of glutamate (Glu, 5 mM) toxicity 16 h after treatment (n=8; ***p<0.001, compared to glutamate treated control).

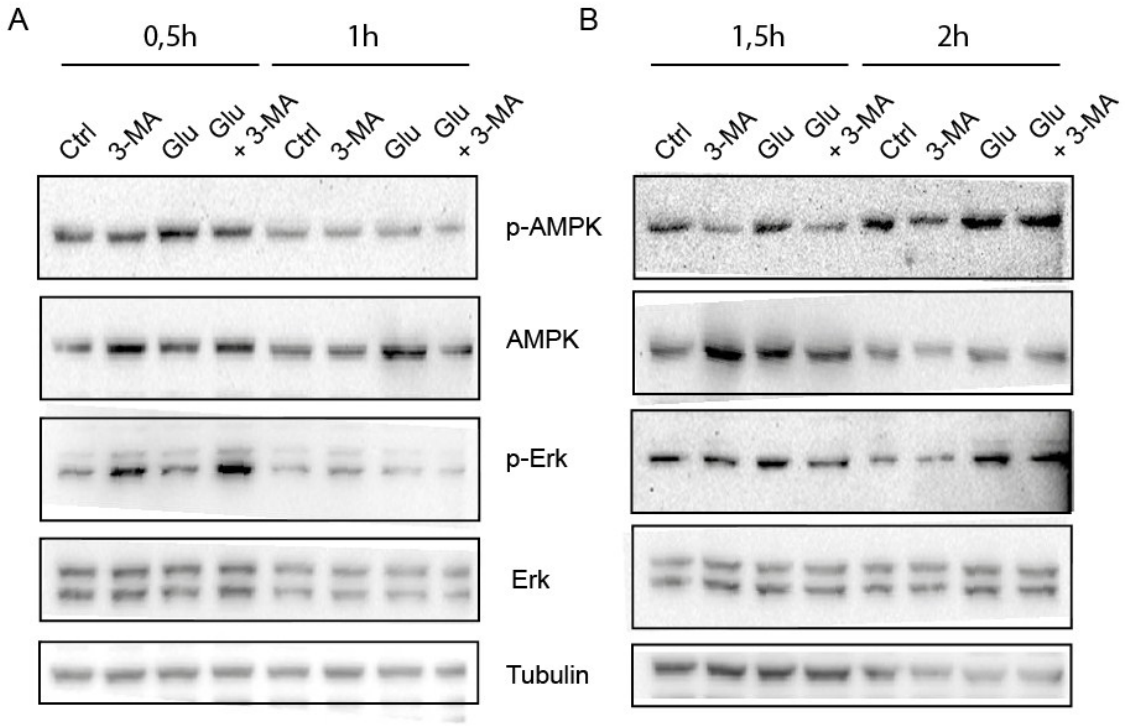

Figure 17. Effects of 3-MA on the AMPK and MAPK/Erk-1/2 signaling pathways. Protein extracts from HT-22 cells were collected 0.5 h, 1 h, 1.5 h and 2 h after treatment with 3-MA (5 mM) ± glutamate (5 mM). Protein levels of pAMPK, AMPK, p-Erk and Erk were determined using immunoblot analysis. Tubulin was used as a loading control.

3.1.7 3-MA treatment preserves mitochondrial integrity

Next, the effects of glutamate and 3-MA on mitochondrial morphology and function were examined. Mitochondria generate most of the cell's supply of ATP. In addition, mitochondria are involved in the regulation of other fundamental cellular functions such as mitochondrial retrograde signaling, cellular differentiation, cell death, as well as the control of the cell cycle and cell growth [192]. Mitochondria have also been implicated in several human diseases, including neurodegenerative diseases [193].

After glutamate treatment, most cells showed significant fragmentation of the mitochondria appearing as small round organelles in the damaged cells in contrast to long tubular mitochondria observed under control conditions [182, 194]. 3-MA preserved mitochondrial morphology despite glutamate exposure, and mitochondria remained as a network of long tubular organelles similar to controls (Fig. 18 A). Quantification of mitochondrial morphology confirmed these results (Fig. 18 B).

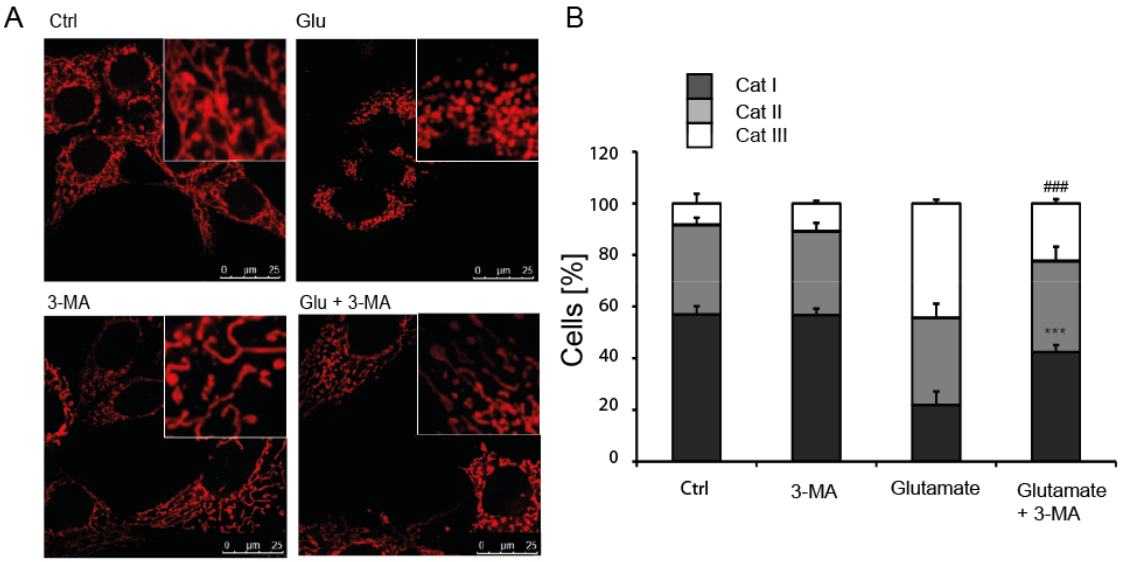

Figure 18. 3-MA preserves mitochondrial morphology after glutamate exposure. A. HT-22 cells were stained with MitoTracker red 30 min before glutamate (Glu, 5 mM) and 3-MA (5 mM) treatment. Fluorescence microscopy was performed 16 h after the treatment. Red color indicated mitochondria. Bar scale 25 µm. **B** Quantification of mitochondrial morphology: Category I (Cat I): fused, Category II (Cat II): intermediate, Category III (Cat III): fragmented mitochondria. At least 500 cells were counted per condition blinded to treatment conditions. Values are given from three independent experiments (###$p<0.001$ compared to category III glutamate treated control; ***$p<0.001$ compared to category I glutamate treated control).

Further, the formation of lipid peroxides, which are associated with irreversible mitochondrial damage and ROS formation, was analyzed. As detected by the fluorescent dye BODIPY (4,4-difluoro- 5-(4-phenyl-1,3-butadienyl)-4-bora-3a,4a-diaza-s-indacene- 3-undecanoic acid) and fluorescence-activated cell sorting (FACS) analysis, glutamate-induced cell death was accompanied by an accumulation of lipid peroxides (Fig. 19 A, B). 3-MA treatment significantly reduced the production of lipid peroxides compared to controls exposed to glutamate. To assess the functional integrity of mitochondria in 3-MA treated cells, we next investigated ATP levels after glutamate exposure. Since glutamate treatment results in a rapid decrease in cytoplasmic ATP levels, we next evaluated if 3-MA is able to reduce the decrease of cytoplasmic ATP levels after glutamate treatment [168, 181]. As shown in Fig. 19 D, luminescence measurements demonstrated that 3-MA is able to prevent the loss of ATP cells after induction of oxidative stress.

In addition, we investigated the mitochondrial membrane potential ($\Delta\Psi m$, MMP) in glutamate and 3-MA treated cells using tetramethylrhodamin ethyl ester (TMRE staining). The loss of mitochondrial membrane potential is detected by a loss of red fluorescence that can be measured by FACS analysis. Carbonyl cyanide m-chlorophenylhydrazone (FCCP, 50 µM) that induced a fast and strong mitochondrial depolarization was used as a positive control. Glutamate caused a high loss of mitochondrial membrane potential as shown by the reduced number of cells with red fluorescence. 3-MA significantly reduced the glutamate-induced loss of mitochondrial membrane potential (Fig. 19 C).

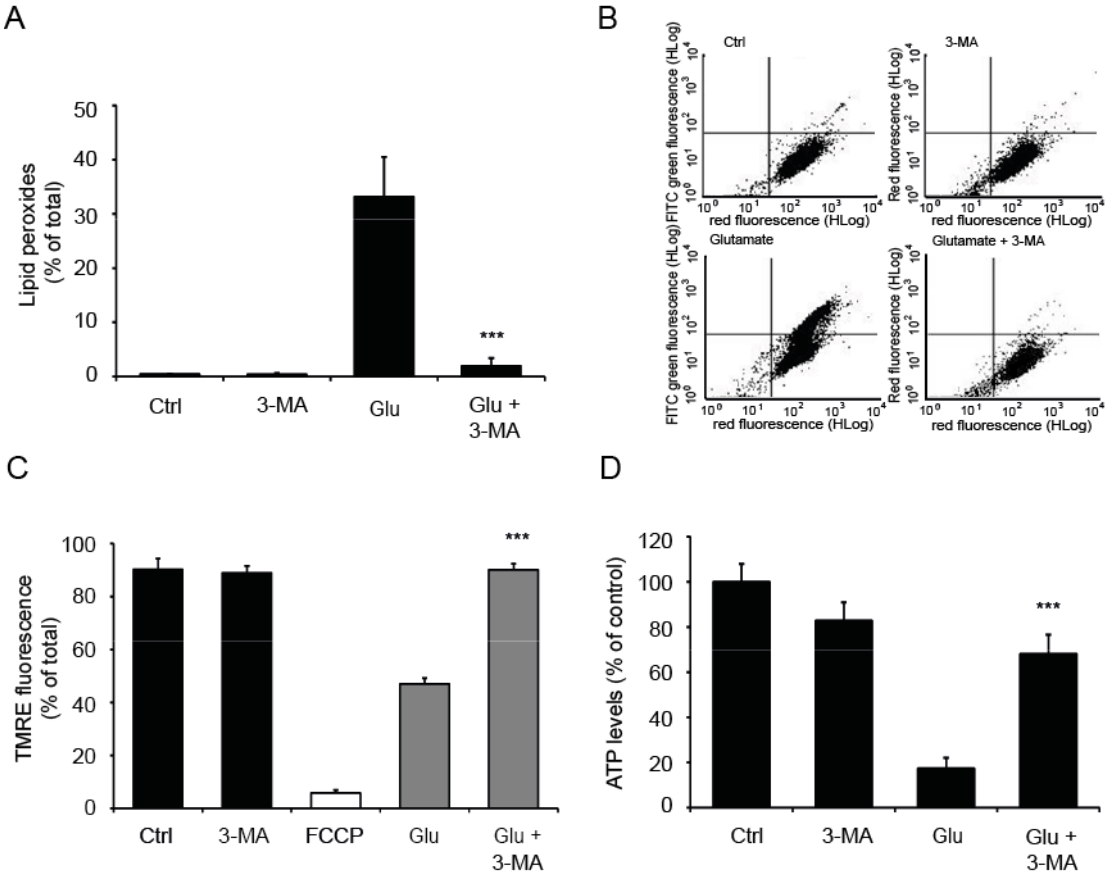

Figure 19. 3-MA preserves mitochondrial function and integrity in HT-22 cells exposed to glutamate. Lipid peroxides were measured by Bodipy FACS analysis 14 h following the onset of 3-MA and glutamate treatment. **A.** Bar graphs showed that 3-MA decreased the amount of lipid peroxides after glutamate cotreatment, ***$p<0.001$ compared to glutamate treated controls (5 mM). **B.** Graphics obtained after FACS analysis. Cells in the upper right quadrant represent cells with increased ROS production. **C.** MMP measured by TMRE is significantly decreased by glutamate treatment (Glu, 5 mM, 15 h) compared to control. Membrane potential is preserved by 3-MA (5 mM) (***$p<0.001$ compared to glutamate treated control cells). FCCP was used to dissipate mitochondrial membrane potential and served as a positive control. Cells were treated with glutamate (5 mM) for 13 h. **D.** ATP levels from 3-MA treated cells (5 mM) were preserved from loss in ATP levels caused after glutamate treatment (n=8;***$p<0.001$ compared to control cells). All statistics were obtained using ANOVA, Scheffé test.

3.1.8 3-MA preserves mitochondrial maximum respiration loss mediated by glutamate

Further, the mitochondrial oxygen consumption rate (OCR) using the XFe extracellular flux analyzer (Seahorse Bioscience) was examined. The rate of OCR is an indicator of mitochondrial respiration and related to catabolic pathways generating ATP. The results revealed that glutamate treatment significantly decreased basal cellular respiration, maximum respiration and the mitochondrial reserve capacity as compared to non-glutamate exposed cells. 3-MA treatment alone did not affect basal respiration, but prevented the decreases of mitochondrial respiration parameters induced by glutamate treatment (Fig. 20). These data confirmed that 3-MA prevented mitochondrial damage, thereby, rescuing the HT-22 cells from glutamate-induced oxidative stress.

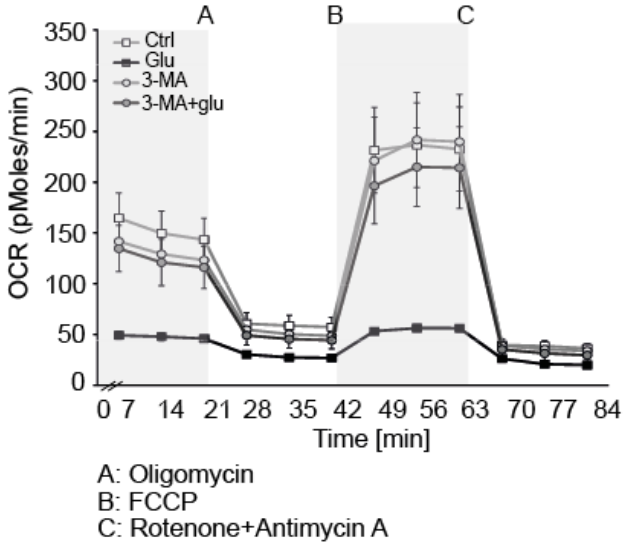

Figure 20. Mitochondrial oxygen utilization in glutamate treated cells. Oxygraph traces showing respiratory activity of HT-22 cells exposed to glutamate (4 mM) with or without 3-MA (5mM) after 16 h of treatment. *A* indicated the additions of oligomycin (OM), *B* the addition of Carbonylcyanide p-trifluoromethoxyphenylhydrazone (FCCP) and *C* the addition of Rotenone and Antimycin A.

3.2 Neuroprotection mediated by conditioned medium (CM) of neuronal cell lines

3.2.1 Conditioned medium of neural progenitor cells protects neuronal cells against growth factor withdrawal and glutamate-induced neurotoxicity

Beneficial effects of neural progenitor cell (NPC) transplantation have been well established in animal models of acute brain damage. However, the cellular and molecular mechanisms underlying these protective effects are largely unknown. Since only very few NPC cells survive intracerebral transplantation, enhanced neurogenesis may only play a minor role for the observed functional and histological protection of brain tissue. Therefore, the aim of this part was to explore the neuroprotective potential of NPC-conditioned medium (CM) that may be exerted by factors released from these cells.

3.2.1.1 Deprivation of growth factors promotes cellular death of NPC

Local transplantation of NPC into injured brain regions in models of acute brain damage revealed significant cellular death of NPC. However, dying NPC mediated protective or regenerative effects on neuronal tissues in various models of brain damage. In this study the conditions after NPC transplantation *in vivo* were mimicked *in vitro* by withdrawal of growth factor support in cultured NPC.

In a first approach to characterize NPC, cellular growth of different cell densities (80,000, 100,000, 120,000 cells/cm^2) was monitored over 48 h (Fig. 21 A). Different seeding densities were easily distinguished by different cell indices. For further experiments a cell density of 120,000 cells/cm^2 was used. Next, NPC were deprived of both EGF and bFGF (Fig. 21 C). The effects of growth factor deprivation on NPC were monitored using the xCELLigence system. Twenty four h after growth factor deprivation, the cell index decreased significantly, indicating time-dependent cellular death of NPC. The impedance of the control group that was kept in medium containing the growth factors increased continuously. After growth factor deprivation the NPC shrunk, rounded up and partly detached from the surface of the culture plate (Fig. 21 B).

To investigate the cell death mechanisms induced by growth factor deprivation, Western blot analysis of caspase-3 and poly [ADP-ribose] polymerase (PARP) was performed. Caspase-3 is a key mediator of apoptosis in mammalian cells and responsible for the proteolytic cleavage of many key proteins such as the nuclear enzyme PARP [195]. PARP is activated in different paradigms of cellular stress, mediating either repair mechanisms or cell death, depending on the context and the strength of the stress stimulus. Cleavage of PARP serves as a marker of cells undergoing caspase-dependent apoptosis [196]. The results showed a time-dependent increase in activation of caspase-3 and cleavage of PARP 6 and 12 h after growth factor deprivation (Fig. 22).

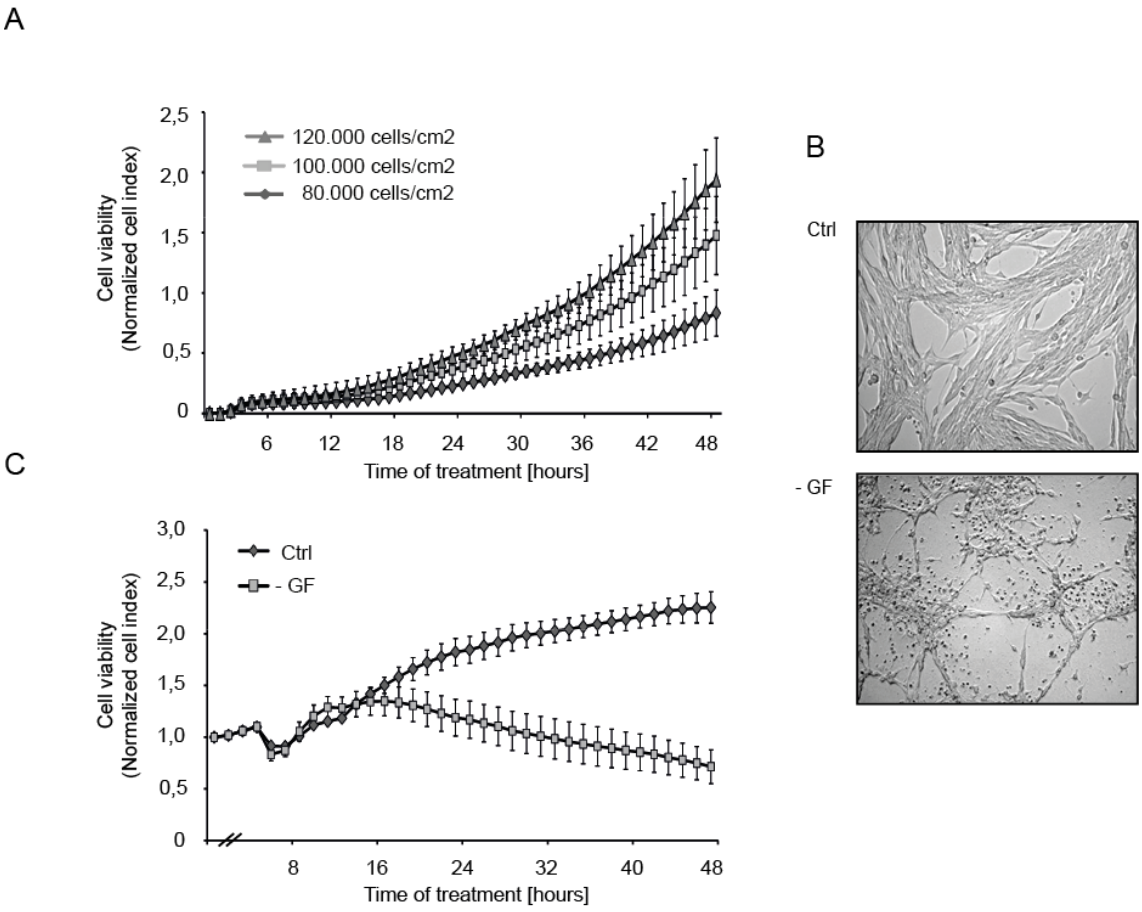

Figure 21. Cellular growth and effects of growth factor deprivation in NPC. A. Measurement of cellular impedance of NPC grown at different densities (80,000 cells/cm^2, 100,000 cells/cm^2 and 120,000 cells/cm^2), (n = 6). **B.** Representative pictures of cell morphology of NPC deprived of growth factors (-GF) (24 h) in comparison to control (Ctrl). **C.** NPC were plated on an E- plate 96 and deprived of the growth factors EGF and bFGF. Cellular impedance was continuously monitored by the xCELLigence system (n=6).

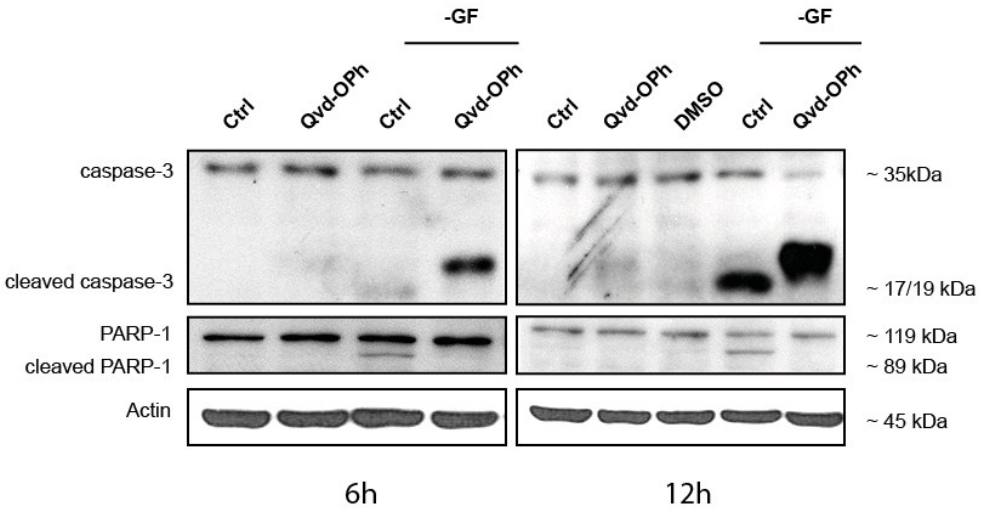

Figure 22. Cellular growth and effects of growth factor deprivation in NPC. Growth factor deprivation induced activation of caspase-3. The immunoblot shows a time-dependent activation of caspase-3 and PARP-cleavage 6 h and 12 h after deprivation of EGF and bFGF. The broad caspase inhibitor Qvd-OPh (20 µM) prevented activation of caspase-3 and cleavage of PARP.

3.2.1.2 Broad caspase inhibitor Qvd-OPh protects NPC from cellular death

Further, the broad caspase inhibitor Qvd-OPh was administered to the medium at a final concentration of 20 µM. DMSO was used as a standard solvent, the concentration was below 0.1% and did not cause any effect on its own. The caspase inhibitor Qvd- OPh partly attenuated cell death after growth factor withdrawal in NPC cultures as determined with the xCELLigence system (Fig. 23 A). The corresponding MTT assay conducted in parallel further supported this observation, thus strengthening the proposed correlation between MTT and impedance measurements (Fig. 23 B). Qvd-OPh alone did not significantly affect cellular viability in relation to non-treated NPC, as detected by the xCELLigence system and the MTT assay. Additionally, Western Blot analysis also showed that Qvd-OPh (20µM) was able to prevent caspase-3 activation and the cleavage of PARP in the model of growth factor deprivation (Fig. 22). Interestingly, a band showing higher molecular weight (~23 kDa) than the large fragment (17, 19 kDa) of cleaved caspase-3 was detected. This may reflect the mode of action of the caspase inhibitor that irreversibly binds to activated caspases thereby likely stabilizing the protein as detected in the current immunoblot analysis [197].

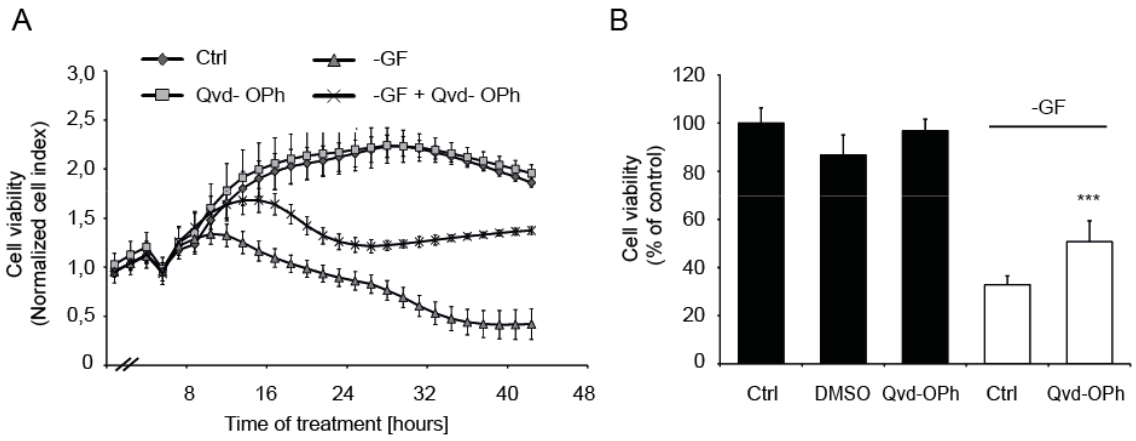

Figure 23. Broad caspase inhibitor Qvd-OPh protects NPC against cell death induced by deprivation of growth factors. A. NPC were treated with Qvd-OPh (20 µM). Real time monitoring of cellular impedance by the xCELLigence system revealed a protective effect of Qvd-OPh 48 h after deprivation of EGF and bFGF (-GF) (n=6). **B.** MTT-assay confirmed the protective effect of Qvd-OPh against growth factor withdrawal (-GF) in NPC (***$p<0.001$ compared to control after growth factor deprivation; n=8, ANOVA, Scheffé test).

3.2.1.3 NPC conditioned medium protects neuronal cells against damage by growth factor withdrawal and glutamate toxicity

The development of a CM from dying NPC reflects the conditions after stem/progenitor cell injection. Therefore, the aim was to explore the potential of NPC-conditioned medium (NPC CM) to attenuate growth factor withdrawal and glutamate-induced neuronal death. In many settings of acute and chronic neurodegeneration, oxidative stress and glutamate-induced deregulation of intracellular calcium homeostasis are considered as the major triggers of neuronal cell death [174, 175]. Here, NPC CM was applied in the model system of glutamate-induced toxicity in order to evaluate the potential neuroprotective effects of factors released by NPC.

In HT-22 cells, millimolar concentrations of glutamate induce NMDA-receptor independent cell death through enhanced oxidative stress, mitochondrial damage and the release of mitochondrial apoptosis-inducing factor (AIF), a process termed oxytosis [167, 182]. In contrast, micromolar concentrations of glutamate induce excitotoxicity and calcium-triggered cell death through activation of NMDA receptors in primary cortical neurons [173]. HT-22 cells, PCN and NPC cells were pre-treated for 6 h with NPC conditioned medium (NPC CM) and then challenged with glutamate for 18 h or deprived of growth factors for 24 h. In the experimental setups growth factor deprivation and glutamate treatment led to cellular death of about 60-90% (Fig. 24 A-

C). NPC CM elicited neuroprotective effects against growth factor deprivation and glutamate-toxicity in both HT-22 (Fig. 24 A) and PCN cells (Fig. 24 B) as shown by MTT analysis. In NPC, NPC CM protected cells significantly against growth factor deprivation (Fig. 24 C). These findings indicated that NPC secrete protective factors that attenuate growth factor withdrawal and glutamate-induced neurotoxicity. To check whether the neuroprotective effects of CM were specific to NPC, the effects of conditioned medium obtained from MEF cultures were also investigated. MEF CM was collected 24 h after nutrient deprivation and prepared like regular NPC CM (see chapter 2.1.2.4). HT-22 cells were pretreated for 6 h and then treated with glutamate for additional 18 h. Cell viability was determined using MTT analysis.

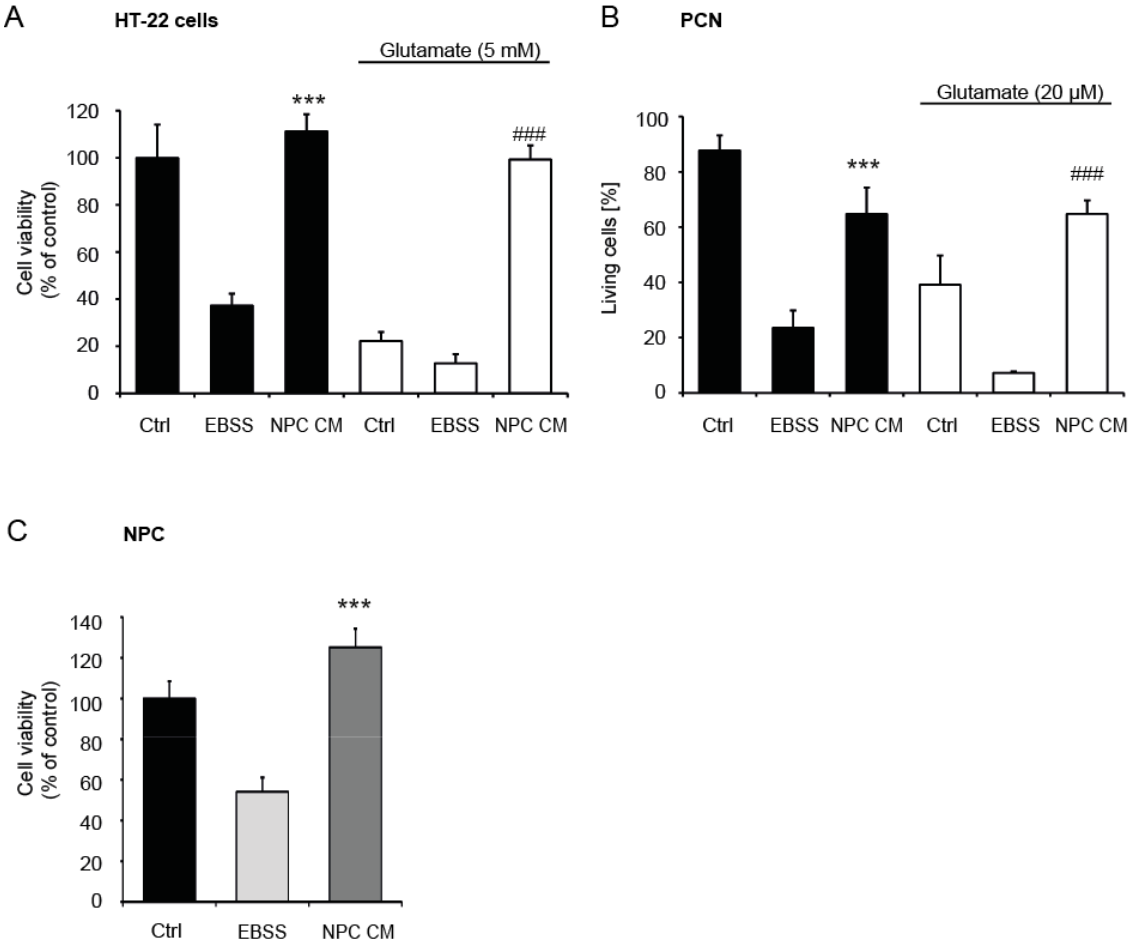

Figure 24. Effects of CM in HT-22 cells, primary cortical neurons (PCN) and neural progenitor cells (NPC). A. HT-22 cells were pre-treated with CM for 6 h before exposure to glutamate (5 mM). Cell viability was determined 18 h after onset of glutamate. NPC CM protected HT-22 cells against growth factor withdrawal (EBSS) and glutamate toxicity. MTT assay was used to determine cell viability (***$p<0.001$ compared to EBSS, ###$p<0.001$ compared to EBSS treated with glutamate, n=8, ANOVA, Scheffé test). **B.** DAPI staining followed by counting revealed a significant protective effect induced by NPC CM against growth factor withdrawal (EBSS) and glutamate toxicity (40 µM) in PCN (***$p<0.001$ compared to EBSS, ###$p<0.001$ compared to EBSS treated with glutamate n=8, ANOVA, Scheffé test). **C.** NPC were treated with NPC CM for 24 h. MTT analysis revealed a strong protective effect against nutrient starvation (***$p<0.001$ compared to EBSS, n=6, ANOVA, Scheffé test).

Interestingly, MEF conditioned medium also protected against growth factor deprivation and glutamate-induced neurotoxicity (Fig. 25). However, the neuroprotective effect of NPC CM was far more pronounced than the effects obtained with the MEF CM.

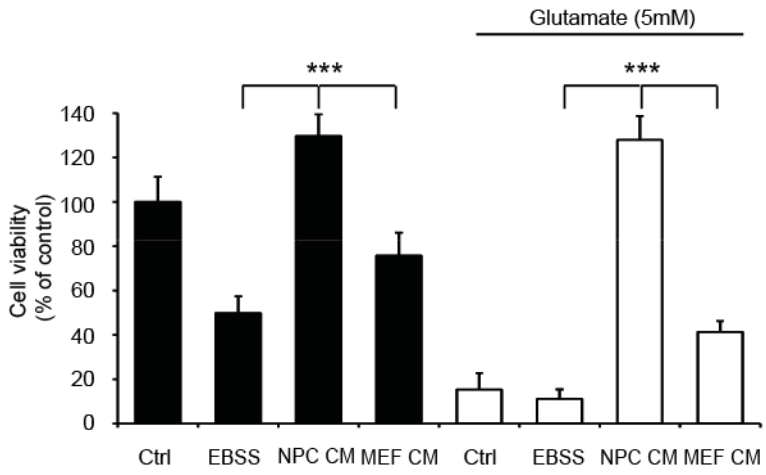

Figure 25. MEF CM protects HT-22 cells against trophic factor withdrawal or glutamate toxicity not as strong as NPC CM. HT-22 cell viability measurement indicated a protective effect by both NPC and MEF CM against growth factor deprivation (EBSS) and glutamate-induced neurotoxicity (5 mM) (***p<0.001 NPC CM and MEF CM compared to EBSS; NPC CM and MEF treated with glutamate compared to EBSS treated with glutamate, n=8, ANOVA, Scheffé test).

3.2.1.4 Heating abolishes the protective effect of NPC CM

Additional experiments aimed at further analyzing the factors that were secreted by NPC mediating neuroprotective effects in HT-22 cells and PCN. In a first approach, the CM was exposed the CM to 95°C for 30 min in order to achieve denaturation of proteins. In contrast to the previously applied native NPC CM, heat-exposed NPC CM failed to protect HT-22 cells from glutamate-induced toxicity (Fig. 26). Interestingly, heat inactivated NPC CM still provided protective effects against growth factor deprivation comparable to native NPC CM.

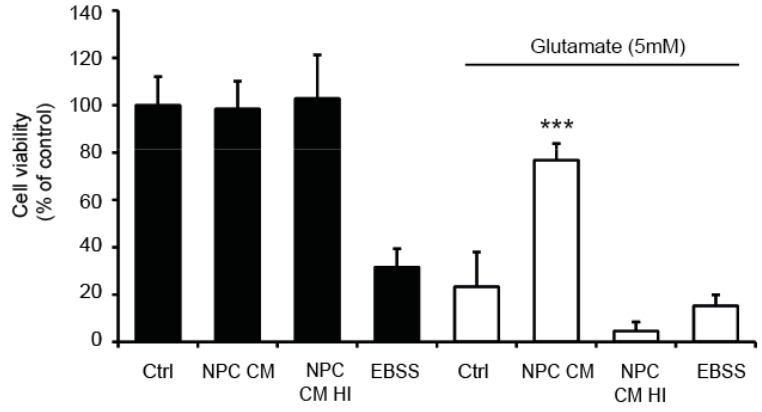

Figure 26. Heating abolishes protective effects of NPC CM. The NPC CM was incubated at 95°C for 30 min to generate heat inactivated CM (NPC CM HI) for treatment in HT-22 cells. MTT analysis demonstrated a protective effect against glutamate-induced toxicity mediated by NPC CM, but not by heat inactivated NPC CM (***p<0.001 compared to EBSS treated with glutamate; n=8, ANOVA, Scheffé test).

3.2.1.5 Apoptotic bodies have a minor role in the mediation of neuroprotection of CM

Apoptotic bodies have been proposed to enhance the differentiation of human endothelial progenitor cells *in vitro* [198]. Therefore Eva Öxler investigated CM for apoptotic bodies to mediate neuroprotection. However, apoptotic bodies isolated from NPC did not protect against glutamate-induced cell death whereas the supernatant still protected HT-22 cells from apoptosis [199].

To exclude the possibility that the process to isolate apoptotic bodies was insufficient, the involvement of apoptotic bodies in NPC CM-mediated neuroprotection was further investigated using a pharmacological approach. NPC were treated with Blebbistatin (50 µM) or Y-27632 (10 µM) in EBSS. The medium was collected after 24 h and prepared for further investigations. Blebbistatin is a selective inhibitor of non-muscle myosin II, Y-27632 is a highly potent, cell-permeable, selective ROCK (Rho-associated coiled coil forming protein serine/threonine kinase) inhibitor. Both substances inhibit the formation of membrane blebs [200]. HT-22 cells were pretreated with Blebbistatin CM (Blebbi CM) or Y-27632 CM for 6 h and then challenged with glutamate for 18 h. MTT analysis showed that also Blebbistatin CM (Fig. 27 A) or Y-27632 CM (Fig. 27 B) protected HT-22 cells against glutamate- induced cell death. It is interesting to note that the protective effect of Blebbi CM was less potent than the protective effect that was mediated by regular NPC CM, indicating that apoptotic bodies do partly participate in NPC CM mediated neuroprotection.

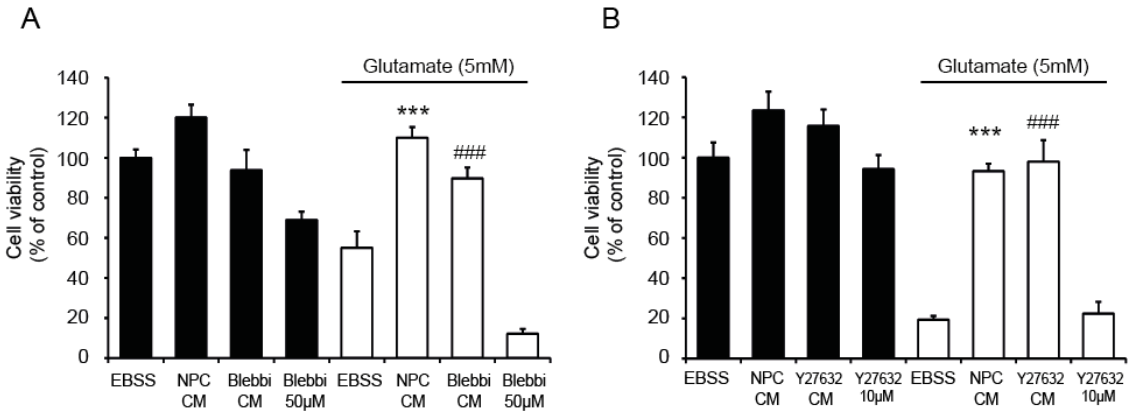

Figure 27. NPC CM prepared with Blebbistatin or Y-27632 mediates neuroprotection. A,B. HT-22 cells were pretreated with Blebbi CM (A) or Y27632 CM (B) for 6 h and then challenged with glutamate for 18 h. MTT assay was used to determine cell viability (n=8, *** $p<0.001$ compared to glutamate-treated EBSS, ###$p<0.001$ compared to glutamate-treated EBSS, ANOVA, Scheffé Test).

3.2.1.6 Activation of PI_3-K/Akt and MAPK/Erk-1/2 in neurons is involved in neuroprotection by preconditioned medium

To gain further insights into neuroprotective signaling triggered by NPC CM, it was next investigated whether this effect was associated with enhanced phosphorylation of proteins that were previously established to mediate trophic factor signaling. The PI_3K/Akt and the MAPK/Erk-1/2 pathways are the most prominent survival signaling cascades that can be stimulated in neurons by a wide variety of cytokines or growth factors [189, 201]. Rat primary cortical neurons were treated with NPC CM for several time points ranging from 10 to 120 min. Western blot analysis was performed to detect the rate of phosphorylation of growth factor activated survival signaling proteins, such as Akt/PKB and Erk 1/2 after treatment with NPC CM. The results were compared with the phosphorylation rate of Akt/PKB and Erk 1/2 after treatment with BDNF (10 ng/ml). Immunoblot analysis showed an enhanced phosphorylation of Akt/PKB and Erk 1/2, which was very pronounced after 10 min and remained significantly elevated up to 120 min after incubation (Fig. 28 A). Quantification of Western blots confirmed these results (Fig. 28 B, C). The effects of NPC CM enhancing Akt/PKB and Erk 1/2 phosphorylation were similar to effects by BDNF. Quantification of immunoblots verified a significant increase in Akt and Erk1/2 phosphorylation from 10 to 120 min in comparison to control. These findings suggested that the components of NPC CM that mediate neuroprotection *in vitro* or improved neural regeneration *in vivo* act very similar to neurotrophic signaling pathways that were previously shown to provide neuroprotection [202].

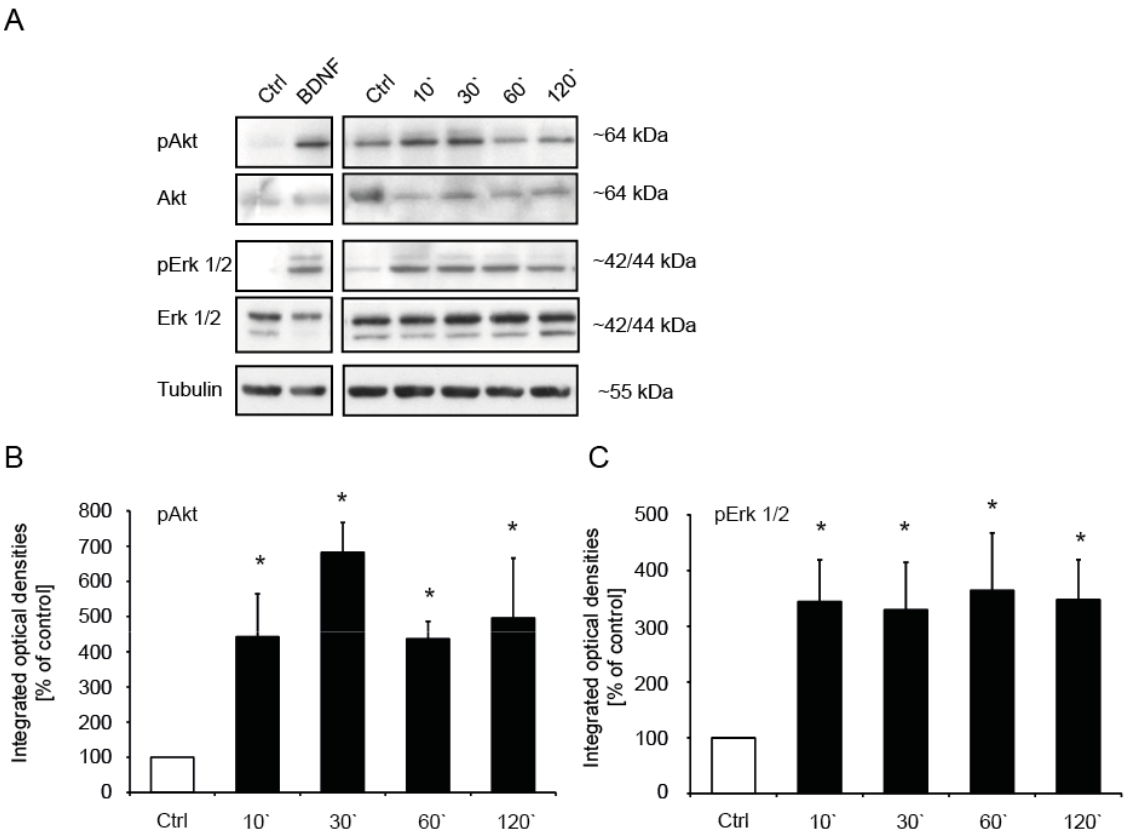

Figure 28. NPC CM and BDNF activate cell survival-related kinases. A. PCN were treated with NPC PCM for several time points ranging from 10 to 120 min. Western blot analysis showed enhanced phosphorylation of Akt/PKB and Erk 1/2, similar to the effects after exposure to BDNF. **B/C.** Quantification of Western blot analysis (*p<0.05 compared to control (Ctrl), n=3, ANOVA, Duncan test).

3.2.1.7 Inhibition of autophagy does not protect NPC against EBSS-induced starvation

Autophagic activity is induced by nutrient starvation and is crucial for cell adaption and survival under extreme conditions [12]. Therefore it was next addressed, whether the process of autophagy contributed to the protective effect of NPC CM in the model system of glutamate-induced cell death. Starvation is the best characterized inducer of autophagy [58]. Hence, immunocytochemistry and Western Blot analysis were performed to investigate if starvation also induces autophagy in NPC. The cells were treated with EBSS for 18 h to induce starvation followed by apoptotic cell death. Western Blot analysis was performed to investigate protein expression of LC3 after 18 h of EBSS treatment. LC3 is an essential protein for the formation of autophagosomes and exists in two forms in the cell. Once, autophagy is activated, LC3-I gets lipidated to LC3-II and is incorporated into the autophagosome membrane. In cells exposed to

serum deprivation both LC3-I and LC3-II were increased in comparison to control cells, indicating induction of autophagy after starvation (Fig. 28 A). 3-MA, a widely used inhibitor of autophagy, was able to slightly reduce the amount of LC3-II that occurred after EBSS treatment (Fig. 29 A), indicating an inhibitory effect on autophagy. Pictures obtained with a fluorescence microscope clearly revealed an increase of green dot agglomerations and an increase in fluorescence intensity in EBSS-treated NPC in comparison to control cells (Fig. 29 B). The increase of green dot agglomerates represents increased formation of autophagosomes [19, 46], indicating activation of autophagy.

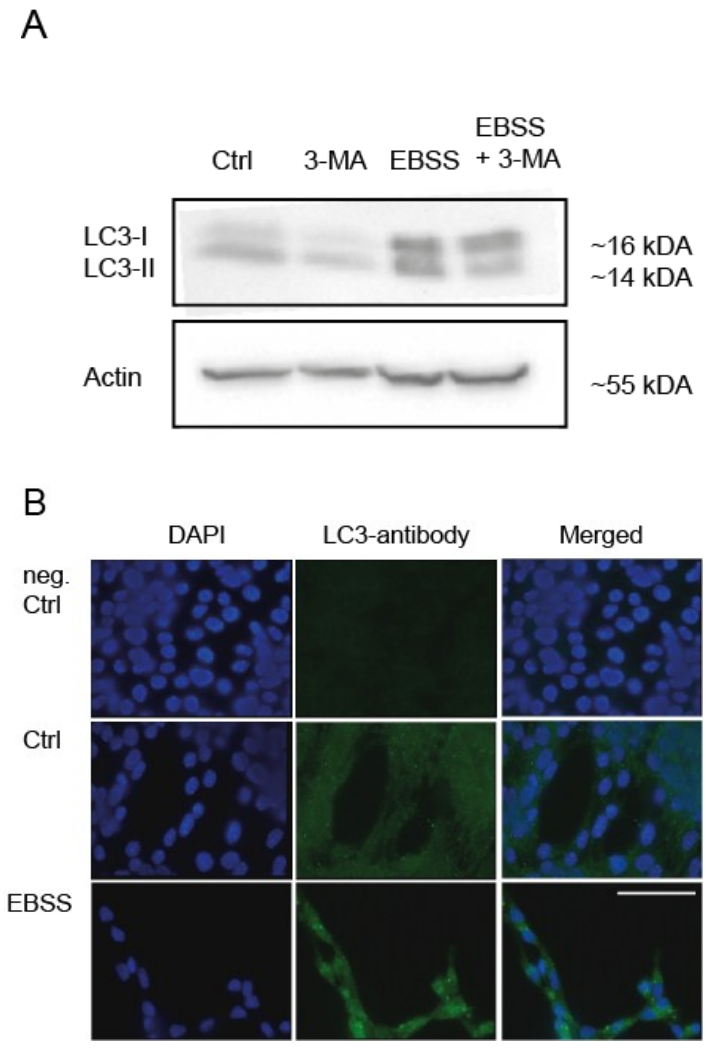

Figure 29. EBSS-induced autophagy in NPC. A. Western Blot analysis of NPC incubated with EBSS and 3-MA (5 mM). Protein expression of LC3-I and II was determined 18 h after the treatment. **B**. NPC were starved with EBSS for 18 h and afterwards incubated with an LC3 antibody (1:150). Dylight goat 488 anti rabbit was used as a second antibody. Fluorescence microscopy was performed using an L5 filter. Bar scale 50 µM.

Next, NPC were pretreated for 2 h or cotreated with 3-MA (5 mM) respectively and then challenged with EBSS for 18 h. MTT analysis demonstrated that 3-MA was not able to protect NPC against starvation-induced cell death, neither in the pretreated nor the cotreated cells (Fig. 30 A).

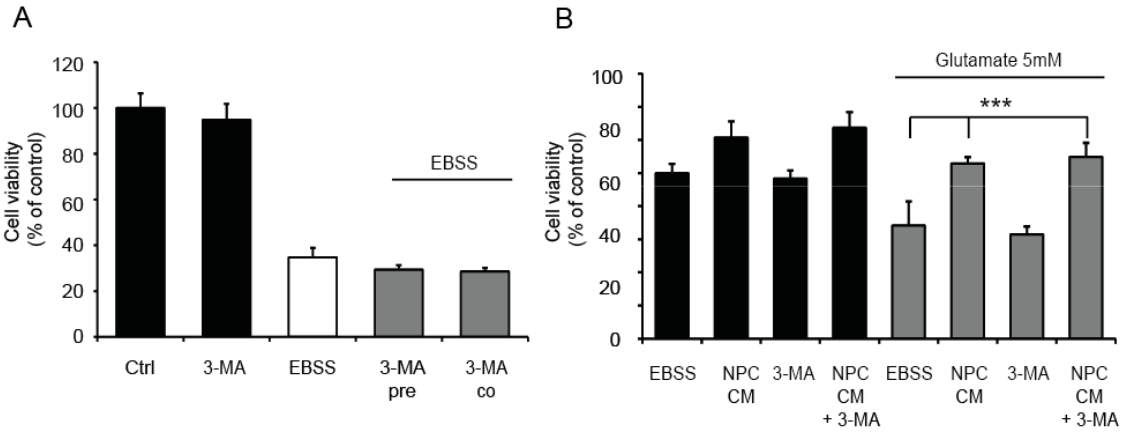

Figure 30. Effects of 3-MA and NPC CM prepared with 3-MA. A. MTT analysis of pretreatment (2 h) or cotreatment with 3-MA (5 mM) of NPC in the model system of EBSS-induced starvation (18 h). **B.** MTT analysis of NPC CM prepared 3-MA compared to regular NPC CM in the model system of glutamate-induced toxicity in HT-22 cells (n=8,***p< 0.001 compared to glutamate treated EBSS, ANOVA, Scheffé test).

3.2.1.8 NPC conditioned medium prepared with 3-MA protects HT-22 cells against glutamate-induced oxidative stress

Further, the medium of NPC treated with 3-MA and deprived of nutrients was collected after 24 h and prepared like regular NPC CM (see chapter 2.1.2.4). Then, NPC CM + 3-MA was tested and compared with regular NPC CM in the model system of glutamate-induced oxidative stress in HT-22 cells. MTT cell viability assay showed that NPC CM + 3-MA was as protective as regular NPC CM (Fig. 30 B) against glutamate (5 mM) toxicity, even though a slight inhibitory effect on autophagy was detected by Western Blot in the cells exposed to EBSS (Fig. 29 A). Therefore it is concluded that autophagy induction by trophic factor withdrawal or serum deprivation has no impact on the protective effect of NPC CM in the model system of glutamate-induced oxidative stress.

3.2.2 Spermidine conditioned medium of HT-22 cells in the model system of glutamate-induced oxidative stress

Spermidine, a polyamine, found in all living organisms, is closely related to cellular growth. Recently, spermidine has been shown to increase the lifespan of yeast, nematodes, and flies in an autophagy-dependent fashion [203]. Spermidine was used to induce autophagy selectively in HT-22 cells. The aim was to investigate, if the preparation of spermidine conditioned medium (Sp CM) mediates neuroprotective effects that are dependent on autophagy activation.

3.2.2.1 Spermidine induces autophagy in HT-22 cells

First, the autophagic marker LC3 was analysed by immunoblot analysis and immunocytochemistry in spermidine treated cells. For this purpose, HT-22 cells were exposed to spermidine (Sp, 1 µM and 20 µM) and chloroquine (CQ, 10 µM) simultaneously. Ten h after the onset of spermidine and CQ, HT-22 cells were harvested and prepared for immunoblot analysis. As shown in Fig. 31 A, spermidine and CQ exposure increased LC3-II accumulation after comparison to control cells. This result was further confirmed with immunocytochemistry studies. As shown in Fig. 31 B, the punctuated LC3 staining increased in HT-22 cells exposed to 16 h of spermidine in comparison to control cells. To analyse effects of chloroquine on cell viability after spermidine treatment, MTT assay was performed 16 h after the treatment. Fig. 31 C showed that CQ had no effect on cell viability in glutamate treated cells. Altogether, these results indicated an increase in autophagic flux after spermidine exposure in HT-22 cells.

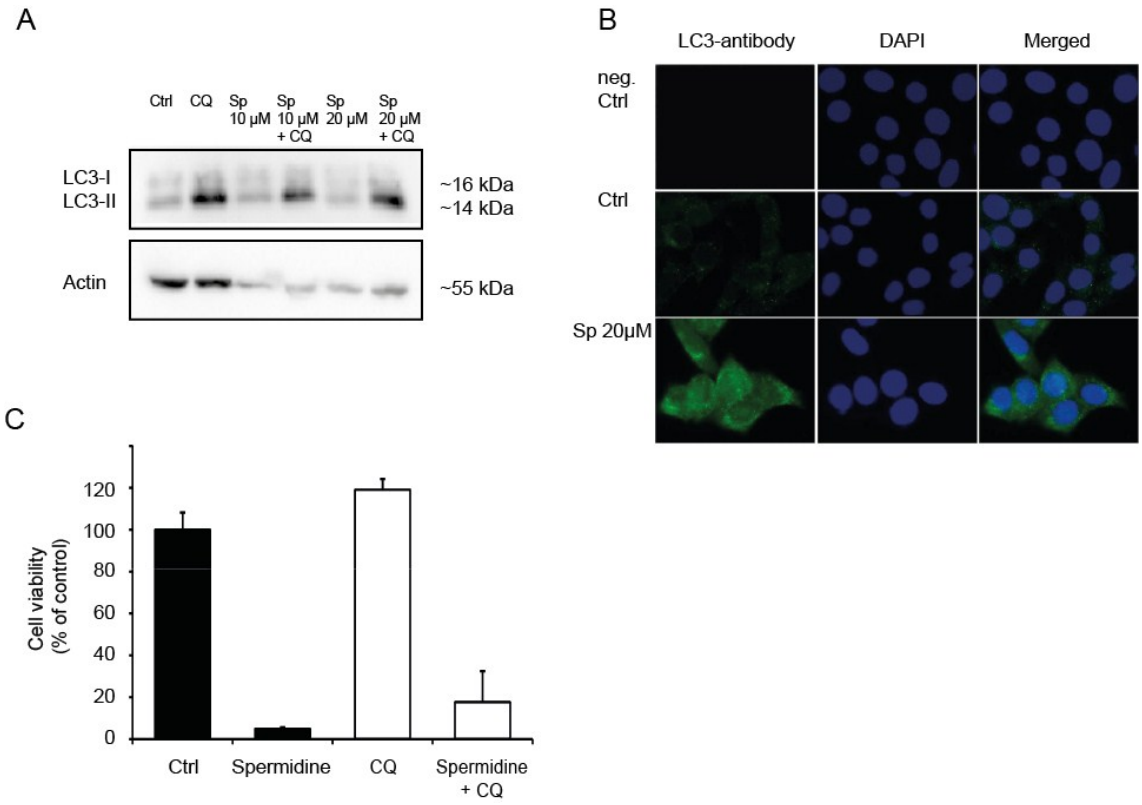

Figure 31. Induction of autophagy after spermidine treatment. A. Spermidine treatment induced autophagy in HT-22 cells. After incubation with spermidine (1 µM and 20 µM) with or without chloroquine (10 µM) for 16 h, cells were analyzed by immunoblot for LC3 conversion. Immunoblot of actin was used as a loading control. **B.** Formation of autophagosomes was increased after spermidine treatment. Immunocytochemistry was performed 16 h after spermidine (20 µM) treatment. The formation of LC3 dots inside of the cells, representing the recruitment of activated LC3 into autophagosomes, was examined by fluorescence microscopy. Bar scale 50 µm. **C.** Chloroquine treatment (10 µM) had no effect on cell viability after spermidine (20 µM) treatment. MTT assay was performed 16 h after the onset of spermidine.

3.2.2.2 3-MA protects HT-22 cells against spermidine-induced toxicity

Next, HT-22 cells were treated with spermidine at different concentrations ranging from 10 µM to 100 µM for 24 h. MTT assay revealed a dose dependent decrease of cell viability in HT-22 cells after the treatment of spermidine (Fig. 32 A). To exclude that spermidine toxicity in HT-22 cells is due to an increase of the pH of the medium after spermidine treatment, measurements of the pH were performed using the S20-SevenEasy™ pH meter (Mettler-Toledo GmbH, Giessen, Germany). Spermidine slightly increased the pH (control medium: 7.48, spermidine 100µM: 7.58), however this effect was not strong enough to induce cell death by a pH shift. Cellular death after the treatment with spermidine (50 µM) could be prevented with 3-MA treatment (5 mM). In contrast, the broad caspase inhibitor Qvd- OPh (40 µM) or the Bid inhibitor

BI-6C9 (10 µM) were not able to protect against neurotoxic effects of spermidine (Fig. 32 B). Real time impedance measurements using the xCELLigence system confirmed the neuroprotective effect of 3-MA (Fig. 32 C). Light microscopic analysis of cellular morphology of HT-22 cells after spermidine challenge and simultaneous 3-MA treatment completed the investigation of cell viability and verified the results from previous experiments (Fig. 32 D). These results further indicated that autophagy might be involved in the cell death mechanism of spermidine. Since 3-MA is not a selective inhibitor of autophagy, a gene silencing approach targeting regulator proteins of autophagy was obligatory to confirm involvement of autophagy in spermidine-induced cell death.

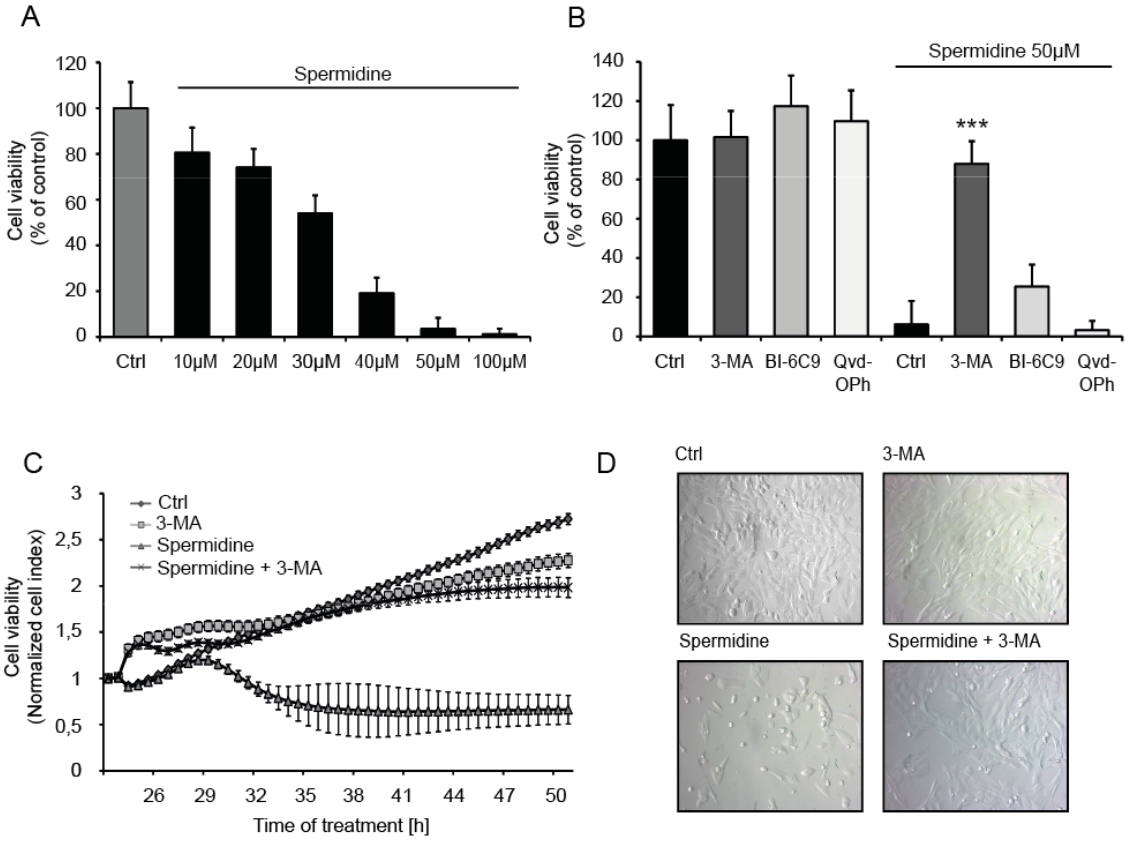

Figure 32. Neuroprotective effect of 3-MA against spermidine cytotoxicity. A. Dose dependent toxicity of spermidine after 18 h of treatment in HT-22 cells. Cell viability was determined using the MTT assay (n=8). **B.** 3-MA significantly prevented cell death following spermidine (50 µM) exposure. 3-MA (5 mM), Qvd-OPh (40 µM) and BI-6C9 (10µM) were added simultaneously with spermidine (50 µM) and the cell viability was measured after 18 h of glutamate exposure using MTT assay (n=8; ***$p<0.001$, compared to glutamate treated control, ANOVA, Scheffé test). **C.** xCELLigence real-time measurement of HT-22 cells treated with spermidine (50 µM) and 3-MA (5 mM) confirmed a neuroprotective effect (n=6). **D.** 3-MA preserved cellular morphologies following glutamate treatment.

3.2.2.3 HT-22 cells transfected with Beclin-1 siRNA and Atg5 siRNA in the model of spermidine toxicity

To inhibit the autophagic process selectively, siRNA targeting Beclin-1 and Atg5 was applied. The knockdown of total Beclin-1 and Atg5 in HT-22 cells was established previously (see chapter 3.1.3). For cell viability experiments, HT-22 cells were transfected with Beclin-1 or Atg5 siRNA (each 40 nM) in 96 well plates and then challenged with spermidine (25 µM) 48 h after transfection. Cell viability was quantified using the MTT assay 18 h after spermidine treatment. The selective knockdown of either Beclin-1 or Atg5 did not protect HT-22cells against spermidine-induced neurotoxicity (Fig. 33 A, B). These results indicated that autophagy is likely not involved in spermidine-induced neurotoxicity, however 3-MA mediated neuroprotection.

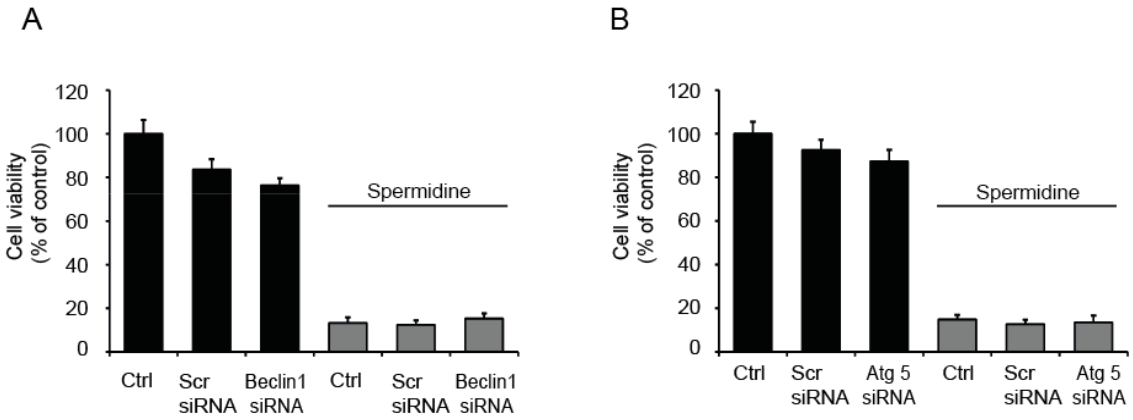

Figure 33. Beclin-1 or Atg5 knockdown did not prevent cell death after spermidine treatment. A. Beclin siRNA (40 nM) did not protect HT-22 cell against spermidine toxicity (25 µM). Cells were challenged with spermidine (25 µM) 48 h after siRNA transfection. Cell viability was determined using the MTT assay. **B.** Atg5 siRNA (40 nM) also did not protect HT-22 cell against spermidine toxicity (50 µM). Cells were challenged with glutamate 48 h after siRNA transfection. Cell viability was again determined using the MTT assay.

The mode of action of spermidine in the execution of cell death has to be further elucidated. Recent findings demonstrated that simultaneous treatment of glutamate (5 mM) and spermidine (25 µM) strongly increased neurotoxicity in HT-22 cells in comparison to single applications (Fig. 34), showing synergistic effects of both neurotoxic substances. This indicated two distinct mechanisms leading to HT-22 cell death. Spermidine-induced cell death is clearly neither dependent on caspases nor on autophagy (Fig 32 B, Fig 33 A, B).

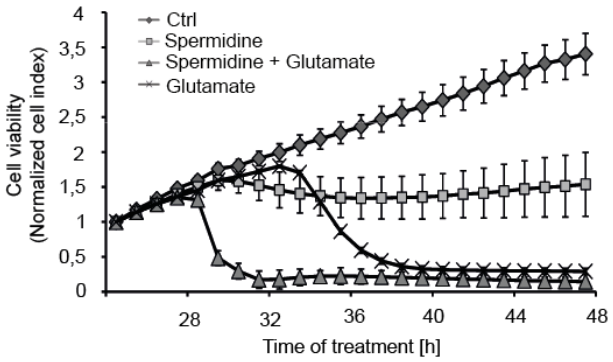

Figure 34. Simultaneous treatment of glutamate and spermidine. xCELLigence real-time measurement of HT-22 cells treated with spermidine (50 µM) and glutamate (5 mM) simultaneously showed stronger neurotoxicity compared to single application of each substance (n=6).

Because of recent findings showing that spermidine improved both survival and locomotor activity of the fruit fly Drosophila melanogaster upon exposure to paraquat [204], nontoxic concentrations of spermidine (1 µM, 10 µM) were used in the model system of glutamate toxicity in HT-22 cells.

In the model system of glutamate toxicity, spermidine did not exert neuroprotective effects (Fig. 35 A). This experiment was followed by the preparation of Sp CM from HT-22 cells (see chapter 2.1.2.5). With the preparation of Sp CM, the aim was to investigate, if the activation of autophagy via spermidine may lead to the release of neuroprotective substances, like it is described for NPC CM, thereby contributing to protection of HT-22 against glutamate toxicity. Spermidine CM prepared with low concentrations of spermidine did not mediate protection (Fig. 35 B), indicating that sole activation of autophagy to release protective substances out of cells into the medium is not sufficient to generate a neuroprotective CM.

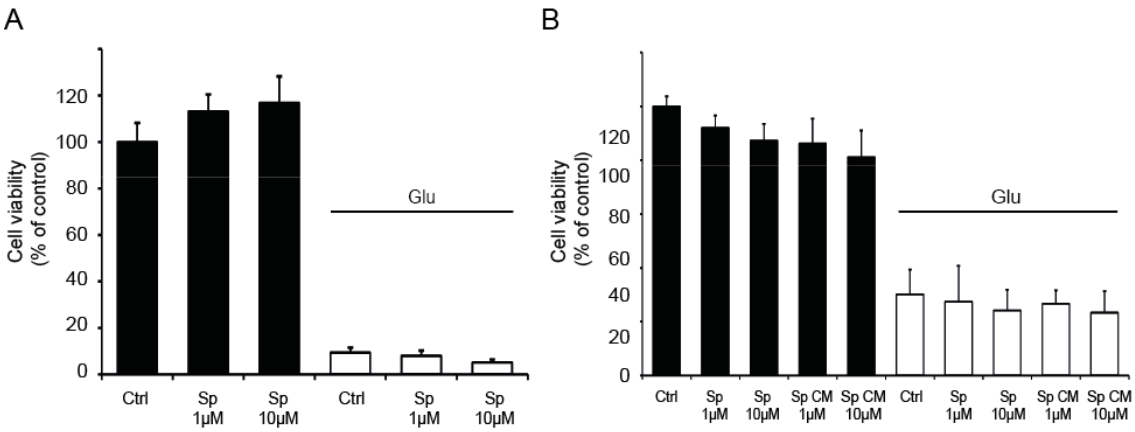

Figure 35. Low concentrations of spermidine are not neuroprotective. **A.** HT-22 cells were cotreated with spermidine (Sp, 1 µM, 10 µM) and glutamate (Glu, 7 mM). MTT analysis was performed 16 h after the treatment. **B.** Spermidine CM (Sp CM) was prepared with low concentrations of spermidine. HT-22 cells were pretreated 6 h with Sp CM and then challenged with glutamate (Glu, 5 mM). Cell viability was determined using the MTT assay 16 h after the onset of glutamate.

3.2.2.4 Spermidine CM from HT-22 cells is not as potent as NPC CM

Results obtained from NPC CM experiments revealed that caspase-dependent, apoptotic cell death of NPC was necessary to obtain neuroprotective NPC CM (see chapter 3.2.1.3). Therefore, Sp CM was prepared incubating HT-22 cells with a toxic concentration of spermidine (25 µM) in regular HT-22 growth medium. Conditioned medium was collected after 24 h, centrifuged, filtered and stored at -80°C until further use. The Sp CM was applied in the model systems of glutamate-induced cell death and spermidine-induced cell death. HT-22 cells were pre-treated with CM for 6 h before exposure to glutamate (5 mM) or spermidine (50 µM). Cell viability was determined 18 h after the onset of each treatment using the MTT assay. Sp CM protected HT-22 cells against spermidine toxicity (Sp 25 µM) but not against glutamate-induced toxicity (Fig. 36 A) or additional spermidine treatment (Fig. 36 B). In conclusion, Sp CM prepared from dying cells showed only moderate protective effects, but it was at least more potent than Sp CM obtained from HT-22 cells that were treated with nontoxic concentrations of spermidine. This finding confirmed that cell death was essential in order to produce substantial amounts of protective factors that enhance neuronal resilience. The content of protective substances in Sp CM, however, is likely very low, which would increase the difficulty of further analysis.

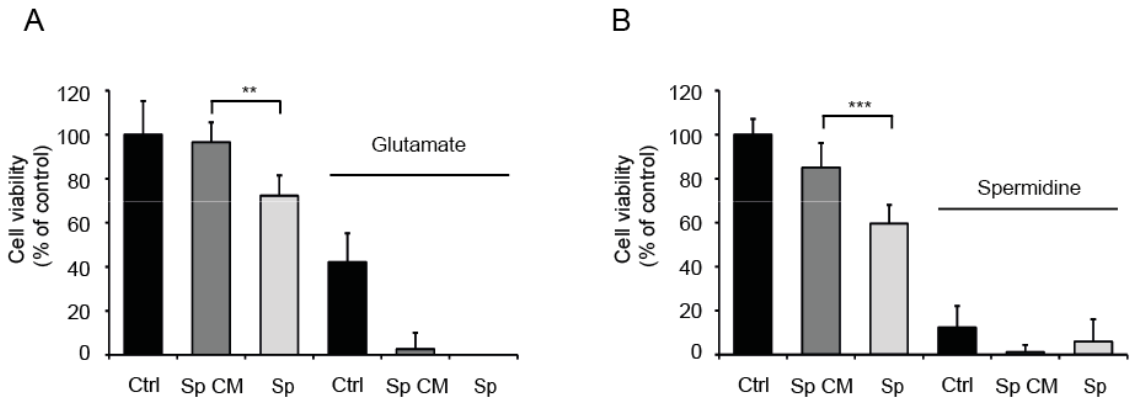

Figure 36. Effects of Sp CM in HT-22 cells. Cells were pre-treated with CM for 6 h before exposure to glutamate or spermidine. Cell viability was determined 18 h after the onset of each treatment. **A.** Sp CM protected HT-22 cells against spermidine toxicity (Sp, 25 μM) but not against glutamate-induced toxicity (5 mM). MTT assay was used to determine cell viability (**$p<0.01$ compared to spermidine control (Sp), n=8, ANOVA, Scheffé test). **B.** Sp CM protected HT-22 cells against spermidine toxicity (Sp, 25 μM) but not against additional spermidine treatment (50 μM). MTT assay was used to determine cell viability (***$p<0.001$ compared to spermidine control (Sp), n=8, ANOVA, Scheffé test)

4 Discussion

4.1 3-MA mediates neuroprotection independently of autophagy inhibition

The aim of the first part of this study was to analyze the role of autophagy in glutamate-induced neuronal cell death. The involvement of autophagy was characterized in immortalized mouse hippocampal HT-22 neurons. Glutamate clearly enhanced autophagy markers and induced cell death in HT-22 cells and PCN. Cell death was prevented by 3-MA, a widely used inhibitor of autophagy. Interestingly, 3-MA itself induced autophagy in HT-22 cells. A gene silencing approach targeting key regulators of autophagy reduced the autophagic flux, but failed to prevent cell death persistently. Further, the aim was to elucidate the exact mechanism of 3-MA mediated protection in the model system of glutamate neurotoxicity. 3-MA prevented the glutamate-induced ROS formation, the loss of ATP, and preserved the mitochondrial membrane potential as well as mitochondrial morphology.

The activation of the PI_3K/Akt pathway and the MAPK/Erk-1/2 pathway were excluded to play a role in 3-MA mediated neuroprotection. In conclusion, these data suggest that glutamate toxicity is associated with increased markers of autophagy. However, specific gene silencing of key regulators of autophagy did not provide protective effects, suggesting that the increased autophagic flux was dispensable for cell death induced by glutamate. Further the findings clearly demonstrate that protective effects by 3-MA occur independently of autophagy inhibition, although the compound is widely used as an inhibitor of autophagy.

4.1.1 Glutamate induces autophagy in HT-22 cells

HT-22 cells do not express ionotropic glutamate receptors such as NMDA receptors or AMPA/Kainate receptors. Therefore, glutamate cannot induce rapid calcium influx and excitotoxicity in HT-22 cells but mediates cellular death by inhibition of cystine import and subsequent GSH depletion. GSH is an important antioxidative system that also regulates the activity of GPx4 and thus indirectly the activity of 12/15 lipoxygenases (12/15-LOX) [164–166]. Activation of 12/15-LOX leads to excessive accumulation of ROS and cellular death [166]. The present study further revealed that glutamate-induced oxidative stress also activated autophagy in HT-22 cells (Fig. 4). In recent publications,

ROS were found to regulate autophagy. For example, starvation was found to stimulate ROS formation. These oxidative conditions were essential for the modulation of a core protein of the autophagic machinery, thereby leading to autophagy activation [59]. Also both, exogenously added hydrogen peroxide (H_2O_2) and endogenous superoxide ($O_2^{\bullet-}$) produced in the mitochondria have been previously shown to upregulate the formation of autophagosomes [205, 206].

Markers for autophagy induction including LC3 conversion, suppression of the mTOR pathway, and GFP-LC3 dot formation were enhanced by glutamate treatment in HT-22 cells [207]. Activation of autophagy markers like Beclin-1 and LC3 were also found by Kumari *et al*. after glutamate treatment [208]. Contrary results were reported by Kubota *et al*., who demonstrated that glutamate did not stimulate autophagy in HT-22 cells [209]. Since LC3-II itself is degraded by autophagy, LC3 immunoblotting is sometimes interpreted inappropriately. Increased levels of LC3-II do not necessarily indicate enhanced autophagic flux by glutamate, but may also reflect reduction in autophagosome turnover or the inability of turnover to keep pace with increased autophagosome formation [45]. Therefore, CQ was applied to investigate whether in the present model system glutamate increased autophagic flux. The antimalarial drug CQ is a weak base accumulating in acidic organelles like lysosomes. The compound elevates lysosomal pH and thereby inhibits autophagy at the step of lysosomal degradation of its substrates [185, 186]. The strong accumulation of LC3-II in Western blot and the strong increase in dot formation detected by immunocytochemistry after simultaneous treatment with glutamate and CQ indicated and increase in autophagic flux by glutamate (Fig. 4). The accumulation of LC3-II in control cells treated with CQ suggested a high basal level of autophagy in the HT-22 cell line, indicating important physiological functions for autophagy in the maintenance of HT-22 cells under standard culturing conditions.

4.1.2 Glutamate does not induce autophagic cell death

The widely used inhibitor of autophagy, 3-MA, suppresses the activity of Vps34, a class III phosphoinositide-3-kinase (PI_3K) that interacts with Beclin-1 in vesicle nucleation during autophagy induction [12, 210]. Inhibition of autophagy by 3-MA was demonstrated in many previous studies. For example, 3-MA reduced autophagy in HT-

22 cells in the model system of serum deprivation [211]. There, addition of 3-MA led to a potentiation of cell death induced by serum deprivation in the HT-22 cells. Further, 3-MA was reported to promote neuroprotection against glutamate in HT-22 cells [207, 209], which is in line with the present results (Fig. 8). Recent studies involving striatal injections of kainate [212] or quinolate [213] showed neuroprotection by 3-MA. Similar protection has been obtained in with 3-MA in various models of focal cerebral ischemia [214–216].

Interestingly, 3-MA was also found to promote autophagic flux when MEFs or LC929 cells were treated under nutrient rich conditions [217], indicating a dual role of 3-MA regulating the autophagic process. The results from the present study also suggested an increase of autophagic flux after 3-MA treatment (Fig. 7), suggesting that 3-MA is not a specific inhibitor of autophagy and that 3-MA did not mediate neuroprotection against glutamate toxicity specifically through autophagy inhibition in HT-22 cells. Activation of autophagy through 3-MA treatment is possible through inhibition of class I PI_3K (Fig. 14) and its downstream target mTOR [68, 69].

In a selective approach to inhibit autophagy, the knockdown of total Beclin-1, Atg5 or LC3 protein reduced autophagic activity, but these approaches were not able to protect HT-22 cells against glutamate-induced oxidative stress (Fig. 11). This result strongly suggested that glutamate-induced oxytosis did not require autophagic cell death, despite the detected increase in autophagic activity after the glutamate treatment. Hence, the increase in autophagic activity may be associated with oxytosis, but is not a major cause of this form of oxidative cell death.

Further, additional treatment with 3-MA in Atg5 or Atg5/Beclin-1 siRNA transfected cells did not affect neuroprotection mediated by 3-MA (Fig. 11). Interestingly, Beclin-1 siRNA treatment increased 3-MA mediated neuroprotection against glutamate toxicity. The finding that Beclin-1 and not Atg5 downregulation increased 3-MA mediated neuroprotection suggested different functions of these proteins in autophagy-dependent or autophagy-independent processes [218]. Taken together, these results indicated that inhibition of autophagy did not primarily mediate neuroprotection by 3-MA against glutamate toxicity.

After serum deprivation (SD) in HT-22 cells, 3-MA was not able to mediate neuroprotection. Unexpectedly, 3-MA even provided a potentiation of cell death

induced by serum deprivation [211], which is in line with our results (data not shown). In a gene silencing approach to inhibit autophagy in the model system of starvation, no protection was achieved (Fig. 13), which emphasizes that the autophagic process is rather pro-survival than detrimental to HT-22 cells. Thus, classic induction of autophagy via starvation or glutamate treatment did not induce autophagic cell death. All cases of cell death that exhibit markers of autophagy such as the lipidation of LC3, but cannot be blocked by autophagy inhibition, should not be classified as autophagic cell death [92]. The massive accumulation of autophagolysosomes after serum deprivation [211] or glutamate treatment (Fig. 4) rather indicated the ultimate attempt to survive by adapting to stress and not to execute cell death. Moreover, the role of autophagy as a protective mechanism in several types of neurodegenerative conditions is well recognized, where it functions to remove ubiquitin aggregates, preventing neuronal degeneration. Consistent with this, loss of function of Atg5 and Atg7 causes neuronal loss and neurodegeneration [26, 27, 29]. Kuma *et al*. showed in 2004 [219], that mice lacking an autophagy related gene (Atg5) are not able to survive longer than 12 h after birth because of nutrient shortage. They concluded that nutrient supply by autophagy was essential for survival.

4.1.3 Class III PI_3K is not affected through 3-MA in HT-22 cells

It has been established that 3-MA acts via interference with class III PI_3K, hVps34 [220]. Recently, inhibition of class III PI_3K through 3-MA was observed only transiently [217]. In a model system of H_2O_2-toxicity, inactivation of the Vps34/phosphatydil-inositol-3-phosphate kinase (PI_3K) III signaling pathway, either by pharmacologic inhibition with 3-MA or by transgenic expression of a dominant-negative Vps34, prevented the onset of autophagy and protected dopaminergic neuroblastoma cells [221]. In the model system of glutamate toxicity, inhibition of class III PI_3K activity using siRNA did not protect HT-22 cells (Fig. 14). Additionally, no change of the neuroprotective effect of 3-MA against glutamate was observed in class III PI_3K siRNA treated cells.

In conclusion, 3-MA mediated neuroprotection against glutamate toxicity is not mediated through class III PI_3K inhibition, further indicating that autophagy-independent mechanisms mediated neuroprotection by 3-MA.

4.1.4 The PI_3K/Akt and the MAPK/Erk-1/2 signaling pathways are not involved in 3-MA mediated neuroprotection

The PI_3-K/Akt and the MAPK/Erk-1/2 pathways are the most prominent survival signaling cascades that can be stimulated in neurons by a wide variety of cytokines or growth factors [189, 201]. In this study, inhibition of class I PI_3K and the downstream target Akt, was conducted using LY294002. LY294002 did not protect HT-22 cells against glutamate and decreased 3-MA mediated neuroprotection against glutamate-induced toxicity (Fig. 15). At first, this result indicated that 3-MA is a positive regulator of the PI_3K/Akt pathway. However, this result can also suggest an additive inhibitory effect by 3-MA on the PI_3K/Akt pathway.

The investigation of direct effects on p-Akt protein levels in our system revealed that 3-MA decreased p-Akt levels in the presence and absence of glutamate (Fig. 15 C, D). Together, these results demonstrated that 3-MA is rather a negative regulator of the PI_3K/Akt pathway. Nevertheless, it is unlikely that negative regulation of the PI_3K/Akt pathway is the main mechanism for 3-MA-mediated neuroprotection. For instance, LY924002, which also decreases Akt phosphorylation, was not protective against glutamate toxicity (Fig. 15 A, B). This is in line with a large body of evidence showing that activation of the PI_3K/Akt signaling cascade mediates survival in neurons [222].

In addition, the MAPK/Erk-1/2 pathway was intensively studied to investigate its contribution for pro-survival signaling in different types of cultured cells, including neurons. It is well documented that activation of MAPK/Erk-1/2 mediated neuroprotection in cultured neurons [223, 224]. The MAPK/Erk-1/2 pathway has also been implicated in glutamate-induced oxidative stress in HT-22 cells. U0126, a specific inhibitor of the ERK-activating kinase MEK-1/2 protected both HT-22 cells and immature primary cortical neuron cultures from glutamate toxicity [225, 226].

Glutamate was also reported to cause a biphasic activation of Erk-1/2 in HT-22 cells. According to these studies, the initial peak of Erk-1/2 activation plays a protective role whereas the second peak was caused by prolonged oxidative stress and mediates cell death [226].

In our system, 3-MA transiently enhanced phosphorylation of MAPK/Erk-1/2 within 30 min (Fig. 16). Erk-1/2 signals declined to control levels already after 1 h. This finding

suggested a transient activation of Erk-1/2 by 3-MA. In a pharmacological approach, the specific MEK 1 inhibitor PD98059 protected HT-22 cells against glutamate-induced oxidative stress, indicating that the underlying mechanism of protection was rather dependent on inhibition of the MAPK/Erk-1/2 pathway (Fig. 15). This result is in line with a previous study that showed, that MAPK/Erk-1/2 pathway is implicated in glutamate-induced oxidative stress HT-22 cells [225]. However, it cannot be excluded if the transient activation of Erk-1/2 by 3-MA after 30 min did contribute to neuroprotection in the model system of glutamate toxicity in HT-22 cells.

Further, the AMP-activated protein kinase (AMPK) signaling pathway was investigated after 3-MA treatment. Recent studies revealed that AMPK activation is implicated in the regulation of neuronal survival and as a key player during ischemic stroke [227]. In addition to Akt, AMPK is one of the main regulators of mTOR. In response to increases in AMP/ATP ratio, AMPK preserves intracellular energy substrate levels by switching off ATP-requiring processes, while switching on ATP-generating catabolic pathways, such as autophagy [228].

AMPK activation may have dual functions in the regulation of neuronal survival [227]. AMPK provides neuroprotective effects during transient energy depletion in a model of intracellular Ca^{2+}-overload, and this effect is partially mediated by the activation of neuronal glucose transporter 3 [229]. In contrast, prolonged AMPK activation can lead to neuronal apoptosis via the transcriptional activation of the proapoptotic Bcl-2 family member Bim [230].

The results of the present study show that 3-MA decreased AMPK phosphorylation transiently (Fig 16), suggesting that the inhibition of the AMPK signaling pathway is likely involved in 3-MA mediated neuroprotection in the model system of glutamate toxicity in HT-22 cells. Further investigations are necessary, however, to confirm the involvement of the AMPK pathway in 3-MA mediated neuroprotection.

Still, the exact mechanisms of 3-MA-mediated neuroprotection in the present model system of glutamate-induced oxytosis are currently unknown. Remarkably, induction of autophagy and other cellular actions via persistent inhibition of class I PI_3K and independent of autophagy inhibition were detected after 3-MA treatment. For example, autophagy promotion activity of 3-MA was found to be due to its differential temporal effects on class I and class III PI_3K; 3-MA blocks class I PI_3K persistently, whereas its

suppressive effect on class III PI_3K is transient [217]. Additionally, 3-MA can affect glycogen metabolism, lysosomal acidification [70], endocytosis [71, 231] and the mitochondrial permeability transition [72]. 3-MA can suppress proteolysis even in Atg5-deficient cells, suggesting that 3-MA may have some additional effects on protein degradation other than autophagy [48].

4.1.5 Modulation of mitochondrial parameters through 3-MA treatment

Mitochondria are crucial organelles in every cell as they are the primary source of energy, and they are involved in many catabolic and anabolic reactions of different metabolites, the regulation of ROS metabolism and calcium homeostasis. In addition to their central role in various biochemical pathways, mitochondria are key regulators of development, aging and programmed cell death, in particular in neurons [232].

Mitochondria are dynamic organelles that undergo permanent fission and fusion under physiological conditions. In damaged neurons, however, this dynamic process is disturbed leading to excessive fragmentation of mitochondria and thereby promoting cell death progression [233–235]. Although the mechanisms controlling mitochondrial morphology under pathological conditions are only partly known, increasing evidence suggests a potential role for oxidative stress and impaired bioenergetics as potential triggers of mitochondrial fission in the cell death program [182].

The present study demonstrated that glutamate-induced cell death was associated with mitochondrial fragmentation, mitochondrial membrane depolarization, ROS production, decreased ATP levels and elevated mitochondrial oxygen consumption (Fig. 18, 19, 20), and disturbance of the mitochondrial dynamic balance towards fission. These effects were prevented by 3-MA. These data suggested that 3-MA modulated regulators of mitochondrial damage that mediate enhanced mitochondrial fission, loss of mitochondrial integrity, loss of energy (ATP), increased ROS production, and elevated mitochondrial oxygen consumption. The exact link between the major survival signaling pathways of 3-MA and mitochondrial signaling in HT-22 cells needs to be further elucidated.

4.1.6 Conclusion and Outlook

In summary, the findings of this part of the thesis work demonstrated that glutamate activated hallmarks of the autophagy machinery in HT-22 cells during cell death. The detected autophagy, however, did not cause cell death and was dispensable for execution of oxytosis. As an intracellular mechanism, the observed induction of autophagy rather indicated the ultimate attempt to survive by adapting to stress and enhancing cellular resilience. Autophagy plays a major role for cellular homeostasis, however in the present model system of oxytosis the autophagy induction was insufficient to ultimately prevent glutamate-induced cell death.

Following established protocols, 3-MA was used in the present study as a tool to inhibit autophagy in glutamate-induced cell death in HT-22 cells. The results of this thesis strongly suggest that 3-MA is not a selective inhibitor of autophagy. In contrast, 3-MA mediated its neuroprotective effect against glutamate toxicity in HT-22 cells independently of autophagy inhibition. The protective effects of 3-MA were associated with the inhibition of PI_3K/Akt and the AMPK pathways and transient activation of the MAPK/Erk-1/2 signaling pathway. Nowadays, 3-MA is used frequently in experimental studies *in vivo* and *in vitro*. Based on the present findings, caution is recommended in the interpretation of data obtained with 3-MA in the context of autophagy studies, in particular, if mitochondrial alterations are connected.

Due to the importance of autophagy for cellular homeostasis, development and survival, and the knowledge that impaired autophagy can contribute to the pathology of various diseases, research in the field autophagy is increasing continuously. Besides *in vitro* and *in vivo* animal studies, first clinical trials were registered recently. To date, 45 clinical trials are registered at http://clinicaltrials.gov involving autophagy modulation. In most trials the drug hydroxychloroquine is used. Hydroxychloroquine is a drug that has been used to treat malaria and rheumatism [236, 237]. It has been recently discovered that hydroxychloroquine inhibits autophagy [186]. In the majority of trials different forms of cancer are in the focus for investigation. Cancer cells use autophagy to survive chemotherapy or hormonal therapy [238]. Also, cancer cells use autophagy to survive in areas of a tumor where there is a low oxygen level [239]. Recent medical science suggests that it is possible to make anticancer therapy work better if autophagy is blocked. The investigators aim to elucidate if blocking autophagy while giving standard

treatment for the particular type of cancer will improve the treatment (NCT00933803, NCT00765765 and others). Another study focuses on the influence of autophagy in nonalcoholic Fatty Liver Disease (NCT01988441). Also, the effect of low protein diet to correct defective autophagy in patients with collagen VI related myopathies in Phase II was investigated (NCT01438788). No clinical trials were found so far that focused on AD, PD or other neurodegenerative diseases that involved the modulation of the autophagic process. This is may be attributed to opposing roles of autophagy as a regulator of cellular homeostasis and resilience in healthy neural tissue in contrast to impaired autophagy as a mechanism of cell death in neurological diseases. For further studies, the development of therapeutic strategies will need to take into account these opposing roles of autophagy.

4.2 Conditioned medium of neuronal cell lines as a therapeutical option for neurodegenerative diseases

Beneficial effects of neuronal progenitor cell (NPC) transplantation have been well established in animal models of acute brain damage. Since only very few NPC cells survive intracerebral transplantation, enhanced neurogenesis may only play a minor role for the observed functional and histological protection of brain tissue. Thus, induction of cell death by trophic factor withdrawal was performed in the present study to mimic the conditions after neural progenitor cell injection. The CM obtained from this *in vitro* approach should contain the putative protective factors that are also delivered by dying NPC in the cellular grafts *in vivo*.

Deprivation of growth factors promoted cellular death of NPC that was accompanied by caspase-3 activation and PARP cleavage. Cell death of NPC was prevented by the broad caspase inhibitor Ovd-OPh. Conditioned medium that was prepared during NPC starvation protected HT-22 cells against glutamate-induced neurotoxicity. Further, heating of NPC CM abolished the protective effect of NPC CM, indicating that proteins were likely responsible for the neuroprotective effect. Apoptotic bodies and also the mechanism of autophagy induction play only a minor role for the mediation of protective effects of NPC CM. In primary neurons, the most prominent pro-survival signaling pathways, namely the PI_3K/ Akt pathway and the Erk 1/2 pathway, were activated upon NPC CM treatment. In a different approach, CM of HT-22 cells exposed to induction of autophagy by spermidine was tested for its ability to mediate neuroprotection. It has been shown previously that spermidine induced autophagy, which increased life span and showed protective effects in several animal models from flies to mice [203]. In the HT-22 cells, spermidine mediated a dose-dependent toxicity, but did not mediate protective effects by itself. 3-MA prevented spermidine-induced toxicity in an autophagy independent manner. The protective effects mediated by Sp CM were not as potent as protection achieved with NPC CM.

In summary, these data demonstrated that CM of NPC and HT-22 cells mediated neuroprotective effects in the model system of glutamate toxicity in PCN and HT-22 cells. Therefore, conditioned medium could serve as potent therapeutical option to treat acute or chronic neurodegenerative diseases that are accompanied by oxidative stress and excitotoxicity.

4.2.1 NPC conditioned medium mediates neuroprotective effects

Nowadays, stem cell based therapy represents a powerful new therapeutic option for the treatment of neuronal diseases. Stem cells and progenitor cells have the potential to enhance neurorestorative processes like neurogenesis, angiogenesis and modulation of inflammation or trophic support, thus facilitating functional recovery and neuroprotection [128–131].

In fact, however, most cells die after transplantation *in vivo* [149] suggesting that the beneficial effect after transplantation is rather mediated by released protective and/or trophic factors than neuron replacement. In the present study an *in vitro* model system was developed to mimic the conditions of stem/progenitor cell transplantation. The NPC were deprived of growth factors, which induced caspase dependent apoptotic cell death (Fig. 21). Caspase-dependent apoptotic cell death after serum deprivation was already described in mesenchymal stem cells [240] and several other types of stem cells suggesting similar mechanisms for serum deprivation-induced cell death in NPC.

In the present model system of serum deprivation-induced cell death in NPC, Qvd-OPh mediated a partial protection (Fig. 23) and prevented the cleavage of caspase-3 and PARP (Fig. 22). Active caspase-3 is a key mediator of apoptosis in mammalian cells and responsible for the proteolytic cleavage of many key proteins such as caspase-6, -7 and -9 or the nuclear enzyme PARP [195]. PARP is activated in different paradigms of cellular stress, mediating either repair mechanisms or cell death, depending on the context and the strength of the stress stimulus. Cleavage of PARP serves as a marker of cells undergoing caspase-dependent apoptosis [196].

Medium from dying NPC (NPC CM) was found to mediate neuroprotection in the model systems of oxidative stress and excitotoxicity in neurons (Fig. 24 A, B). Moreover, Eva Öxler demonstrated in our laboratory that the rescue of NPC from starvation by the caspase inhibitor Qvd-OPh abolished the neuroprotective effect of NPC CM [199], indicating that caspase-dependent cell death was essential for generating the highly protective NPC CM.

Previous studies using conditioned medium from a variety of different stem cells also demonstrated protective effects. For example, a previous study in our laboratory showed that application of adult bone marrow stromal cells (BMSC) CM attenuated staurosporine (STS) or amyloid-beta peptide-induced apoptosis and triggered

endogenous survival signaling pathways that mediate protection against apoptotic insults in primary embryonic rat neurons [154]. Others showed that NSC conditioned medium (NSC CM) was neuroprotective *in vitro,* in a model of Huntington's disease [157]. In another study with human MSCs CM, the authors found that MSCs secrete brain-derived neurotrophic factor (BDNF) which promoted neuronal survival in cultured rodent cortical neurons against trophic factor withdrawal or nitric oxide (NO) exposure [160]. Further, BMSC CM that contained insulin-like growth factor (IGF)-1, hepatocyte growth factor (HGF), vascular endothelial growth factor (VEGF), and transforming growth factor (TGF)-β1, promoted neuronal survival and neurite outgrowth in hippocampal neurons [241].

Together, these data suggested that dying NPC secrete substances that protect neighboring cells. It turned out that NPC CM is an adequate tool for the investigation of the factors and mechanisms mediating protective effects after stem/progenitor cell transplantation *in vitro*.

4.2.2 Characterization of the protective effect of the NPC CM

The hypothesis that NPC secrete protective factors during cell death led to further experiments that focused on the analysis of the composition of the NPC CM and the related mechanisms of protection. During the previous characterization process of BMSC CM [154], heating over 90°C abolished the neuroprotective effect of BMSC CM, suggesting that heat labile factors, i.e. proteins, released by BMSC mediated the observed anti-apoptotic effect in the neurons. In mammalian cells, enzymes and proteins show a functional optimum around 35-40°C and they denature if exposed to temperatures higher than 60°C. During denaturation, proteins lose their quaternary, tertiary and secondary structure, which typically results in the loss of their biological function. The loss of biological function is irreversible, if the protein cannot regain its native state when the denaturing influence is removed. The thermostability of proteins depends on various factors such as amino acid composition, hydrophobic interactions, ion pairing or hydrogen bonds within the protein [242]. Heat exposed NPC CM (95°C for 30 min) no longer protected HT-22 cells in the model of glutamate-induced neurotoxicity (Fig. 26). This result clearly indicated an involvement of proteins for NPC

CM mediated neuroprotection, which was further confirmed in our laboratory by Eva Öxler [199].

Apoptotic bodies have been demonstrated to enhance the differentiation of human endothelial progenitor cells *in vitro* [198]. Isolated apoptotic bodies that were obtained after serum deprivation-induced cell death in NPC did not mediate neuroprotection [199]. Further, Y-27632, which blocks the formation of apoptotic bodies, did not affect the protective effects of CM against glutamate-induced toxicity. However, treatment with Blebbistatin revealed a decrease in the protective effect of NPC CM, indicating that apoptotic bodies may partly participate in NPC CM mediated neuroprotection.

To test the specificity of NPC CM, mouse embryonic fibroblast CM (MEF CM) was compared to NPC CM in the model system of glutamate toxicity in HT-22 cells. MEF CM was much less protective than regular NPC CM indicating that neuronal progenitor cells are necessary for the production of potent CM (Fig. 25). Additionally, Eva Öxler found that also CM prepared from HT-22 cells and other neuronal stem cell lines mediated neuroprotective properties during starvation [199], which approved that the protective effect is specific for neuronal cells or stem/progenitor cells.

Prosurvival signaling pathways linked to CM-mediated neuroprotection are the PI_3K/Akt and the MAPK/Erk-1/2 pathway. The PI_3-K/Akt and the MAPK/Erk-1/2 pathways are important survival signaling cascades that can be stimulated in neurons by a variety of cytokines or growth factors [189, 201]. As a proto-oncoprotein and the primary target of PI_3K, Akt was first characterized for its function in regulating cell survival and cell proliferation in neurons [222]. Constitutive activation of Akt signaling is sufficient to block cell death induced by a variety of apoptotic stimuli [243]. It was already described that also activation of MAPK/Erk-1/2-mediated neuroprotection in cultured neurons [223, 224] and in models of cerebral ischemia *in vivo* [244, 245].

In the primary neurons, phosphorylation of Akt and Erk-1/2 increased within 10 min up to 120 min after exposure to NPC CM (Fig. 28). These findings implicated that NPC secrete neuroprotective factors that may stimulate neurotrophin-like survival signaling thereby contributing to the protective effects against growth factor withdrawal and glutamate neurotoxicity. This assumption was supported by size exclusion filtration experiments that indicated that the components of CM mediating the neuroprotective

effect have a molecular size between 10 and 50 kDa [199]. Growth factors like BDNF, VEGF, EGF or FGF have a molecular weight between 6 kDa and 27 kDa. However, it is conceivable that also substances with another molecular weight may contribute to or reinforce the potency of NPC CM. Also the finding that proteins are likely responsible for the mediation of neuroprotection of NPC CM support the hypothesis that growth factors or neurotrophins participate in the survival signaling of NPC CM. Heating of NPC CM to 95°C abolished its neuroprotective effect (Fig. 26). Though, heating of NPC CM to 50-80°C further increased the protective effect against glutamate-induced neurotoxicity [199]. This thermostability was so far not demonstrated for growth factors. Moreover, the recombinant growth factor BDNF did not protect HT-22 cells against glutamate toxicity, because HT-22 cells do not express functional TrkB receptors [246]. Further, MALDI TOF analysis revealed that NPC CM did not contain growth factors like BDNF, VEGF, EGF, FGF or NGF. So far, Peroxiredoxin-1 and galectin-1 were found that are jointly responsible for mediating neuroprotection [199].

4.2.3 Autophagy induction does not contribute to the protective effect of NPC CM

Autophagic activity is essential for numerous physiological processes, including cell survival, cell metabolism, development, aging and immunity, and is generally considered to mediate cell survival [12]. Starvation is the best characterized inducer of autophagy [58]. Here, starvation of NPC was achieved by growth factor deprivation leading to caspase-dependent apoptotic cell death. This process was accompanied with a clear increase of autophagic activity (Fig. 29). Inhibition of autophagy with 3-MA did not protect NPC against EBSS-induced starvation, indicating that starvation did not induce autophagic cell death. NPC CM that was prepared with 3-MA still protected HT-22 cells against glutamate- induced toxicity (Fig. 30), which indicated that the process of autophagy was not essential for the mediation of neuroprotection through NPC CM.

So far, the mechanisms underlying the neuroprotective effect of NPC CM are not fully understood and are matter of ongoing studies.

4.2.4 Spermidine conditioned medium is not neuroprotective in the model system of glutamate toxicity

However, the induction of autophagic activity by starvation in NPC was not essential for the protective effect of NPC CM in the model system of glutamate-induced oxidative stress, spermidine was used to induce autophagy selectively in HT-22 cells. The aim was to investigate, if the preparation of spermidine conditioned medium (Sp CM) mediated neuroprotective effects that were dependent on autophagy activation.

Spermidine (Sp) is a ubiquitous polycation that is synthesized from putrescine and serves as a precursor of spermine. Putrescine, spermidine and spermine are polyamines that play a role in multiple biological processes. Spermidine has recently been shown to promote longevity across species in an autophagy-dependent manner [203, 247]. The regulatory mechanism underlying this effect might be of epigenetic origin. In yeast, spermidine inhibits the activity of histone acetyltransferases and leads to a global hypoacetylation of histone H3 at all acetylation sites spanning the N-terminus of the histone. Thus, the promoter of the *ATG7* gene required for autophagy is hyperacetylated after post-treatment with spermidine. These results support that spermidine activates a global transcriptional response which may involve epigenetic regulation [247].

Genetic inactivation of genes essential for autophagy abolishes the life span-prolonging effect of spermidine in yeast, nematodes and flies [248]. Additionally, spermidine improved both survival and locomotor activity of the fruit fly Drosophila melanogaster upon exposure to paraquat [204]. Simple spermidine feeding not only restored juvenile polyamine levels, but also suppressed age-induced memory impairment [249].

These findings complement expanding evidence that autophagy mediates cytoprotection against a variety of noxious agents and can confer longevity when induced at the level of the whole organism.

In HT-22 cells, spermidine induced an increase of LC3-II accumulation (Fig. 31), indicating activation of autophagy also in the presently used system of neuronal cells. Dose-dependent cell death after the challenge of spermidine was prevented with 3-MA (Fig. 32), but not with siRNA targeting key regulators of autophagy, namely Beclin-1 and Atg5 (Fig. 33), which further proves the theory that autophagy is rather protective than detrimental to cells.

In the present study, subtoxic concentrations of spermidine, which were previously reported to promote longevity and mediate both survival and locomotor activity of the

fruit fly Drosophila melanogaster upon exposure to the superoxide generator and neurotoxic agent paraquat [204], could not mediate neuroprotection in the model system of glutamate-induced oxidative stress (Fig. 35 A). This result suggested that spermidine has various functions in different cell types independent or dependent of autophagic activity. With the preparation of Sp CM, the aim was to investigate, if autophagy activation in HT-22 cells leads to the release of neuroprotective substances. Spermidine CM prepared with low concentrations of spermidine did not mediate protection (Fig. 35), indicating that sole activation of autophagy to release protective substances out of the cell into the medium is simply not enough to promote survival.

As outlined before, results obtained from NPC CM experiments revealed that cell death of NPC was necessary to obtain conditioned medium that promoted neuronal survival [199]. However, Sp CM obtained from dying HT-22 cells did not protect cells against glutamate induced toxicity or spermidine toxicity, and it was only protective in the control groups in comparison to the regular spermidine treatment (Fig. 36). In conclusion, Sp CM prepared from dying cells exerted only moderate effects, but was at least more potent than Sp CM from HT-22 cells that were alive. This weak neuroprotective effect of Sp CM is likely due to cell death of the HT-22 cells which released protective factors and, therefore, this effect is unlikely specific for spermidine treatment. Therefore, autophagy can rather be excluded as the mediator of neuroprotection. Additionally, Eva Öxler already demonstrated that CM from HT-22 cells that underwent starvation was protective against glutamate toxicity [199]. Although starvation and spermidine treatment led to cell death, the CM obtained from these two processes act differently in the model system of glutamate toxicity. A problem of Sp CM might be that it was not possible to remove spermidine from CM. Attempts were made to remove spermidine from CM with cut off filtration experiments (Milipore, 3kDA filter). Unfortunately spermidine accumulated in the concentrate of the filter, likely due to interactions with the membrane of the filter tube. The filtrate was not protective and the concentrate was toxic, likely because spermidine accumulated in the supernatant and that was further accompanied by a strong pH elevation.

In addition to the life span-prolonging effects, improved survival and locomotor activity and suppression of age-induced memory impairment of PAs in several *in vitro* model systems, recent findings demonstrated that PAs were also involved in the direct or

indirect regulation of programmed cell death (PCD). Direct correlation of PAs with cell death refers to their association with particular biological processes, and their physical contact with molecules or structures involved in cell death. Indirectly, PAs regulate PCD through their metabolic derivatives, such as catabolic and interconversion products. Cytotoxic products of PA metabolism are involved in PCD cascades, whereas it remains largely elusive how PAs directly control pathways leading to PCD [250]. Caspase-dependent and independent apoptotic cell death was already observed after treatment with several PA analogues [251]. PAs could contribute directly to PCD through their regulatory effect on ion channels. For example, spermine directly regulates acid sensing anion channels on neurons that are involved in PCD induction [252]. Surprisingly, both activation and prevention of apoptosis due to PA depletion are reported for several cell lines, but also elevation of PA levels may lead to apoptosis or to malignant transformation [253]. In mammals, the PA-dependent PCD perhaps involves mitochondrial dysfunction. Polyamine oxidation results in mitochondrial dysfunction and related intrinsic cell death pathways [254, 255].

So far, PA treatment was not regularly used as a model system to induce neurotoxicity in HT-22 cells. Therefore, further experiments aimed on the investigation of the molecular mechanism of spermidine toxicity in HT-22 cells. Dose-dependent cell death after the challenge of spermidine was caspase-independent and Bid-independent and could be prevented with 3-MA treatment (Fig. 32), but not with siRNA targeting key regulators of autophagy, namely Beclin-1 and Atg5 (Fig. 33), which further proves the theory that autophagy is rather protective than detrimental to HT-22 cells.

Thus, the exact mechanism of spermidine mediated cell death requires further studies that should evaluate how spermidine mediates neurotoxicity.

4.2.5 The final aim: clinical use of NPC CM

The results of this thesis expose CM from dying NPCs as a viable and promising tool for the treatment of neurodegenerative insults, which could bypass several technical and clinical limitations of direct stem/progenitor cell transplantation. Stem cell transplantation holds risks for severe long-term effects, such as severe immune responses or tumor formation. To date it remains unknown, which type and number of

stem cells are the most suitable regarding safety and efficacy, and which is the optimal route of delivery for therapeutic approaches in neurodegenerative diseases. For that reason it is highly important to ensure safety of stem and progenitor cell transplantation and to develop alternative strategies such as the application of stem cell conditioned medium that may overcome risks and limitations of classic stem cell therapy. Further analysis of NPC CM to identify as much components as possible could be the basis for the development of a highly potent, standardized composition for the therapy of neurodegenerative diseases.

The neuroprotective benefit of CM as well as safety, uniformity and reproducible generation, and the exact application of CM have to be tested in extensive studies *in vivo* before transferring this therapeutic concept to patients in clinical trials. First *in vivo* experiments using the CM in animal models of ischemic brain damage are already conducted in collaboration with Nikolaus Plesnila (Department of Neurosurgery, University of Munich Medical Center Grosshadern, Ludwig-Maximilians University, Munich, Germany) and Klas Blomgren (Department of Pediatric Oncology, The Queen Silvia Children's Hospital, University of Gothenburg, Sweden). First *in vivo* experiments were performed in a neonatal mouse model of hypoxia/ischemia (HI) with highly concentrated NPC CM. Experiments started at post natal day (PND) 9, with a NPC CM pretreatment, followed by hypoxic ischemia. Short term evaluation was executed after PND 10, long term evaluation started after PND 40 with behavior tests, such as open field test (a locomotion activity and anxiety test) and rearing test (exploratory activity and emotionality test). First positive and significant results showed that NPC CM was neuroprotective in an *in vivo* hypoxia model system.

These results from this promising *in vivo* study support the conclusion that NPC CM could serve as therapeutical option for the treatment of acute or chronic neurodegenerative diseases in human patients. The NPC CM may be further developed into a drug that could be applied systematically, stored and used ‘off the shelf’ which is impossible for stem cells. Depending on the cause of the disease and the related therapeutic time window, the cells producing therapeutic CM could be even obtained from the very same patient through generation of inducible pluripotent stem cells from fibroblasts or hair follicle cells of the patient.

4.3 Conclusion: Mechanisms of cell death such as autophagy and apoptosis can contribute to neuronal survival

The aim of this thesis was to investigate the role of two different, but well investigated cell death mechanisms, namely autophagy and apoptosis, in the model system of glutamate toxicity in cultured neurons.

Autophagy was found to act as an intracellular mechanism contributing to cellular survival and intracellular homeostasis in HT-22 cells. Induction of lethal stress led to activation of autophagy, but autophagy did apparently not contribute to the execution of cellular death. Thus, the observed induction of autophagy is interpreted as the ultimate attempt of the neural cells to adapt to lethal stress.

In the system of starvation-induced apoptosis in NPC, cellular death led to the preparation of a conditioned medium that mediated potent neuroprotective effects at the cellular level in model systems of glutamate toxicity. Induced apoptosis via starvation released substances that were neuroprotective, demonstrating that apoptotic cell death was required to mediate neuroprotection of other cells and possibly for entire organs in a whole organism. The preparation of conditioned medium *in vitro* mimicked the process of stem cell transplantation *in vivo*. Adult stem cells that contribute to neurogenesis and stem cells that are transplanted in case of neurodegenerative diseases contribute to neuronal survival and can improve brain functions. Nevertheless, these cells also die after transplantation and disappear after a few weeks. This finding indicated that the results obtained from the *in vitro* model system in this thesis are transferable to the adult organism, as recently confirmed in a model of neonatal hypoxia-ischemia in mice.

For future studies on autophagy and apoptosis it could be interesting not to contemplate both mechanisms as isolated mechanisms or to link them solely to cellular demise. Recent studies strongly indicated that a crosstalk between autophagy and apoptosis exists. The mechanisms linking autophagy and apoptosis are not fully understood. However, recent publications have revealed that several pro-apoptotic proteins (e.g., PUMA, Noxa, Nix, Bax, XIAP, and Bim) modulate autophagy. Moreover, autophagic proteins that control nucleation and elongation regulate intrinsic apoptosis through calpain- and caspase-mediated cleavage of autophagy-related proteins, which switches

the cellular program from autophagy to apoptosis. Similarly, several autophagic proteins are implicated in extrinsic apoptosis [256]. The crosstalk between autophagy and apoptosis has also been associated with trauma (e.g., haemorrhage and sepsis) [257], AD [258], HIV infection [259], and neural damage [246]. Although apoptosis is the major mechanism of cell death in these disease processes, autophagy plays dual roles by mediating cell death or cytoprotection, and, the latter may also apply for apoptosis, depending on the context of tissue damage and cellular stress. Elucidating the mechanisms underlying the connection between autophagy and apoptosis in these diseases may be useful for the development of targeted treatments as well as considering both mechanisms also contributing to cellular resilience.

5 Summary

Autophagy and apoptosis play major roles in determining the cellular fate. Accordingly, they participate in development, cellular homeostasis, and both in physiological as well as in pathological processes. Apoptosis is executed by activated caspases, which are specific enzymes that participate in signaling cascades that culminate in the rapid removal of organelles and other cellular structures. Autophagy is a highly conserved cytoprotective process whereby cytoplasmic contents are sequestered, transported via double-membrane autophagosomes to lysosomes, and degraded. Along with regulated necrosis and other forms of programmed cell death, pathological mechanisms of autophagy and apoptosis have been detected in neurodegenerative diseases, such as Parkinson's disease or Alzheimer's disease and acute brain injuries.
The aim of this thesis was to investigate the role of autophagy and apoptosis for neuronal resilience versus neuronal cell death in model systems of glutamate toxicity *in vitro*.

The role of autophagy was investigated in the model system of glutamate-induced oxidative stress, i.e. oxytosis in neural HT-22 cells. The objectives were to determine the effect of oxidative glutamate toxicity on autophagic flux and to investigate if oxytosis involves autophagy pathways of cell death. Moreover the neuroprotective effect of 3-Methyladenine (3-MA), a widely used autophagy inhibitor, was explored in the model systems of glutamate-induced oxytosis and excitotoxicity in neural HT-22 cells and primary cortical neurons, respectively.
Glutamate clearly enhanced autophagy markers and induced cell death in HT-22 cells and PCN. Cell death was prevented by 3-MA, a widely used inhibitor of autophagy. Interestingly, 3-MA itself induced autophagy in HT-22 cells. A gene silencing approach targeting key regulators of autophagy reduced the autophagic flux, but failed to prevent cell death persistently. 3-MA prevented the glutamate-induced ROS formation, the loss of ATP, and preserved the mitochondrial membrane potential as well as mitochondrial morphology. The activation of the PI_3K/Akt pathway and the MAPK/Erk-1/2 pathway do not play a role in 3-MA mediated neuroprotection.
In conclusion, these data suggest that glutamate toxicity is associated with increased markers of autophagy. However, specific gene silencing of key regulators of autophagy

did not provide protective effects, suggesting that the increased autophagic flux was dispensable for cell death induced by glutamate. The induction of autophagy can rather be interpreted as the ultimate attempt to adapt to lethal stress after glutamate challenge und is rather prosurvival and contributes to cellular homeostasis in HT-22 cells. Further, the findings clearly demonstrate that protective effects by 3-MA occur independently of autophagy inhibition, although the compound is widely used as an inhibitor of autophagy. Nowadays, 3-MA is used frequently in experimental studies *in vivo* and *in vitro*. Based on the present findings, caution is recommended in the interpretation of data obtained with 3-MA in the context of autophagy studies, in particular, if mitochondrial alterations are connected.

The contribution of apoptosis to neuronal survival through intercellular signaling between dying cells and neurons was investigated using conditioned medium of neural progenitor cells (NPC) and HT-22 cells. Stem cells as well as progenitor cells have been widely used in model systems of neurodegenerative diseases and acute brain injuries where transplantation of these cells into the brain improved neuronal survival and brain functions in experimental settings. However, most transplanted cells die after transplantation *in vivo*, and the exact mechanism of action of stem cell or progenitor cell transplantation still remains unknown. To investigate mechanisms of intercellular signaling underlying the protective effects of transplanted stem cells, the transplantation conditions were mimicked *in vitro* by preparation of conditioned medium (CM) obtained from dying neuronal progenitor cells. This CM should contain similar cellular components as released during cell death of the progenitor cell transplants, and this CM should therefore also provide neuroprotective effects. Thus, the CM of dying/apoptotic cells was applied in model systems of cell death *in vitro* for to test its potential to mediate neuroprotection. Further, the composition of the conditioned medium obtained from the dying progenitor cells was analysed for identifying the most potent protective components that may be applied as neuroprotectants *in vitro* and *in vivo* instead of the CM or the cellular transplants.

In order to mimic the conditions of transplantation, NPC were exposed to medium lacking growth factors such as FGF and EGF. Such growth factor deprivation induced caspase-dependent cell death in NPC in a time-dependent manner. The conditioned medium obtained from apoptotic NPC significantly attenuated cell death induced by

growth factor withdrawal and glutamate exposure in HT-22 cells and cortical neurons in a dose-dependent manner. The protective effect of NPC CM against glutamate neurotoxicity was abolished by heat inactivation at 95°C for 30 min. Further, NPC CM enhanced phosphorylation of PKB/Akt and Erk 1/2 in neurons in a similar time frame as the neurotrophin BDNF. Inhibition of autophagy did not diminish the protective effect of NPC CM. Also the use of spermidine conditioned medium (Sp CM) from HT-22 cells, whose production aimed on the specific activation of autophagy, indicated that the induction of autophagy is not essential for the protective effect of conditioned medium.

In total, these findings suggest that NPC secrete neuroprotective factors that stimulate neurotrophin-like survival signaling thereby providing protective effects against growth factor withdrawal and glutamate neurotoxicity. The results obtained from the *in vitro* model system in this thesis are transferable to the adult organism. Thus, the results are the basis for the development of a highly potent, standardized composition for the therapy of neurodegenerative diseases and acute brain injury. Therefore, CM and its active components could serve as an alternative therapeutic option to stem cell transplantation.

6 Zusammenfassung

Autophagie und Apoptose sind hochregulierte, komplexe Mechanismen, die eine bedeutende Rolle in der Entwicklung, Funktion und Homöostase von Zellen und Geweben eines Organismus einnehmen. Apoptose ist durch die Aktivität spezifischer Enzyme, der Caspasen, gekennzeichnet, die festgelegte programmierte Signalkaskaden in Gang setzten, was u.a. einen schnellen Abbau von Organellen und anderen zellulären Strukturen zur Folge hat. Autophagie ist ein hoch konservierter und in der Regel protektiver Prozess, bei dem zytoplasmatische Bestandteile in so genannte Autophagosomen eingeschlossen und transportiert werden und schließlich in den in Lysosomen degradiert werden. Bei neurodegenerativen Erkrankungen, wie Morbus Parkinson, Morbus Alzheimer und akuten Gehirnerkrankungen sind in den letzten Jahren zunehmend auch Mechanismen der Autophagie und Apoptose detektiert worden. Diese Befunde führten zu der Schlussfolgerung, dass bei diesen Erkrankungen die erhöhte Aktivität von Apoptose und Autophagie zum fortschreitenden Zelltod der Neurone und dem progressiven Verlust der Hirnfunktionen essentiell beitragen.

Das Ziel dieser Arbeit war es daher, die möglichen Funktionen von Autophagie und Apoptose in Modellsystemen von Glutamat-Toxizität in kultivierten Neuronen *in vitro* zu untersuchen, um die Rolle dieser Mechanismen beim neuronalem Zelltod zu klären. Die Rolle von Autophagie wurde im Modellsystem von Glutamat-induziertem oxidativem Stress in neuronalen HT-22 Zellen untersucht. Eine Zielsetzung war, den Effekt von oxidativer Glutamat-Toxizität auf die Aktivierung von Autophagie-Mechanismen in den Neuronen zu bestimmen und so zu klären, ob und in welchem Ausmaß hier Autophagie zum Zelltod beiträgt. Zudem wurde in Modellsystemen der Glutamat-Toxizität auch der neuroprotektive Effekt des vielfach verwendeten Autophagie-Inhibitors 3-Methyladenin (3-MA) untersucht.

In HT-22 Zellen und primären kortikalen Neuronen (PCN) war die Glutamat-induzierte Toxizität von einem deutlichen Anstieg von Autophagie-Markern begleitet. Der Glutamat-induzierte Zelltod wurde durch den Autophagie-Inhibitor 3-MA signifikant vermindert. Allerdings induzierte 3-MA selbst Autophagie in HT-22 Zellen. Im Gegensatz dazu gelang es nicht, die Zellen mit Hilfe von genetischer Regulation der Autophagie gegen die Glutamat-Schädigung zu schützen. Die siRNA-vermittelte

Expressionshemmung von Schlüsselregulatoren der Autophagie reduzierte zwar erwartungsgemäß die autophagische Aktivität, war aber nicht in der Lage, den Zelltod dauerhaft aufzuhalten. Der Inhibitor 3-MA verhinderte zudem die Glutamat-induzierte Bildung von reaktiven Sauerstoffspezies und den Verlust von ATP, wobei sowohl das Mitochodrienmembranpotential als auch die mitochondriale Morphologie erhalten blieben. Die Aktvierung der PI_3K/Akt- und der MAPK/Erk-1/2 Signalwege sind offenbar nicht an der 3-MA vermittelten Neuroprotektion beteiligt.
Schlussfolgernd zeigen diese Daten, dass Glutamat-Toxizität mit einer Aktivierung der Autophagie einhergeht. Allerdings lieferte die siRNA-vermittelte spezifische Hemmung der Expression von Schlüsselregulatoren der Autophagie keine protektiven Effekte, so dass die gemessene autophagische Aktivität nicht entscheidend zum Glutamat-induzierten Zelltod beiträgt. Die Induktion von Autophagie ist in diesem Zusammenhang offenbar eine Gegenregulation der Zellen, über die eine Anpassung an den Stress vermittelt wird. In den untersuchten Neuronen trägt die Autophagie eher zum Überleben und zur zellulären Homöostase bei und ist nicht als Mechanismus des Zelltodes zu verstehen. Weiterhin zeigen die Ergebnisse, dass der protektive Effekt von 3-MA in den Mitochondrien der Neurone unabhängig von einer Inhibition der Autophagie erfolgt, obwohl die Substanz vielfach als Inhibitor der Autophagie verwendet wird. Basierend auch auf den vorliegenden Ergebnissen sind also Daten, die mit 3-MA in Autophagiestudien erhoben werden, zurückhaltend zu interpretieren, insbesondere dann, wenn mitochondriale Schädigungen den Zelltod vermitteln.

Der Beitrag von Apoptose zu neuronalem Überleben durch interzelluläre Signale zwischen sterbenden (Stamm) Zellen und Neuronen wurde in Modellen des Nährstoffentzugs in neuronalen Vorläuferzellen und im Glutamat-Schädigungsmodell in den HT-22 Zellen untersucht. Therapeutische Effekte von Stammzellen und neuronalen Vorläuferzellen sind in Modellsystemen von akuten und chronischen neurodegenerativen Erkrankungen umfangreich nachgewiesen worden. In experimentellen Studien steigerten beispielsweise entsprechende Zelltransplantate das neuronale Überleben und die Erhaltung und Regeneration von Gehirnfunktionen. Jedoch sterben die meisten Zellen nach der Transplantation in das Gehirngewebe schnell ab und auch der exakte Mechanismus der therapeutischen Effekte von solchen Zelltransplantationen ist bislang weitgehend unbekannt. Die vorliegende Arbeit

untersuchte, inwieweit das Absterben von neuronalen Vorläuferzellen für die beobachteten protektiven Effekte von transplantierten Zellen von Bedeutung ist. Zu diesem Zweck wurden die Transplantationsbedingungen *in vitro* nachgeahmt indem aus dem Medium von neuronalen Vorläuferzellen (NPC) die Wachstumsfaktoren EGF und FGF entfernt wurden, um so apoptotischen Zelltod zu induzieren. Das konditionierte Medium von diesen apoptotischen Zellen sollte ähnliche zelluläre Komponenten enthalten, die auch nach der Transplantation von den sterbenden Stamm- oder Vorläuferzellen im Gehirn *in vivo* freigesetzt werden und die möglicherweise die neuroprotektiven Effekte vermitteln. Das konditionierte Medium der apoptotischen neuronalen Vorläuferzellen wurde im Modell der Glutamatschädigung in HT-22 Zellen auf neuroprotektive Effekte untersucht. Weiterhin wurde die Zusammensetzung des konditioniertem Mediums der sterben Progenitorzellen analysiert, um die wirksamsten protektiven Komponenten zu identifizieren, die dann vielleicht *in vitro* und *in vivo* an Stelle des konditionierten Mediums oder zellulärer Transplantate appliziert werden könnten.

Der Wachstumsfaktorentzug induzierte in den NPC einen Caspase-abhängigen Zelltod. Das konditionierte Medium (CM) von den apoptotischen NPC zeigte deutliche dosisabhängige protektive Effekte und verhinderte in HT-22 Zellen und kortikalen Neuronen den Zelltod nach Wachstumsfaktorentzug und Glutamatbehandlung. Der protektive Effekt des konditionierten Mediums wurde durch Hitzeinaktivierung bei 95°C für 30 Minuten aufgehoben. Weiterhin verstärkte das CM die Phosphorylierung von Erk 1/2 und PKB/Akt in primären Neuronen in einem ähnlichen Zeitrahmen wie das Neurotrophin BDNF. Autophagieinhibition in NPC schwächte die beschriebene neuroprotektive Wirkung nicht ab. Konditioniertes Medium, das von den NPC nach Induktion von Autophagie durch Spermidin gewonnen wurde, zeigte keinerlei protektiven Effekte in dem Modell der Glutamat-Schädigung in HT-22 Zellen. Die Aktivierung von Autophagie in NPC ist also im Gegensatz zur Apoptose offenbar nicht ausreichend, um protektive Faktoren zu bilden und in das konditionierte Medium abzugeben.

Zusammenfassend deuten diese Ergebnisse deuten darauf hin, dass apoptotische NPC neuroprotektive Faktoren sezernieren, die neurotrophin-ähnliche Überlebenssignalwege stimulieren und so protektive Effekte gegen Nährstoffentzug und Glutamat-Toxizität vermitteln. Die Resultate des *in vitro* Modellsystems in dieser Arbeit sind übertragbar

zum adulten Organismus. Die vorliegenden Erkenntnisse sind die Basis für die Entwicklung einer zellfreien, standardisierten und potenten neuroprotektiven Komposition, die eine Alternative zur Stammzelltransplantation darstellt und neue therapeutische Optionen für die zukünftige Behandlung von akuten und chronischen neurodegenerativen Erkrankungen bieten kann.

7 References

1. Eisenberg-Lerner A, Bialik S, Simon H, Kimchi A. Life and death partners: apoptosis, autophagy and the cross-talk between them. Cell Death Differ 2009; 16 (7): 966–975.
2. Lockshin RA, Zakeri Z. Apoptosis, autophagy, and more. Int. J. Biochem. Cell Biol. 2004; 36 (12): 2405–2419.
3. Yang Z, Klionsky DJ. Eaten alive: a history of macroautophagy. Nat Cell Biol 2010; 12 (9): 814–822.
4. Galluzzi L, Vitale I, Abrams JM et al. Molecular definitions of cell death subroutines: recommendations of the Nomenclature Committee on Cell Death 2012. Cell Death Differ 2011; 19 (1): 107–120.
5. Kim SU, Vellis J de. Stem cell-based cell therapy in neurological diseases: A review. J. Neurosci. Res. 2009; 87 (10): 2183–2200.
6. Reuck AVS de, Cameron MP, Duve C de. Lysosomes, London: J. & A. Churchill 1963.
7. Ciechanover A, Orian A, Schwartz AL. Ubiquitin-mediated proteolysis: biological regulation via destruction. Bioessays 2000; 22 (5): 442–451.
8. Ding W, Ni H, Gao W et al. Linking of Autophagy to Ubiquitin-Proteasome System Is Important for the Regulation of Endoplasmic Reticulum Stress and Cell Viability. The American Journal of Pathology 2007; 171 (2): 513–524.
9. Wang XJ, Yu J, Wong SH et al. A novel crosstalk between two major protein degradation systems: Regulation of proteasomal activity by autophagy. Autophagy 2013; 9 (10).
10. Shaid S, Brandts CH, Serve H, Dikic I. Ubiquitination and selective autophagy. Cell Death Differ. 2013; 20 (1): 21–30.
11. Takeshige K, Baba M, Tsuboi S et al. Autophagy in yeast demonstrated with proteinase-deficient mutants and conditions for its induction. J. Cell Biol. 1992; 119 (2): 301–311.
12. Mizushima N, Levine B, Cuervo AM, Klionsky DJ. Autophagy fights disease through cellular self-digestion. Nature 2008; 451 (7182): 1069–1075.
13. He C, Klionsky DJ. Regulation Mechanisms and Signaling Pathways of Autophagy. Annu. Rev. Genet. 2009; 43 (1): 67–93.
14. Klionsky DJ, Emr SD. Autophagy as a regulated pathway of cellular degradation. Science 2000; 290 (5497): 1717–1721.
15. Kraft C, Peter M, Hofmann K. Selective autophagy: ubiquitin-mediated recognition and beyond. Nat Cell Biol 2010; 12 (9): 836–841.
16. Komatsu M, Ichimura Y. Physiological significance of selective degradation of p62 by autophagy. FEBS Letters 2010; 584 (7): 1374–1378.
17. Kirkin V, McEwan DG, Novak I, Dikic I. A Role for Ubiquitin in Selective Autophagy. Molecular Cell 2009; 34 (3): 259–269.
18. Jeong H, Then F, Melia TJ et al. Acetylation Targets Mutant Huntingtin to Autophagosomes for Degradation. Cell 2009; 137 (1): 60–72.
19. Rami A. Review: Autophagy in neurodegeneration: firefighter and/or incendiarist? Neuropathology and Applied Neurobiology 2009; 35 (5): 449–461.
20. Mijaljica D, Prescott M, Devenish RJ. Microautophagy in mammalian cells: revisiting a 40-year-old conundrum. Autophagy 2011; 7 (7): 673–682.

21. Kaushik S, Cuervo AM. Chaperone-mediated autophagy: a unique way to enter the lysosome world. Trends in Cell Biology 2012; 22 (8): 407–417.
22. Esclatine A, Chaumorcel M, Codogno P. Macroautophagy signaling and regulation. Curr. Top. Microbiol. Immunol. 2009; 335: 33–70.
23. Levine B, Kroemer G. Autophagy in the Pathogenesis of Disease. Cell 2008; 132 (1): 27–42.
24. Ravikumar B, Sarkar S, Davies JE et al. Regulation of Mammalian Autophagy in Physiology and Pathophysiology. Physiological Reviews 2010; 90 (4): 1383–1435.
25. Boland B, Kumar A, Lee S et al. Autophagy Induction and Autophagosome Clearance in Neurons: Relationship to Autophagic Pathology in Alzheimer's Disease. Journal of Neuroscience 2008; 28 (27): 6926–6937.
26. Komatsu M, Waguri S, Chiba T et al. Loss of autophagy in the central nervous system causes neurodegeneration in mice. Nature 2006; 441 (7095): 880–884.
27. Hara T, Nakamura K, Matsui M et al. Suppression of basal autophagy in neural cells causes neurodegenerative disease in mice. Nature 2006; 441 (7095): 885–889.
28. Nishiyama J, Miura E, Mizushima N et al. Aberrant membranes and double-membrane structures accumulate in the axons of Atg5-null Purkinje cells before neuronal death. Autophagy 2007; 3 (6): 591–596.
29. Komatsu M, Wang QJ, Holstein GR et al. Essential role for autophagy protein Atg7 in the maintenance of axonal homeostasis and the prevention of axonal degeneration. Proc. Natl. Acad. Sci. U.S.A. 2007; 104 (36): 14489–14494.
30. Martinez-Vicente M, Talloczy Z, Wong E et al. Cargo recognition failure is responsible for inefficient autophagy in Huntington's disease. Nat Neurosci 2010; 13 (5): 567–576.
31. Matsuda N, Sato S, Shiba K et al. PINK1 stabilized by mitochondrial depolarization recruits Parkin to damaged mitochondria and activates latent Parkin for mitophagy. The Journal of Cell Biology 2010; 189 (2): 211–221.
32. Geisler S, Holmström KM, Skujat D et al. PINK1/Parkin-mediated mitophagy is dependent on VDAC1 and p62/SQSTM1. Nat Cell Biol 2010; 12 (2): 119–131.
33. Lee J, Yu WH, Kumar A et al. Lysosomal Proteolysis and Autophagy Require Presenilin 1 and Are Disrupted by Alzheimer-Related PS1 Mutations. Cell 2010; 141 (7): 1146–1158.
34. Nakatogawa H, Suzuki K, Kamada Y, Ohsumi Y. Dynamics and diversity in autophagy mechanisms: lessons from yeast. Nat Rev Mol Cell Biol 2009; 10 (7): 458–467.
35. Itakura E, Mizushima N. Characterization of autophagosome formation site by a hierarchical analysis of mammalian Atg proteins. Autophagy 2010; 6 (6): 764–776.
36. Suzuki K, Kubota Y, Sekito T, Ohsumi Y. Hierarchy of Atg proteins in pre-autophagosomal structure organization. Genes Cells 2007; 12 (2): 209–218.
37. Hayashi-Nishino M, Fujita N, Noda T et al. A subdomain of the endoplasmic reticulum forms a cradle for autophagosome formation. Nat Cell Biol 2009; 11 (12): 1433–1437.
38. Hailey DW, Rambold AS, Satpute-Krishnan P et al. Mitochondria supply membranes for autophagosome biogenesis during starvation. Cell 2010; 141 (4): 656–667.
39. Hamasaki M, Yoshimori T. Where do they come from? Insights into autophagosome formation. FEBS Lett. 2010; 584 (7): 1296–1301.
40. Ravikumar B, Moreau K, Rubinsztein DC. Plasma membrane helps autophagosomes grow. Autophagy 2010; 6 (8): 1184–1186.
41. Chen Y, Klionsky DJ. The regulation of autophagy - unanswered questions. Journal of Cell Science 2010; 124 (2): 161–170.

42. Chang Y, Neufeld TP. Autophagy takes flight in Drosophila. FEBS Letters 2010; 584 (7): 1342–1349.
43. Yang Z, Klionsky DJ. Mammalian autophagy: core molecular machinery and signaling regulation. Current Opinion in Cell Biology 2010; 22 (2): 124–131.
44. McPhee CK, Baehrecke EH. Autophagy in Drosophila melanogaster. Biochimica et Biophysica Acta (BBA) - Molecular Cell Research 2009; 1793 (9): 1452–1460.
45. Klionsky DJ, Abdalla FC, Abeliovich H et al. Guidelines for the use and interpretation of assays for monitoring autophagy. Autophagy 2012; 8 (4): 445–544.
46. Kabeya Y, Mizushima N, Ueno T et al. LC3, a mammalian homologue of yeast Apg8p, is localized in autophagosome membranes after processing. EMBO J. 2000; 19 (21): 5720–5728.
47. Maiuri MC, Zalckvar E, Kimchi A, Kroemer G. Self-eating and self-killing: crosstalk between autophagy and apoptosis. Nat. Rev. Mol. Cell Biol. 2007; 8 (9): 741–752.
48. Mizushima N, Yamamoto A, Hatano M et al. Dissection of autophagosome formation using Apg5-deficient mouse embryonic stem cells. J. Cell Biol. 2001; 152 (4): 657–668.
49. Pyo J, Jang M, Kwon Y et al. Essential roles of Atg5 and FADD in autophagic cell death: dissection of autophagic cell death into vacuole formation and cell death. J. Biol. Chem. 2005; 280 (21): 20722–20729.
50. Schmelzle T, Hall MN. TOR, a central controller of cell growth. Cell 2000; 103 (2): 253–262.
51. Jacinto E, Loewith R, Schmidt A et al. Mammalian TOR complex 2 controls the actin cytoskeleton and is rapamycin insensitive. Nat. Cell Biol. 2004; 6 (11): 1122–1128.
52. Corradetti MN, Guan K. Upstream of the mammalian target of rapamycin: do all roads pass through mTOR? Oncogene 2006; 25 (48): 6347–6360.
53. Brazil DP, Hemmings BA. Ten years of protein kinase B signalling: a hard Akt to follow. Trends Biochem. Sci. 2001; 26 (11): 657–664.
54. Meley D, Bauvy C, Houben-Weerts JHPM et al. AMP-activated protein kinase and the regulation of autophagic proteolysis. J. Biol. Chem. 2006; 281 (46): 34870–34879.
55. Sarkar S, Ravikumar B, Floto RA, Rubinsztein DC. Rapamycin and mTOR-independent autophagy inducers ameliorate toxicity of polyglutamine-expanded huntingtin and related proteinopathies. Cell Death Differ 2008; 16 (1): 46–56.
56. Mehrpour M, Esclatine A, Beau I, Codogno P. Overview of macroautophagy regulation in mammalian cells. Cell Res 2010; 20 (7): 748–762.
57. Ding W, Manley S, Ni H. The emerging role of autophagy in alcoholic liver disease. Exp. Biol. Med. (Maywood) 2011; 236 (5): 546–556.
58. Todde V, Veenhuis M, van der Klei IJ. Autophagy: Principles and significance in health and disease. Biochimica et Biophysica Acta (BBA) - Molecular Basis of Disease 2009; 1792 (1): 3–13.
59. Scherz-Shouval R, Shvets E, Fass E et al. Reactive oxygen species are essential for autophagy and specifically regulate the activity of Atg4. EMBO J. 2007; 26 (7): 1749–1760.
60. Ravikumar B, Vacher C, Berger Z et al. Inhibition of mTOR induces autophagy and reduces toxicity of polyglutamine expansions in fly and mouse models of Huntington disease. Nat. Genet. 2004; 36 (6): 585–595.
61. Sarkar S, Krishna G, Imarisio S et al. A rational mechanism for combination treatment of Huntington's disease using lithium and rapamycin. Hum. Mol. Genet. 2008; 17 (2): 170–178.

62. Sarkar S, Krishna G, Imarisio S et al. A rational mechanism for combination treatment of Huntington's disease using lithium and rapamycin. Hum. Mol. Genet. 2008; 17 (2): 170–178.
63. Sarkar S, Rubinsztein DC. Small molecule enhancers of autophagy for neurodegenerative diseases. Mol. BioSyst. 2008; 4 (9): 895.
64. Sarkar S, Davies JE, Huang Z et al. Trehalose, a novel mTOR-independent autophagy enhancer, accelerates the clearance of mutant huntingtin and alpha-synuclein. J. Biol. Chem. 2007; 282 (8): 5641–5652.
65. Rubinsztein DC, Gestwicki JE, Murphy LO, Klionsky DJ. Potential therapeutic applications of autophagy. Nat Rev Drug Discov 2007; 6 (4): 304–312.
66. Blommaart EF, Krause U, Schellens JP et al. The phosphatidylinositol 3-kinase inhibitors wortmannin and LY294002 inhibit autophagy in isolated rat hepatocytes. Eur. J. Biochem. 1997; 243 (1-2): 240–246.
67. Itakura E, Kishi C, Inoue K, Mizushima N. Beclin 1 Forms Two Distinct Phosphatidylinositol 3-Kinase Complexes with Mammalian Atg14 and UVRAG. Molecular Biology of the Cell 2008; 19 (12): 5360–5372.
68. Matsunaga K, Saitoh T, Tabata K et al. Two Beclin 1-binding proteins, Atg14L and Rubicon, reciprocally regulate autophagy at different stages. Nat Cell Biol 2009; 11 (4): 385–396.
69. Knight ZA, Gonzalez B, Feldman ME et al. A pharmacological map of the PI3-K family defines a role for p110alpha in insulin signaling. Cell 2006; 125 (4): 733–747.
70. Caro LH, Plomp PJ, Wolvetang EJ et al. 3-Methyladenine, an inhibitor of autophagy, has multiple effects on metabolism. Eur. J. Biochem. 1988; 175 (2): 325–329.
71. Punnonen EL, Marjomäki VS, Reunanen H. 3-Methyladenine inhibits transport from late endosomes to lysosomes in cultured rat and mouse fibroblasts. Eur. J. Cell Biol. 1994; 65 (1): 14–25.
72. Xue L, Borutaite V, Tolkovsky AM. Inhibition of mitochondrial permeability transition and release of cytochrome c by anti-apoptotic nucleoside analogues. Biochem. Pharmacol. 2002; 64 (3): 441–449.
73. Jahreiss L, Menzies FM, Rubinsztein DC. The itinerary of autophagosomes: from peripheral formation to kiss-and-run fusion with lysosomes. Traffic 2008; 9 (4): 574–587.
74. Kimura S, Noda T, Yoshimori T. Dynein-dependent movement of autophagosomes mediates efficient encounters with lysosomes. Cell Struct. Funct. 2008; 33 (1): 109–122.
75. Kim KW, Hwang M, Moretti L et al. Autophagy upregulation by inhibitors of caspase-3 and mTOR enhances radiotherapy in a mouse model of lung cancer. Autophagy 2008; 4 (5): 659–668.
76. Sou Y, Waguri S, Iwata J et al. The Atg8 Conjugation System Is Indispensable for Proper Development of Autophagic Isolation Membranes in Mice. Molecular Biology of the Cell 2008; 19 (11): 4762–4775.
77. Qu X, Yu J, Bhagat G et al. Promotion of tumorigenesis by heterozygous disruption of the beclin 1 autophagy gene. J. Clin. Invest. 2003; 112 (12): 1809–1820.
78. Yue Z, Jin S, Yang C et al. Beclin 1, an autophagy gene essential for early embryonic development, is a haploinsufficient tumor suppressor. Proc. Natl. Acad. Sci. U.S.A. 2003; 100 (25): 15077–15082.

79. Komatsu M, Waguri S, Ueno T et al. Impairment of starvation-induced and constitutive autophagy in Atg7-deficient mice. J. Cell Biol. 2005; 169 (3): 425–434.
80. Saitoh T, Fujita N, Hayashi T et al. Atg9a controls dsDNA-driven dynamic translocation of STING and the innate immune response. Proceedings of the National Academy of Sciences 2009; 106 (49): 20842–20846.
81. Cadwell K, Liu JY, Brown SL et al. A key role for autophagy and the autophagy gene Atg16l1 in mouse and human intestinal Paneth cells. Nature 2008; 456 (7219): 259–263.
82. Saitoh T, Fujita N, Jang MH et al. Loss of the autophagy protein Atg16L1 enhances endotoxin-induced IL-1β production. Nature 2008; 456 (7219): 264–268.
83. Hara T, Takamura A, Kishi C et al. FIP200, a ULK-interacting protein, is required for autophagosome formation in mammalian cells. The Journal of Cell Biology 2008; 181 (3): 497–510.
84. Fimia GM, Stoykova A, Romagnoli A et al. Ambra1 regulates autophagy and development of the nervous system. Nature 2007; 447 (7148): 1121–1125.
85. Kroemer G, Levine B. Autophagic cell death: the story of a misnomer. Nat Rev Mol Cell Biol 2008; 9 (12): 1004–1010.
86. Virgin HW, Levine B. Autophagy genes in immunity. Nat Immunol 2009; 10 (5): 461–470.
87. Gump JM, Thorburn A. Autophagy and apoptosis: what is the connection? Trends in Cell Biology 2011; 21 (7): 387–392.
88. Boya P, González-Polo R, Casares N et al. Inhibition of macroautophagy triggers apoptosis. Mol. Cell. Biol. 2005; 25 (3): 1025–1040.
89. Denton D, Shravage B, Simin R et al. Autophagy, Not Apoptosis, Is Essential for Midgut Cell Death in Drosophila. Current Biology 2009; 19 (20): 1741–1746.
90. Fazi B, Bursch W, Fimia GM et al. Fenretinide induces autophagic cell death in caspase-defective breast cancer cells. Autophagy 2008; 4 (4): 435–441.
91. Laane E, Tamm KP, Buentke E et al. Cell death induced by dexamethasone in lymphoid leukemia is mediated through initiation of autophagy. Cell Death Differ 2009; 16 (7): 1018–1029.
92. Shen H, Codogno P. Autophagic cell death: Loch Ness monster or endangered species? Autophagy 2011; 7 (5): 457–465.
93. Klionsky DJ, Abeliovich H, Agostinis P et al. Guidelines for the use and interpretation of assays for monitoring autophagy in higher eukaryotes. Autophagy 2008; 4 (2): 151–175.
94. Kepp O, Galluzzi L, Lipinski M et al. Cell death assays for drug discovery. Nat Rev Drug Discov 2011; 10 (3): 221–237.
95. Kerr JF, Wyllie AH, Currie AR. Apoptosis: a basic biological phenomenon with wide-ranging implications in tissue kinetics. Br. J. Cancer 1972; 26 (4): 239–257.
96. Kerr JFR. History of the events leading to the formulation of the apoptosis concept. Toxicology 2002; 181-182: 471–474.
97. Vaux DL, Korsmeyer SJ. Cell death in development. Cell 1999; 96 (2): 245–254.
98. Oppenheim RW. Cell death during development of the nervous system. Annu. Rev. Neurosci. 1991; 14: 453–501.
99. Norbury CJ, Hickson ID. Cellular responses to DNA damage. Annu. Rev. Pharmacol. Toxicol. 2001; 41: 367–401.

100. Mattson MP. Apoptosis in neurodegenerative disorders. Nat. Rev. Mol. Cell Biol. 2000; 1 (2): 120–129.
101. Wajant H. The Fas signaling pathway: more than a paradigm. Science 2002; 296 (5573): 1635–1636.
102. Schütze S, Tchikov V, Schneider-Brachert W. Regulation of TNFR1 and CD95 signalling by receptor compartmentalization. Nat Rev Mol Cell Biol 2008; 9 (8): 655–662.
103. Barnhart BC, Alappat EC, Peter ME. The CD95 type I/type II model. Semin. Immunol. 2003; 15 (3): 185–193.
104. Scaffidi C, Fulda S, Srinivasan A et al. Two CD95 (APO-1/Fas) signaling pathways. EMBO J. 1998; 17 (6): 1675–1687.
105. Yin XM, Wang K, Gross A et al. Bid-deficient mice are resistant to Fas-induced hepatocellular apoptosis. Nature 1999; 400 (6747): 886–891.
106. Li H, Zhu H, Xu CJ, Yuan J. Cleavage of BID by caspase 8 mediates the mitochondrial damage in the Fas pathway of apoptosis. Cell 1998; 94 (4): 491–501.
107. Kroemer G, Galluzzi L, Brenner C. Mitochondrial membrane permeabilization in cell death. Physiol. Rev. 2007; 87 (1): 99–163.
108. Li P, Nijhawan D, Budihardjo I et al. Cytochrome c and dATP-dependent formation of Apaf-1/caspase-9 complex initiates an apoptotic protease cascade. Cell 1997; 91 (4): 479–489.
109. Zou H, Henzel WJ, Liu X et al. Apaf-1, a human protein homologous to C. elegans CED-4, participates in cytochrome c-dependent activation of caspase-3. Cell 1997; 90 (3): 405–413.
110. Joza N, Susin SA, Daugas E et al. Essential role of the mitochondrial apoptosis-inducing factor in programmed cell death. Nature 2001; 410 (6828): 549–554.
111. Li LY, Luo X, Wang X. Endonuclease G is an apoptotic DNase when released from mitochondria. Nature 2001; 412 (6842): 95–99.
112. Büttner S, Eisenberg T, Carmona-Gutierrez D et al. Endonuclease G regulates budding yeast life and death. Mol. Cell 2007; 25 (2): 233–246.
113. Chai J, Du C, Wu JW et al. Structural and biochemical basis of apoptotic activation by Smac/DIABLO. Nature 2000; 406 (6798): 855–862.
114. Yang Q, Church-Hajduk R, Ren J et al. Omi/HtrA2 catalytic cleavage of inhibitor of apoptosis (IAP) irreversibly inactivates IAPs and facilitates caspase activity in apoptosis. Genes Dev. 2003; 17 (12): 1487–1496.
115. Vande Walle L, van Damme P, Lamkanfi M et al. Proteome-wide Identification of HtrA2/Omi Substrates. J. Proteome Res. 2007; 6 (3): 1006–1015.
116. Hegde R, Srinivasula SM, Zhang Z et al. Identification of Omi/HtrA2 as a mitochondrial apoptotic serine protease that disrupts inhibitor of apoptosis protein-caspase interaction. J. Biol. Chem. 2002; 277 (1): 432–438.
117. Chipuk JE, Green DR. Do inducers of apoptosis trigger caspase-independent cell death? Nat. Rev. Mol. Cell Biol. 2005; 6 (3): 268–275.
118. Kroemer G, Martin SJ. Caspase-independent cell death. Nat. Med. 2005; 11 (7): 725–730.
119. Yuan J, Lipinski M, Degterev A. Diversity in the mechanisms of neuronal cell death. Neuron 2003; 40 (2): 401–413.
120. Zong W, Thompson CB. Necrotic death as a cell fate. Genes Dev. 2006; 20 (1): 1–15.

121. Majno G, Joris I. Apoptosis, oncosis, and necrosis. An overview of cell death. Am. J. Pathol. 1995; 146 (1): 3–15.
122. Vandenabeele P, Galluzzi L, Vanden Berghe T, Kroemer G. Molecular mechanisms of necroptosis: an ordered cellular explosion. Nat Rev Mol Cell Biol 2010; 11 (10): 700–714.
123. Degterev A, Huang Z, Boyce M et al. Chemical inhibitor of nonapoptotic cell death with therapeutic potential for ischemic brain injury. Nat. Chem. Biol. 2005; 1 (2): 112–119.
124. Gage FH. Mammalian neural stem cells. Science 2000; 287 (5457): 1433–1438.
125. Seaberg RM, van der Kooy D. Stem and progenitor cells: the premature desertion of rigorous definitions. Trends Neurosci. 2003; 26 (3): 125–131.
126. Gould E. How widespread is adult neurogenesis in mammals? Nat. Rev. Neurosci. 2007; 8 (6): 481–488.
127. Deng W, Aimone JB, Gage FH. New neurons and new memories: how does adult hippocampal neurogenesis affect learning and memory? Nat. Rev. Neurosci. 2010; 11 (5): 339–350.
128. Lindvall O, Kokaia Z. Stem cells for the treatment of neurological disorders. Nature 2006; 441 (7097): 1094–1096.
129. Lindvall O, Kokaia Z. Stem cell research in stroke: how far from the clinic? Stroke 2011; 42 (8): 2369–2375.
130. Wang F, Maeda N, Yasuhara T et al. The therapeutic potential of human umbilical cord blood transplantation for neonatal hypoxic-ischemic brain injury and ischemic stroke. Acta Med. Okayama 2012; 66 (6): 429–434.
131. Chen WW, Blurton-Jones M. Concise review: Can stem cells be used to treat or model Alzheimer's disease? Stem Cells 2012; 30 (12): 2612–2618.
132. Dutta S, Singh G, Sreejith S et al. Cell Therapy: The Final Frontier for Treatment of Neurological Diseases. CNS Neurosci Ther 2013; 19 (1): 5–11.
133. Takahashi K, Yamanaka S. Induction of pluripotent stem cells from mouse embryonic and adult fibroblast cultures by defined factors. Cell 2006; 126 (4): 663–676.
134. Petit I, Salman Kesner N, Karry R et al. Induced pluripotent stem cells from hair follicles as a cellular model for neurodevelopmental disorders. Stem Cell Research 2012; 8 (1): 134–140.
135. Takagi Y, Takahashi J, Saiki H et al. Dopaminergic neurons generated from monkey embryonic stem cells function in a Parkinson primate model. J. Clin. Invest. 2005; 115 (1): 102–109.
136. Redmond DE, Bjugstad KB, Teng YD et al. Behavioral improvement in a primate Parkinson's model is associated with multiple homeostatic effects of human neural stem cells. Proc. Natl. Acad. Sci. U.S.A. 2007; 104 (29): 12175–12180.
137. Blurton-Jones M, Kitazawa M, Martinez-Coria H et al. Neural stem cells improve cognition via BDNF in a transgenic model of Alzheimer disease. Proc. Natl. Acad. Sci. U.S.A. 2009; 106 (32): 13594–13599.
138. Kelly S, Bliss TM, Shah AK et al. Transplanted human fetal neural stem cells survive, migrate, and differentiate in ischemic rat cerebral cortex. Proc. Natl. Acad. Sci. U.S.A. 2004; 101 (32): 11839–11844.
139. Darsalia V, Kallur T, Kokaia Z. Survival, migration and neuronal differentiation of human fetal striatal and cortical neural stem cells grafted in stroke-damaged rat striatum. Eur. J. Neurosci. 2007; 26 (3): 605–614.

140. Chen S, Chang C, Tsai S et al. Functional Improvement of Focal Cerebral Ischemia Injury by Subdural Transplantation of Induced Pluripotent Stem Cells with Fibrin Glue. Stem Cells and Development 2010; 19 (11): 1757–1767.
141. Park HJ, Lee PH, Bang OY et al. Mesenchymal stem cells therapy exerts neuroprotection in a progressive animal model of Parkinson's disease. Journal of Neurochemistry 2008; 107 (1): 141–151.
142. Bang OY, Lee JS, Lee PH, Lee G. Autologous mesenchymal stem cell transplantation in stroke patients. Ann. Neurol. 2005; 57 (6): 874–882.
143. Lee JS, Hong JM, Moon GJ et al. A long-term follow-up study of intravenous autologous mesenchymal stem cell transplantation in patients with ischemic stroke. Stem Cells 2010; 28 (6): 1099–1106.
144. Venkataramana NK, Kumar SK, Balaraju S et al. Open-labeled study of unilateral autologous bone-marrow-derived mesenchymal stem cell transplantation in Parkinson's disease. Translational Research 2010; 155 (2): 62–70.
145. Luan Z, Liu W, Qu S et al. Effects of Neural Progenitor Cell Transplantation in Children With Severe Cerebral Palsy. cell transplant 2012; 21 (1): 91–98.
146. Lindvall O, Kokaia Z, Martinez-Serrano A. Stem cell therapy for human neurodegenerative disorders-how to make it work. Nat. Med. 2004; 10: S42-50.
147. Kopen GC, Prockop DJ, Phinney DG. Marrow stromal cells migrate throughout forebrain and cerebellum, and they differentiate into astrocytes after injection into neonatal mouse brains. Proc. Natl. Acad. Sci. U.S.A. 1999; 96 (19): 10711–10716.
148. Chen X, Li Y, Wang L et al. Ischemic rat brain extracts induce human marrow stromal cell growth factor production. Neuropathology 2002; 22 (4): 275–279.
149. Menasché P. Stem cells for clinical use in cardiovascular medicine: current limitations and future perspectives. Thromb. Haemost. 2005; 94 (4): 697–701.
150. Silva GV, Litovsky S, Assad JAR et al. Mesenchymal stem cells differentiate into an endothelial phenotype, enhance vascular density, and improve heart function in a canine chronic ischemia model. Circulation 2005; 111 (2): 150–156.
151. Chen J, Li Y, Wang L et al. Therapeutic benefit of intravenous administration of bone marrow stromal cells after cerebral ischemia in rats. Stroke 2001; 32 (4): 1005–1011.
152. Piemonte F, Rossi F, Carletti B. Neuroprotection: The Emerging Concept of Restorative Neural Stem Cell Biology for the Treatment of Neurodegenerative Diseases. CN 2011; 9 (2): 313–317.
153. Madhavan L, Ourednik V, Ourednik J. Neural stem/progenitor cells initiate the formation of cellular networks that provide neuroprotection by growth factor-modulated antioxidant expression. Stem Cells 2008; 26 (1): 254–265.
154. Isele NB, Lee H, Landshamer S et al. Bone marrow stromal cells mediate protection through stimulation of PI3-K/Akt and MAPK signaling in neurons. Neurochem. Int. 2007; 50 (1): 243–250.
155. Joyce N, Annett G, Wirthlin L et al. Mesenchymal stem cells for the treatment of neurodegenerative disease. Regen Med 2010; 5 (6): 933–946.
156. Zhu JM, Zhao YY, Chen SD et al. Functional recovery after transplantation of neural stem cells modified by brain-derived neurotrophic factor in rats with cerebral ischaemia. J. Int. Med. Res. 2011; 39 (2): 488–498.
157. Lim H, Lee S, Chu K et al. Neuroprotective effect of neural stem cell-conditioned media in in vitro model of Huntington's disease. Neuroscience Letters 2008; 435 (3): 175–180.

158. Windmolders S, Boeck A de, Koninckx R et al. Mesenchymal stem cell secreted platelet derived growth factor exerts a pro-migratory effect on resident Cardiac Atrial appendage Stem Cells. Journal of Molecular and Cellular Cardiology 2013.
159. Boomsma RA, Geenen DL, Hofmann TG. Mesenchymal Stem Cells Secrete Multiple Cytokines That Promote Angiogenesis and Have Contrasting Effects on Chemotaxis and Apoptosis. PLoS ONE 2012; 7 (4): e35685.
160. Wilkins A, Kemp K, Ginty M et al. Human bone marrow-derived mesenchymal stem cells secrete brain-derived neurotrophic factor which promotes neuronal survival in vitro. Stem Cell Research 2009; 3 (1): 63–70.
161. Morimoto BH, Koshland DE. Excitatory amino acid uptake and N-methyl-D-aspartate-mediated secretion in a neural cell line. Proc. Natl. Acad. Sci. U.S.A. 1990; 87 (9): 3518–3521.
162. Blandini F, Porter RH, Greenamyre JT. Glutamate and Parkinson's disease. Mol. Neurobiol. 1996; 12 (1): 73–94.
163. Coyle JT, Puttfarcken P. Oxidative stress, glutamate, and neurodegenerative disorders. Science 1993; 262 (5134): 689–695.
164. Maher P, Davis JB. The role of monoamine metabolism in oxidative glutamate toxicity. J. Neurosci. 1996; 16 (20): 6394–6401.
165. Murphy TH, Miyamoto M, Sastre A et al. Glutamate toxicity in a neuronal cell line involves inhibition of cystine transport leading to oxidative stress. Neuron 1989; 2 (6): 1547–1558.
166. Li Y, Maher P, Schubert D. A role for 12-lipoxygenase in nerve cell death caused by glutathione depletion. Neuron 1997; 19 (2): 453–463.
167. Landshamer S, Hoehn M, Barth N et al. Bid-induced release of AIF from mitochondria causes immediate neuronal cell death. Cell Death Differ 2008; 15 (10): 1553–1563.
168. Tobaben S, Grohm J, Seiler A et al. Bid-mediated mitochondrial damage is a key mechanism in glutamate-induced oxidative stress and AIF-dependent cell death in immortalized HT-22 hippocampal neurons. Cell Death Differ 2010; 18 (2): 282–292.
169. Tan S, Sagara Y, Liu Y et al. The regulation of reactive oxygen species production during programmed cell death. J. Cell Biol. 1998; 141 (6): 1423–1432.
170. Tan S, Schubert D, Maher P. Oxytosis: A novel form of programmed cell death. Curr Top Med Chem 2001; 1 (6): 497–506.
171. Culmsee C, Zhu C, Landshamer S et al. Apoptosis-inducing factor triggered by poly(ADP-ribose) polymerase and Bid mediates neuronal cell death after oxygen-glucose deprivation and focal cerebral ischemia. J. Neurosci. 2005; 25 (44): 10262–10272.
172. Choi DW, Koh JY, Peters S. Pharmacology of glutamate neurotoxicity in cortical cell culture: attenuation by NMDA antagonists. J. Neurosci. 1988; 8 (1): 185–196.
173. Berliocchi L, Bano D, Nicotera P. Ca2+ signals and death programmes in neurons. Philos. Trans. R. Soc. Lond., B, Biol. Sci. 2005; 360 (1464): 2255–2258.
174. Robinson SR, Bishop GM. Abeta as a bioflocculant: implications for the amyloid hypothesis of Alzheimer's disease. Neurobiol. Aging 2002; 23 (6): 1051–1072.
175. Helton TD, Otsuka T, Lee M et al. Pruning and loss of excitatory synapses by the parkin ubiquitin ligase. Proc. Natl. Acad. Sci. U.S.A. 2008; 105 (49): 19492–19497.
176. Danysz W, Parsons CG. The NMDA receptor antagonist memantine as a symptomatological and neuroprotective treatment for Alzheimer's disease: preclinical evidence. Int J Geriatr Psychiatry 2003; 18 (Suppl 1): S23-32.

177. Jung K, Chu K, Lee S et al. Augmentation of nitrite therapy in cerebral ischemia by NMDA receptor inhibition. Biochem. Biophys. Res. Commun. 2009; 378 (3): 507–512.
178. Fan MMY, Raymond LA. N-methyl-D-aspartate (NMDA) receptor function and excitotoxicity in Huntington's disease. Prog. Neurobiol. 2007; 81 (5-6): 272–293.
179. Ray J, Gage FH. Differential properties of adult rat and mouse brain-derived neural stem/progenitor cells. Mol. Cell. Neurosci. 2006; 31 (3): 560–573.
180. Liu Y, Peterson DA, Kimura H, Schubert D. Mechanism of cellular 3-(4,5-dimethylthiazol-2-yl)-2,5-diphenyltetrazolium bromide (MTT) reduction. J. Neurochem. 1997; 69 (2): 581–593.
181. Diemert S, Dolga A, Tobaben S et al. Impedance measurement for real time detection of neuronal cell death. Journal of Neuroscience Methods 2012; 203 (1): 69–77.
182. Grohm J, Plesnila N, Culmsee C. Bid mediates fission, membrane permeabilization and peri-nuclear accumulation of mitochondria as a prerequisite for oxidative neuronal cell death. Brain Behav Immun 2010; 24 (5): 831–838.
183. Gohil VM, Sheth SA, Nilsson R et al. Nutrient-sensitized screening for drugs that shift energy metabolism from mitochondrial respiration to glycolysis. Nat. Biotechnol. 2010; 28 (3): 249–255.
184. Walker JM. The bicinchoninic acid (BCA) assay for protein quantitation. Methods Mol. Biol. 1994; 32: 5–8.
185. Poole B, Ohkuma S. Effect of weak bases on the intralysosomal pH in mouse peritoneal macrophages. J. Cell Biol. 1981; 90 (3): 665–669.
186. Suzuki T, Nakagawa M, Yoshikawa A et al. The first molecular evidence that autophagy relates rimmed vacuole formation in chloroquine myopathy. J. Biochem. 2002; 131 (5): 647–651.
187. Shintani T, Klionsky DJ. Autophagy in health and disease: a double-edged sword. Science 2004; 306 (5698): 990–995.
188. Denton D, Nicolson S, Kumar S. Cell death by autophagy: facts and apparent artefacts. Cell Death Differ. 2012; 19 (1): 87–95.
189. Philpott KL, McCarthy MJ, Klippel A, Rubin LL. Activated phosphatidylinositol 3-kinase and Akt kinase promote survival of superior cervical neurons. J. Cell Biol. 1997; 139 (3): 809–815.
190. Shaw RJ. LKB1 and AMP-activated protein kinase control of mTOR signalling and growth. Acta Physiol (Oxf) 2009; 196 (1): 65–80.
191. Cowley S, Paterson H, Kemp P, Marshall CJ. Activation of MAP kinase kinase is necessary and sufficient for PC12 differentiation and for transformation of NIH 3T3 cells. Cell 1994; 77 (6): 841–852.
192. McBride HM, Neuspiel M, Wasiak S. Mitochondria: more than just a powerhouse. Curr. Biol. 2006; 16 (14): R551-60.
193. Filosto M, Scarpelli M, Cotelli MS et al. The role of mitochondria in neurodegenerative diseases. J. Neurol. 2011; 258 (10): 1763–1774.
194. Grohm J, Kim S, Mamrak U et al. Inhibition of Drp1 provides neuroprotection in vitro and in vivo. Cell Death Differ. 2012; 19 (9): 1446–1458.
195. Fernandes-Alnemri T, Litwack G, Alnemri ES. CPP32, a novel human apoptotic protein with homology to Caenorhabditis elegans cell death protein Ced-3 and mammalian interleukin-1 beta-converting enzyme. J. Biol. Chem. 1994; 269 (49): 30761–30764.

196. Oliver FJ, La Rubia G de, Rolli V et al. Importance of poly(ADP-ribose) polymerase and its cleavage in apoptosis. Lesson from an uncleavable mutant. J. Biol. Chem. 1998; 273 (50): 33533–33539.
197. Renolleau S, Fau S, Goyenvalle C et al. Specific caspase inhibitor Q-VD-OPh prevents neonatal stroke in P7 rat: a role for gender. J. Neurochem. 2007; 100 (4): 1062–1071.
198. Hristov M, Erl W, Linder S, Weber PC. Apoptotic bodies from endothelial cells enhance the number and initiate the differentiation of human endothelial progenitor cells in vitro. Blood 2004; 104 (9): 2761–2766.
199. Eva-Maria Öxler. Molecular and cellular preconditioning - powerful strategies for neuroprotection. Doktorarbeit, Marburg 2012.
200. Orlando KA, Stone NL, Pittman RN. Rho kinase regulates fragmentation and phagocytosis of apoptotic cells. Exp. Cell Res. 2006; 312 (1): 5–15.
201. Crowder RJ, Freeman RS. Phosphatidylinositol 3-kinase and Akt protein kinase are necessary and sufficient for the survival of nerve growth factor-dependent sympathetic neurons. J. Neurosci. 1998; 18 (8): 2933–2943.
202. Culmsee C, Gerling N, Lehmann M et al. Nerve growth factor survival signaling in cultured hippocampal neurons is mediated through TrkA and requires the common neurotrophin receptor P75. Neuroscience 2002; 115 (4): 1089–1108.
203. Morselli E, Mariño G, Bennetzen MV et al. Spermidine and resveratrol induce autophagy by distinct pathways converging on the acetylproteome. J. Cell Biol. 2011; 192 (4): 615–629.
204. Minois N, Carmona-Gutierrez D, Bauer MA et al. Spermidine promotes stress resistance in Drosophila melanogaster through autophagy-dependent and -independent pathways. Cell Death Dis 2012; 3: e401.
205. Xu Y, Kim SO, Li Y, Han J. Autophagy contributes to caspase-independent macrophage cell death. J. Biol. Chem. 2006; 281 (28): 19179–19187.
206. Matsui Y, Takagi H, Qu X et al. Distinct roles of autophagy in the heart during ischemia and reperfusion: roles of AMP-activated protein kinase and Beclin 1 in mediating autophagy. Circ. Res. 2007; 100 (6): 914–922.
207. Kim H, Choi J, Ryu J et al. Activation of autophagy during glutamate-induced HT22 cell death. Biochem Biophys Res Commun 2009; 388 (2): 339–344.
208. Kumari S, Mehta SL, Li PA. Glutamate induces mitochondrial dynamic imbalance and autophagy activation: preventive effects of selenium. PLoS ONE 2012; 7 (6): e39382.
209. Kubota C, Torii S, Hou N et al. Constitutive reactive oxygen species generation from autophagosome/lysosome in neuronal oxidative toxicity. J. Biol. Chem. 2010; 285 (1): 667–674.
210. Seglen PO, Gordon PB. 3-Methyladenine: specific inhibitor of autophagic/lysosomal protein degradation in isolated rat hepatocytes. Proc. Natl. Acad. Sci. U.S.A. 1982; 79 (6): 1889–1892.
211. Steiger-Barraissoul S, Rami A. Serum deprivation induced autophagy and predominantly an AIF-dependent apoptosis in hippocampal HT22 neurons. Apoptosis 2009; 14 (11): 1274–1288.
212. Wang Y, Han R, Liang Z et al. An autophagic mechanism is involved in apoptotic death of rat striatal neurons induced by the non-N-methyl-D-aspartate receptor agonist kainic acid. Autophagy 2008; 4 (2): 214–226.

213. Wang Y, Dong X, Cao Y et al. p53 induction contributes to excitotoxic neuronal death in rat striatum through apoptotic and autophagic mechanisms. Eur. J. Neurosci. 2009; 30 (12): 2258–2270.
214. Gao L, Jiang T, Guo J et al. Inhibition of autophagy contributes to ischemic postconditioning-induced neuroprotection against focal cerebral ischemia in rats. PLoS ONE 2012; 7 (9): e46092.
215. Wen Y, Sheng R, Zhang L et al. Neuronal injury in rat model of permanent focal cerebral ischemia is associated with activation of autophagic and lysosomal pathways. Autophagy 2008; 4 (6): 762–769.
216. Puyal J, Vaslin A, Mottier V, Clarke PGH. Postischemic treatment of neonatal cerebral ischemia should target autophagy. Ann. Neurol. 2009; 66 (3): 378–389.
217. Wu Y, Tan H, Shui G et al. Dual Role of 3-Methyladenine in Modulation of Autophagy via Different Temporal Patterns of Inhibition on Class I and III Phosphoinositide 3-Kinase. Journal of Biological Chemistry 2010; 285 (14): 10850–10861.
218. Cao Y, Klionsky DJ. Physiological functions of Atg6/Beclin 1: a unique autophagy-related protein. Cell Res. 2007; 17 (10): 839–849.
219. Kuma A, Hatano M, Matsui M et al. The role of autophagy during the early neonatal starvation period. Nature 2004; 432 (7020): 1032–1036.
220. Petiot A, Ogier-Denis E, Blommaart EF et al. Distinct classes of phosphatidylinositol 3'-kinases are involved in signaling pathways that control macroautophagy in HT-29 cells. J. Biol. Chem. 2000; 275 (2): 992–998.
221. Castino R, Bellio N, Follo C et al. Inhibition of PI3k class III-dependent autophagy prevents apoptosis and necrosis by oxidative stress in dopaminergic neuroblastoma cells. Toxicol. Sci. 2010; 117 (1): 152–162.
222. Brunet A, Datta SR, Greenberg ME. Transcription-dependent and -independent control of neuronal survival by the PI3K-Akt signaling pathway. Curr. Opin. Neurobiol. 2001; 11 (3): 297–305.
223. Anderson CN, Tolkovsky AM. A role for MAPK/ERK in sympathetic neuron survival: protection against a p53-dependent, JNK-independent induction of apoptosis by cytosine arabinoside. J. Neurosci. 1999; 19 (2): 664–673.
224. Zhu Y, Yang G, Ahlemeyer B et al. Transforming growth factor-beta 1 increases bad phosphorylation and protects neurons against damage. J. Neurosci. 2002; 22 (10): 3898–3909.
225. Stanciu M, Wang Y, Kentor R et al. Persistent activation of ERK contributes to glutamate-induced oxidative toxicity in a neuronal cell line and primary cortical neuron cultures. J. Biol. Chem. 2000; 275 (16): 12200–12206.
226. Luo Y, DeFranco DB. Opposing roles for ERK1/2 in neuronal oxidative toxicity: distinct mechanisms of ERK1/2 action at early versus late phases of oxidative stress. J. Biol. Chem. 2006; 281 (24): 16436–16442.
227. Weisová P, Dávila D, Tuffy LP et al. Role of 5'-adenosine monophosphate-activated protein kinase in cell survival and death responses in neurons. Antioxid. Redox Signal. 2011; 14 (10): 1863–1876.
228. Kahn BB, Alquier T, Carling D, Hardie DG. AMP-activated protein kinase: ancient energy gauge provides clues to modern understanding of metabolism. Cell Metab. 2005; 1 (1): 15–25.

229. Weisová P, Concannon CG, Devocelle M et al. Regulation of glucose transporter 3 surface expression by the AMP-activated protein kinase mediates tolerance to glutamate excitation in neurons. J. Neurosci. 2009; 29 (9): 2997–3008.
230. Concannon CG, Tuffy LP, Weisová P et al. AMP kinase-mediated activation of the BH3-only protein Bim couples energy depletion to stress-induced apoptosis. J. Cell Biol. 2010; 189 (1): 83–94.
231. Hendil KB, Lauridsen AM, Seglen PO. Both endocytic and endogenous protein degradation in fibroblasts is stimulated by serum/amino acid deprivation and inhibited by 3-methyladenine. Biochem. J. 1990; 272 (3): 577–581.
232. Nunnari J, Suomalainen A. Mitochondria: in sickness and in health. Cell 2012; 148 (6): 1145–1159.
233. Knott AB, Perkins G, Schwarzenbacher R, Bossy-Wetzel E. Mitochondrial fragmentation in neurodegeneration. Nat. Rev. Neurosci. 2008; 9 (7): 505–518.
234. Cho D, Nakamura T, Fang J et al. S-nitrosylation of Drp1 mediates beta-amyloid-related mitochondrial fission and neuronal injury. Science 2009; 324 (5923): 102–105.
235. Yuan H, Gerencser AA, Liot G et al. Mitochondrial fission is an upstream and required event for bax foci formation in response to nitric oxide in cortical neurons. Cell Death Differ. 2007; 14 (3): 462–471.
236. Kalia S, Dutz JP. New concepts in antimalarial use and mode of action in dermatology. Dermatol Ther 2007; 20 (4): 160–174.
237. Steere AC, Angelis SM. Therapy for Lyme arthritis: strategies for the treatment of antibiotic-refractory arthritis. Arthritis Rheum. 2006; 54 (10): 3079–3086.
238. Sui X, Chen R, Wang Z et al. Autophagy and chemotherapy resistance: a promising therapeutic target for cancer treatment. Cell Death Dis 2013; 4: e838.
239. Schlie K, Spowart JE, Hughson LRK et al. When Cells Suffocate: Autophagy in Cancer and Immune Cells under Low Oxygen. Int J Cell Biol 2011; 2011: 470597.
240. Zhu W, Chen J, Cong X et al. Hypoxia and serum deprivation-induced apoptosis in mesenchymal stem cells. Stem Cells 2006; 24 (2): 416–425.
241. Nakano N, Nakai Y, Seo T et al. Characterization of conditioned medium of cultured bone marrow stromal cells. Neurosci. Lett. 2010; 483 (1): 57–61.
242. Karlson P, Doenecke D. Karlsons Biochemie und Pathobiochemie: [Falttafel mit Stoffwechselübersicht], 15th edition, Stuttgart [u.a.]: Thieme 2005.
243. Datta SR, Brunet A, Greenberg ME. Cellular survival: a play in three Akts. Genes Dev. 1999; 13 (22): 2905–2927.
244. Gonzalez-Zulueta M, Feldman AB, Klesse LJ et al. Requirement for nitric oxide activation of p21(ras)/extracellular regulated kinase in neuronal ischemic preconditioning. Proc. Natl. Acad. Sci. U.S.A. 2000; 97 (1): 436–441.
245. Han BH, Holtzman DM. BDNF protects the neonatal brain from hypoxic-ischemic injury in vivo via the ERK pathway. J. Neurosci. 2000; 20 (15): 5775–5781.
246. Xue L, Fletcher GC, Tolkovsky AM. Autophagy is activated by apoptotic signalling in sympathetic neurons: an alternative mechanism of death execution. Mol. Cell. Neurosci. 1999; 14 (3): 180–198.
247. Eisenberg T, Knauer H, Schauer A et al. Induction of autophagy by spermidine promotes longevity. Nat. Cell Biol. 2009; 11 (11): 1305–1314.
248. Madeo F, Eisenberg T, Büttner S et al. Spermidine: a novel autophagy inducer and longevity elixir. Autophagy 2010; 6 (1): 160–162.

249. Gupta VK, Scheunemann L, Eisenberg T et al. Restoring polyamines protects from age-induced memory impairment in an autophagy-dependent manner. Nat. Neurosci. 2013; 16 (10): 1453–1460.
250. Moschou PN, Roubelakis-Angelakis KA. Polyamines and programmed cell death. J. Exp. Bot. 2013.
251. Chen Y, Kramer DL, Li F, Porter CW. Loss of inhibitor of apoptosis proteins as a determinant of polyamine analog-induced apoptosis in human melanoma cells. Oncogene 2003; 22 (32): 4964–4972.
252. Duan B, Wang Y, Yang T et al. Extracellular spermine exacerbates ischemic neuronal injury through sensitization of ASIC1a channels to extracellular acidosis. J. Neurosci. 2011; 31 (6): 2101–2112.
253. Seiler N, Raul F. Polyamines and apoptosis. J. Cell. Mol. Med. 2005; 9 (3): 623–642.
254. Mendivil-Perez M, Velez-Pardo C, Jimenez-Del-Rio M. TPEN induces apoptosis independently of zinc chelator activity in a model of acute lymphoblastic leukemia and ex vivo acute leukemia cells through oxidative stress and mitochondria caspase-3- and AIF-dependent pathways. Oxid Med Cell Longev 2012; 2012: 313275.
255. Brenner C, Grimm S. The permeability transition pore complex in cancer cell death. Oncogene 2006; 25 (34): 4744–4756.
256. Mukhopadhyay S, Panda PK, Sinha N et al. Autophagy and apoptosis: where do they meet? Apoptosis 2014; 19 (4): 555–566.
257. Hsieh Y, Athar M, Chaudry IH. When apoptosis meets autophagy: deciding cell fate after trauma and sepsis. Trends Mol Med 2009; 15 (3): 129–138.
258. Rohn TT, Wirawan E, Brown RJ et al. Depletion of Beclin-1 due to proteolytic cleavage by caspases in the Alzheimer's disease brain. Neurobiol. Dis. 2011; 43 (1): 68–78.
259. Espert L, Denizot M, Grimaldi M et al. Autophagy is involved in T cell death after binding of HIV-1 envelope proteins to CXCR4. J. Clin. Invest. 2006; 116 (8): 2161–2172.

8 Abbreviations

3-MA	3-Methyladenine
AD	Alzheimer´s disease
AIF	Apoptosis inducing factor
ALS	Amyotrophic lateral sclerosis
AMP	Adenosine monophosphate
AMPA	α-amino-3-hydroxy-5-methylisoxazole-4-propionate
AMPK	5' Adenosine monophosphate-activated protein kinase
ANOVA	Analysis of variance
Apaf-1	Apoptosis protease-activating factor-1
ATP	Adenosinetriphosphate
BCA	Bicinchonic acid
Bcl-2	B-cell lymphoma-2
BDNF	Brain-derived neurotrophic factor
bFGF	basic Fibroblast growth factor
BMSC	Bone mesenchymal stem cells
BODIPY	4,4-Difluoro-5-(4-phenyl-1,3-butadienyl)- 4-bora-3a,4a-diaza-sindacene-3-undecanoic acid
BSA	Bovine serum albumin
CAD	Caspase-activated deoxyribonuclease
CCCP	2-[2-(3-Chlorophenyl)hydrazinylyidene]propanedinitrile
CM	Conditioned medium
CMA	Chaperone- mediated autophagy
CNS	Central nervous system
CQ	Chloroquine
CVEC	Coronary venular endothelial cell
CYTC	Cytochrome C
DAPI	4',6-Diamidino-2-phenylindole
DMEM	Dulbecco’s Modified Eagle Medium
DMSO	Dimethyl sulfoxide
DNA	Desoxyribonucleic acid
DTT	DL-Dithiothreitol
EBSS	Earle's Balanced Salt Solution
EDTA	Ethylenediaminetetraacetic acid
eEF 2	eukaryotic Elongation factor 2

EGF	Endothelian growth factor
EGTA	Ethylene glycol-bis (2-aminoethylether)-*N,N,N′,N′*- tetraacetic acid
ENDOG	Endonuclease G
ESC	Embryonic stem cell
FACS	Fluorescence activated cell sorting
FasL	Fas-ligand
FCCP	Carbonyl cyanide-4-(trifluoromethoxy)phenylhydrazone
FCS	Fetal calf serum
FGF	Fibroblast growth factor
Gal-1	Galectin-1
Gpx4	Glutathion peroxidase 4
GSH	Glutathione
H_2O_2	Hydrogen peroxide
HBSS	Hank's Balanced Salt Solution
HD	Huntington´s disease
hNSCs	Human neural stem cells
HRP	Horseradish peroxidase
IAP	Inhibitor of apoptosis protein
IGF	Insulin growth factor
iNCs	induced neuronal cells
iNSCs	induced neural stem cells
IP_3	Inositol trisphosphate
iPSCs	induced pluripotent stem cells
KA	Kainic acid
LC3	Microtubule- associated protein light chain 3
LY294002	2-(4-Morpholinyl)-8-phenyl-4H-1-benzopyran-4-one
MAPK	Mitogen-activated protein kinase
MCAO	Middle cerebral artery occlusion
MEF	Mouse embryonic fibroblast
MEK	Mitogen activated protein kinase kinase
MMP	Mitochondrial membrane potential
MOMP	Mitochondrial Outer Membrane Permeabilization
MSCs	Mesenchymal stem cell
mTOR	mammalian target of Rapamycin
MTT	3-(4,5-Dimethylthiazol-2-yl)-2,5-diphenyltetrazolium bromide

NaOH	Sodium hydroxide
NF-κB	Nuclear factor κB
NMDA	*N*-methyl-*D*-aspartic acid
Noxa	Phorbol-12-myristate-13-acetate-induced protein 1
NPC	Neural progenitor cell
NSCs	Neural stem cells
OCR	Measurement of cellular oxygen consumption rate
Omi/HtrA2	High temperature requirement protein A2
PA	Polyamine
PAR	Poly (ADP-ribose)
PARP-1	Poly (ADP-ribose) polymerase 1
PBS	Phosphate buffered solution
PCD	Programmed cell death
PD	Parkinson´s disease
PE	Phosphatidylethanolamine
PFA	Paraformaldehyde
PI_3K	Phosphoinositide-3-kinase
PIP_2	Phosphatidylinositol (3,4)-bisphosphate
PIP_3	Phosphatidylinositol (3,4,5)-triphosphate
PKC	Protein kinase C
PLA 2	Phospholipase A 2
PND	Post natal day
Prdx	Peroxiredoxin
PSCs	Pluripotent stem cells
PUMA	p53 upregulated modulator of apoptosis
PVDF	Polyvinylidenfluorid
Qvd-OPh	N-(2-Quinolyl) valyl-aspartyl-(2,6-difluorophenoxy) methyl ketone
RIP 1,3	Receptor interacting protein 1,3
RMS	Rostral migratory stream
ROS	Reactive oxygen species
SDS	Sodium dodecyl sulfate
SDS-PAGE	Sodium dodecyl sulfate polyacrylamide gel electrophoresis
SGZ	Subgranular zone
siRNA	Small interfering ribonucleic acid

SMAC/DIABLO	Second mitochondria–derived activator of caspase/direct IAP binding protein with low pI
STS	Staurosporine
SVZ	Subventricular zone
TBE	Tris/borate/EDTA
TBI	Traumatic brain injury
tBid	truncated Bid
TBST	Tris-buffered solution with Tween 20
TEMED	Tetramethylenethylendiamin
TMRE	Tetramethylrhodamin ethyl ester
TNFR	Tumor necrosis factor receptor
TSC 1,2	Tuberous sclerosis protein 1,2
VEGF	Vascular endothelian growth factor
xCT	Glutamine-cystine antiporter
XIAP	X-chromosomal linked inhibitor of apoptosis

9 Publications

9.1 Original papers

J Neurosci Methods. 2012 Jan 15;203(1):69-77. Epub 2011 Sep 22. Impedance measurement for real time detection of neuronal cell death. Diemert S, Dolga AM, Tobaben S, Grohm J, **Pfeifer S**, Oexler E, Culmsee C.

In preparation: 3-Methyladenine mediates neuroprotection against glutamate toxicity in HT-22 cells independent of autophagy inhibition. **Neunteibl S**., Dolga A. M., Elsaesser K., Culmsee C.

9.2 Oral presentations and posters

Selected talks:

Oral presentation for the abstract "Preconditioned medium from neuronal progenitor cells provides neuroprotective effects" presented at the 51th Jahrestagung der Deutschen Gesellschaft für Experimentelle und Klinische Pharmakologie und Toxikologie (DGPT), 2010, Mainz, Germany.

Selected abstracts and poster presentations:

Pfeifer, S., Dolga, A.M., Engel, S., Culmsee, C. (2009) Neuronal progenitor cells provide trophic support and protection against glutamate-induced neurotoxicity, DPhG Jena, 2009

S. Pfeifer, A.M. Dolga, S. Engel, C. Culmsee, Preconditioned medium from neuronal progenitor cells provides neuroprotective effects. 51th Jahrestagung der Deutschen Gesellschaft für Experimentelle und Klinische Pharmakologie und Toxikologie (DGPT), 2010, Mainz, Germany.

S. Diemert, **S. Pfeifer**, J. Grohm, S. Tobaben, A.M. Dolga, C. Culmsee Real-time detection of neuronal cell death by the xCELLigence system. 51th Jahrestagung der Deutschen Gesellschaft für Experimentelle und Klinische Pharmakologie und Toxikologie (DGPT), 2010, Mainz, Germany.

A.M. Dolga, J. Grohm, **S. Pfeifer**, S. Tobaben, C. Culmsee, (2010) Activation of small conductance $K_{Ca}2$ channels prevents neuronal death induced by delayed calcium deregulation, 11th Meeting of the European Calcium Society, Warsaw, Poland

Pfeifer, S., Dolga, A.M., Engel, S., Blomgren, K., Culmsee, C. (2010) Conditioned medium of neural progenitor cells protects neuronal cells against growth factor withdrawal and glutamate-induced neurotoxicity, Society for Neuroscience Annual Meeting , Neuroscience 2010, San Diego, USA, 11.2010

Culmsee C., **Pfeifer S**., Dolga A.M., Blomgren K., Öxler E.M**.** Life from death: Apoptotic neural progenitor cells protect neurons against growth factor withdrawal and glutamate toxicity. Society for Neuroscience Annual Meeting, Neuroscience 2012, New Orleans, USA, 13.10.2012-17.10.2012

Öxler E.M., **Pfeifer S.**, Dolga A.M., Blomgren K., Culmsee C. "Phoenix rising": The potential of apoptotic neural progenitor cells to provide neuroprotection. Fraunhofer Life Science Symposium, 29.11.2012-30.11.2012, Leipzig, Germany

9.3 Patent

Patent No. 12166390.0 - 2107, Culmsee C. Blomgren K., **Pfeifer S.**, Öxler E.M**.**, Sato Y., Zhu C., Stem cell derived composition for the treatment of acute injury and degenerative diseases, date of filing 02.05.2012

10 Acknowledgements, Danksagung

Ich danke meinem Doktorvater Professor Dr. Carsten Culmsee, der mich durch meine Promotionszeit geführt hat. Er stand mir immer mit seinem Fachwissen zur Seite, führte mich gut strukturiert durch meine Projekte und hatte stets ein offenes Ohr für all die Probleme, die während der Promotionszeit auftauchten.

Ich danke Amalia Dolga, die mir stets ein Ansprechpartner war und meine Projekte durch ihre Ideen, Anregungen und ihre konstruktive Kritik bereicherte.

Weiterhin danke ich Eva Meißner, die die Arbeit an den NPC während meiner Elternzeit fortführte und sehr spannende Erkenntnisse gewinnen konnte. Sie stand mir jederzeit mit Rat und Tat zur Seite.

Ich danke Sandra Engel und Renate Hartmannsgruber, die mich in die Arbeit in der Zellkultur eingeführt haben. Zudem danke ich Manuela Gellert, Eileen Daube und im Besonderen Katharina Elsässer, ohne die ein erfolgreicher Abschluss nicht möglich gewesen wäre.

Ein riesen Dank geht an Emma Esser und Niki Gröning für die tolle Arbeit im Sekretariat.

Ich danke all meinen wunderbaren Kollegen, die mir viele Aufgaben abnahmen und mich auch in angespannter und gestresster Laune ertrugen.

Ich danke meinem Mann, der mir stets Mut zugesprochen und mich in meiner Arbeit bestärkt hat. Hätte er mir nicht den Rücken freigehalten, wäre meine Arbeit in dieser Form nicht möglich gewesen.

Meiner Tochter Hannah danke ich dafür, dass sie mir auch in stressigen Zeiten immer ein Lächeln ins Gesicht zauberte.

Und nicht zuletzt danke ich meinen Eltern, die in jeglicher Hinsicht die Grundsteine für meinen Weg gelegt haben.

11 Curriculum vitae